CHAPTER 5

CONCLUSIONS AND OUTLOOK

5.1 Summary of the main results and general conclusion

With its marine configuration possibly prone to self-reinforcing mechanisms, the question of whether and when the WAIS will collapse under a warming climate remains unclear (Fox-Kemper et al., 2021), and reducing this uncertainty is an urgent and prior matter. Despite the uncertainties, recent studies suggest that the WAIS will lose mass in the future and eventually (partially) collapse. The uncertainties essentially pertain to when, and to whether the weak Earth structure beneath that area of the ice sheet may be a stabilising factor, as a rapid bedrock uplift in response to ice mass loss has been shown to delay or even limit mass loss. In addition, the future behaviour of the EAIS (with its sea-level potential of about 52 m SLE; Morlighem et al., 2020) is associated with even larger uncertainties (Stokes et al., 2022; Fox-Kemper et al., 2021). The pending question is: will the EAIS lose or gain mass in the future? More specifically, will the grounding line retreat in its marine basins, and if so, can the associated mass loss be compensated by sufficient mass gain due to increased snow accumulation in the interior of the ice sheet?

In this thesis, we have contributed to clarify and provide new insights to these questions, and therefore on the long-term future of the Antarctic ice sheet. To do so, we have investigated the influence of uncertainties in ice sheet–Earth system interactions on its future stability. Especially, we have focused on the influence of the interactions with the bedrock and sea surface via GIA, with the atmosphere via surface mass balance changes, and the ocean via sub-shelf melt changes.

In Chapter 3, while considering the regional heterogeneity in Antarctic Earth structure as well as the influence of local gravitationally-consistent sea-surface changes, we have explored for the first time the complete uncertainty range in Antarctic solid-Earth characteristics in a probabilistic assessment where we analysed their impact on the response of the AIS to future warming. We hence have produced Antarctic projections whose uncertainty ranges are solely due to the uncertainty in viscoelastic properties. In Chapter 4, we have produced observationally-calibrated projections of the future contribution of the AIS to GMSL changes based on an ensemble of simulations considering key uncertainties in ice sheet–climate interactions. This ensemble thus allows to investigate the future balance between sub-shelf melting and ice discharge on the one hand, and the changing surface mass balance on the other.

In other words, we have investigated in this thesis two main uncertainties about the future evolution of the AIS: (i) will GIA be able to stabilise its marine areas, and (ii) will the surface mass balance compensate for the ocean-driven mass loss? When tackling these questions, we have mainly focused on the centennial-to-multi-millennial timescales. In addition, considering ice–climate uncertainties only, we have proposed new estimates, with quantified uncertainties, of the evolution of the Antarctic ice sheet over the current millennium.

Overall, we have shown that the ocean will be the main driver of Antarctic short-term mass loss, leading to significant retreat in the WAIS (especially in the ASE), even under limited warming. Under sustained warming, however, this may lead to a complete WAIS collapse over the course of the millennium, despite a stabilising weak solid Earth structure beneath West Antarctica. In addition, our results suggest that a sustained warming will likely turn the EAIS into a positive contributor to SLR over the course of the next century. Indeed, we project that the ocean-driven grounding line retreat in its marine basins, which cannot be efficiently stabilised by GIA feedbacks given the rigid structure of the solid Earth in that area, will progressively outweigh the SMB. Finally, we have shown that the mitigating role of the SMB may strongly be reduced under sustained warming, due to a significant increase in surface runoff with increasing temperatures, hence further increasing the net AIS contribution to sea-level rise.

Below, we summarise the main results obtained in Chapter 3 and 4 by axing them following the two main objectives of this thesis. We then provide directions for future research in the next and last section.

5.1.1 The contribution of Antarctica to future sea-level rise

A first objective of this thesis was to contribute to the estimation of the future contribution of the AIS to sea-level changes and its uncertainty by producing credible projections of long-term AIS mass changes. In this framework, while the scope of Chapter 3 was not to carry out realistic projections of the AIS, we produced in Chapter 4 observationally-calibrated projections of the future contribution of the AIS to global mean sea-level changes considering key uncertainties in ice–climate interactions. Such projections thus contribute to estimating with quantified uncertainties what may be the magnitude and the rate of the contribution of the AIS to future SLR.

Under a **sustainable SSP1-2.6 socio-economic pathway** (in which global warming is very likely to be 1.3–2.4°C above pre-industrial levels by 2081-2100 and remain stable or even decrease thereafter; IPCC, 2021), our calibrated ensemble, similar to earlier studies (Golledge et al., 2015; Bulthuis et al., 2019; Rodehacke et al., 2020; Garbe et al., 2020), projects that **only part of WAIS would be lost, limiting the AIS contribution to SLR to +0.79 m [-0.22 to +1.56 m] by 2300 and +1.6 m [-0.47 to +3.12 m] by 3000 CE** (with a high-end contribution attributed to less likely ice–climate interactions, such as high sensitivity of sub-shelf melting to ocean thermal forcing).

Under a **high-emission SSP5-8.5 socio-economic pathway** (in which global warming is very likely to be 3.3–5.7°C above pre-industrial levels by 2081-2100 and keep increasing thereafter; IPCC, 2021), our calibrated ensemble projects a **complete collapse of the WAIS, likely to be completed before the year 2500 as well as significant retreat in the marine basins of the EAIS** occuring by the end of the millennium, also in agreement with previous estimates (Garbe et al., 2020; Fox-Kemper et al., 2021; Bulthuis et al., 2019). More specifically, we find a higher probability of grounding-line retreat in the Wilkes and Recovery basins than in the Aurora basin (similar to, e.g., Garbe et al., 2020; Golledge et al., 2019), despite the fact that the latter is currently showing signs of ocean-driven ice-shelf thinning and associated mass loss (also reproduced by our projections). Such continent-wide mass loss would lead to **AIS contribution to SLR equivalent to +2.82 m [+0.58 to 4.45 m] by 2300 +7.2 m [+3.5 to +13.45 m] by 3000 CE**.

The above calibrated estimates of future AIS mass loss did not account for the lateral variability nor the uncertainties in Antarctic viscoelastic properties. Therefore, taking into account the findings from Chapter 3, we may expect

(i) a stabilising influence of the weak Earth structure beneath West Antarctica, and more particularly the ASE, likely leading to a reduction and/or delay in mass loss arising from the WAIS, though probably not enabling to counteract the WAIS collapse projected under high-emission scenarios at multi-centennial timescales, as well as

(ii) a longer tail towards high values at multi-centennial-to-millennial timescales, due to the rigid rheology of the solid Earth beneath East Antarctica, hence providing a reduced stabilising effect compared with simulations that use a spatially-uniform Earth deformation model.

Therefore, our results confirm the already proposed point of view (e.g., Garbe et al., 2020; Seroussi et al., 2020; Bulthuis et al., 2019; DeConto et al., 2021) that the trigger of future Antarctic mass loss will occur in the WAIS. Thereby, we have contributed to reducing the uncertainty in the shorter-term future evolution of the AIS. Our results also provide additional support to the assessment that *'a threshold for WAIS stability may be close to 1.5-2°C'* (Oppenheimer et al., 2019; Fox-Kemper et al., 2021; McKay et al., 2022). Additionally, our projections seem to point out that (similar to Golledge et al., 2019) **present-day climate conditions are sufficient to commit to a continuous retreat of Thwaites glacier.**

5.1.2 What have we learned about the interactions of the ice sheet with the Earth System?

A second objective of this thesis was to assess the influence on future AIS mass changes of uncertainties approximating the current limits of our scientific understanding in the interactions of the AIS with the other components of the Earth system. Overall, we have shown that such uncertainties strongly modulate the response of the ice sheet to climate changes. In this context, our results have allowed to reduce uncertainties and better identify the drivers of future Antarctic mass loss, as well as the likely influence of GIA feedbacks.

Interactions with the solid Earth and sea surface In Chapter 3, we have highlighted, similar to previous studies (e.g., Gomez et al., 2015; Konrad et al., 2015; Larour et al., 2019), the overall[1] stabilising influence of GIA feedbacks on ice dynamics. Our results suggest that GIA feedbacks are not expected to substantially reduce SLR from marine-based ice in Antarctica over the 21st century, although the local weak Earth structure beneath the ASE may give rise to a delay of grounding-line retreat in this area at decadal timescales (as also suggested Kachuck et al., 2020). We showed, also in line with previous studies (e.g., Gomez et al., 2015; DeConto et al., 2021), that these processes may, however, become important at longer (multi-centennial-to-millennial) timescales (Gomez et al., 2015), even leading in some cases to a re-advance of the grounding line. Importantly, we have highlighted the importance of accounting for the spatial variability in the Antarctic viscoelastic properties and shown that the pathway followed by the future AIS is very sensitive to the solid-Earth structure adopted when evaluating the solid-Earth component of GIA across Antarctica. Especially, we have shown that, at multi-millenial timescales, large uncertainties arise from solid Earth structure below the EAIS (and in particular the Aurora basin), hence highlighting that if we want to robustly predict the long-term future of the AIS, its solid-Earth structure should be better constrained.

Interactions with the atmosphere As expected, the influence of the interactions with the atmosphere is less clear, due to an increase in competing processes (snow accumulation and surface runoff) in a warming climate. Nevertheless, we have contributed in Chapter 4 to a better approximation of how the Antarctic SMB may evolve in a warming climate. Especially, we have shown that, at first, the signal of SMB changes in a warming climate will be dominated by an increase in snow accumulation, as surface runoff remains limited. However, if regional surface warming increases beyond a threshold of 7.5°C above present-day (typically associated with a slightly lower global warming), we have highlighted that the increase in surface runoff will progressively compensate for the increase in snow accumulation, therefore reducing the mitigating potential of the ice-sheet SMB. In addition, under such regional warming (+7.5°C), we find a likely negative SMB over the ice shelves, hence directly contributing to the weakening of their buttressing potential. Beyond +15°C, we find that runoff rates on the grounded ice sheet would likely be sufficient to fully compensate for the snow accumulation, implying that SMB no longer mitigates mass losses and directly contributes to SLR. Whether such thresholds may be crossed and when will be dictated by the trajectories of future atmospheric warming. In addition, our results, similar to others before (Seroussi et al., 2020; Gilbert and Kittel, 2021; Trusel et al., 2015), have pointed out that the increase in surface runoff as atmospheric warming takes place may favour an acceleration of mass loss by way of hydrofracturing-driven weakening of the buttressing ice shelves. Finally, we have also highlighted the importance of the melt-elevation feedback, which has a significant influence of the future evolution of the AIS, and this already at centennial timescales.

Interactions with the ocean In line with recent findings (e.g., Paolo et al., 2015; Gudmundsson et al., 2019; Golledge et al., 2019; Bulthuis et al., 2019), we have highlighted in Chaper 4 the

[1]with the exception of less frequent classes of behaviour, see section 3.1

crucial importance of ice–ocean interactions on the future evolution of the AIS, as ocean thermal forcing triggers mass loss by way of ice-shelf thinning. Especially, our results pointed out that the ocean will be the main driver of Antarctic short-term mass loss, triggering significant ice loss in the WAIS already during this century. Additionally, we have highlighted the strong potential influence of ice–ocean interactions at longer (multi-centennial) timescales under high-emission pathways, under which they will likely trigger a complete WAIS collapse, as well as significant grounding-line retreat in the EAIS, where ocean-driven mass loss will take over atmospheric-driven mass gain as of the beginning of the next century. Overall, we have shown that ice–ocean interactions currently represent the biggest contributor to uncertainties in future AIS mass changes amongst ice–Earth system interactions at decadal-to-multicentennial timescales.

5.2 Discussion and directions for future research

5.2.1 Improving the representation of ice–Earth system interactions

It is important to underline that not all interactions between the AIS and its surrounding environment have been explored here. For example, we have not evaluated the influence of the geothermal heat flux, subglacial water pressure, nor the interactions of the ice sheet with the sea ice (Fyke et al., 2018). Some of the two-way interactions between the ice sheet and other components of the Earth system have been approximated here by using parameterisations or reduced-order models (such as the PDD model, parameterisations of the ocean circulation below the ice shelves, and the Elementary GIA model), allowing to (sometimes roughly) approximate the influence of changes in ice-sheet/shelf geometry on the surface mass balance (SMB–elevation feedback), sub-shelf melting, and isostasy and gravity (GIA feedbacks). However, several additional two-way interactions between the ice sheet and the Earth system (Fyke et al., 2018) have not been explored here, leading to the underestimation of feedback mechanisms, such as the influence of ice-sheet topography changes on atmospheric circulation, of AIS mass changes on the Earth's rotation vector or other ice masses, or of fresh water input (essentially from iceberg fluxes and sub-shelf melting) on the oceanic stratification and circulation, and others, which, in turn, influence the ice-sheet evolution.

Clearly, the future of Antarctic (or more generally climate) projections resides in a full coupling between the different components of the Earth system. Unfortunately, the significant computational resources requested by such coupled simulations hampers the realisation of large ensemble of projections and hence the application of an uncertainty quantification framework. Therefore, while high priority should be (and currently is, e.g., Siahaan et al., 2021; Pelletier et al., 2022) accorded to facilitating and improving fully coupled simulations, a simultaneous direction for future research resides in improving our current approximations of the ice-sheet interactions with the Earth system. In this framework, we believe that the Elementary GIA model developed in the context of this thesis represents an interesting tool and improvement for approximating GIA feedbacks in a computationally-efficient way. Further research may, for example, focus on better constraining the influence of local ice-sheet elevation/geometry changes on, notably, the magnitude and the pattern of precipitations, allowing to improve the relatively crude approximations of elevation feedback used here. For example, a line of research may be, as an intermediate step to two-way coupling between an ice-sheet model and an atmospheric model, to evaluate the evolution of RCM projections using an evolving ice-sheet geometry and try to derive/constrain updated parameterisation(s) of SMB–elevation feedbacks.

5.2.2 Towards credible sea-level projections

Capturing observed trends of mass change remains a challenge for ice-sheet models. As a consequence, uncertainty in AIS projections is increased, especially for this century (Fox-Kemper et al., 2021; Seroussi et al., 2020; Reese et al., 2020; Aschwanden et al., 2021). Nevertheless, AIS projections are increasingly evaluated or calibrated with modern or past observational constraints (Nias et al., 2019; Edwards et al., 2019; DeConto et al., 2021; Lowry et al., 2021). Such conditioning on observations allows to obtain more realistic present-day (i.e., initial) ice-sheet conditions (typically geometry and velocity) and also to constrain uncertainty in a probabilistic framework (Fox-Kemper et al., 2021; Aschwanden et al., 2021). AIS projections are also increasingly better designed to quantify uncertainties, for example by way of model intercomparison projects (Seroussi et al., 2019, 2020; Levermann et al., 2020), statistical emulation (Edwards et al., 2019, 2021; Bulthuis et al., 2019), and large ensembles with space-filling perturbed parameter spaces (Bulthuis et al., 2019; Nias et al., 2019). Providing a protocol for the historical runs used to bring the ice sheet to present day and apply criteria for sub-selecting projections from the multi-model ensemble based on the ability to reproduce historical changes will likely become standard in future model intercomparison projects, such as ISMIP7. With such improvements, we are on the way towards increasingly credible and robust projections of ice-sheet mass changes (Aschwanden et al., 2021; Fox-Kemper et al., 2021).

In this framework, although not fully accounting for all types of uncertainties, we believe that this thesis represents a step forward in its exploration of parametric uncertainties and its application of a Bayesian framework allowing to historically-constrain the ice-sheet model projections. Applied in a multi-model ensemble as well as on a broader (less climate and solid Earth-oriented) parametric uncertainty exploration, it would constitute a significant step forward in producing credible projections of the contribution of the AIS to sea-level changes (Edwards et al., 2019; Aschwanden et al., 2021). To continue in this direction, future work should focus on applying a similar Bayesian calibration approach on an ensemble considering (i) climate and solid-Earth uncertainties together as well as (ii) including uncertainties in ice-dynamical parameters that approximate the current limits of our scientific understanding.

Nevertheless, one may wonder whether calibrating ice-sheet models with respect to observations really leads to more credible projections. Indeed, ensemble members may be evaluated as well-matching the observations while, in fact, projections compensate for some drift associated with the model initialisation (though the latter has been significantly reduced in our case), or applied model physics compensate for biases in the imposed climate forcing. In this context, we believe that an advantage/improvement of the calibration method applied in Chapter 4 with respect to previous works (e.g., Nias et al., 2019; DeConto et al., 2021; Lowry et al., 2021) is that it relies on different sources of mass change triggered by processes which are known to drive current AIS mass changes: sub-shelf melting, surface mass balance, iceberg calving. The method applied here may however be improved by forcing the ice-sheet model with outputs from RCMs downscaling climate reanalysis (such as the ERA5 reanalysis; Hersbach et al., 2020) for the atmosphere and from reanalysis directly for the ocean (e.g., ORAS5; Zuo et al., 2018, 2019), instead of using atmospheric and oceanic forcings derived from ESMs.

In addition, modern ice-sheet and climate conditions may not necessarily reflect the future ones. In such case, model projections that do not match observed mass changes may yet better perform at reproducing the future evolution of the AIS. This is all the more problematic as, due to the lack of observational data, we are currently only able to calibrate for relatively short modern periods. To address this, another advantage of a Bayesian approach such as applied here is that model projections with physics or parameter values that do not ideally match current observed trends are still attributed a weight in the projections, even though a lower one. Similarly, projections from ice-sheet models are crucially dependent on the model physics that they include. However, despite our constantly improving knowledge and understanding of ice-sheet dynamics, we know for a fact that current ice-sheet models do not include all physics characterising ice sheets. Model projections may thus reproduce current trends, but lack accounting for processes that may be triggered in the future. A known example of such process/mechanism is MICI, which occurs through brittle failure (Bassis et al., 2021). Ice is known to be brittle, but large scale ice-sheet models do not yet include such brittle deformation. By definition, current ice-sheet models would thus not be able to properly predict the occurrence of such a behaviour in the future. Therefore, attention should be directed towards the understanding and representation of processes that may be triggered or increased in a warmer climate, such as ice-shelf weakening through damage (Lhermitte et al., 2020) which may facilitate cliff collapse (Pollard et al., 2015; Bassis et al., 2021), or the injection of surface melt water into the ice-sheet subglacial environment (Bell et al., 2018). Further steps may also consist in (similarly to, e.g., DeConto and Pollard, 2016; DeConto et al., 2021) additionally calibrate projections for available paleo observations, allowing to (potentially) account for conditions different than modern. However, this requires tackling some additional challenges typically associated with modelling the past evolution of the AIS, such as uncertainties in the paleo-climate and the initialisation procedure (how do you initialise an ice-sheet model when you only know little about the past conditions of the ice sheet?).

Finally, it is important to underline that model evaluation and calibration remains hampered by uncertainties in processes that may currently play a significant role but are yet not well taken into account in ice-sheet models, such as calving (Benn et al., 2017), firn densification processes (Verjans et al., 2020), or the influence of subglacial hydrology on basal sliding (Kazmierczak et al., 2022). Opportunities in reducing uncertainties in AIS projections hence lie in improving our understanding of such processes.

5.2.3 On the road to decadal (regional) predictability?

Although the title and focus of this thesis is *'The long-term future of the Antarctic ice sheet'*, some of the aspects tackled in this work may open new perspectives on the investigation of shorter timescales. First, the improvements made on the initialisation procedure (section 2.3.1) allowed for a significant diminution in model drift (noise), hence limiting the aforementioned risk of having model projections that reproduce observations for the wrong reasons (i.e., compensate for such drift). In addition, the development of a simplified GIA model enables to account for the fast (potentially at decadal timescales) uplift likely occurring in the Amundsen Sea sector of West Antarctica, as well as for the instantaneous influence of gravitationally-consistent sea-surface changes in response to Antarctic mass changes. Finally, applying a Bayesian framework as realised in Chapter 4 enables to evaluate the performance of ice-sheet models over the historical period and retain (or attribute more weight to) the projections that closely match observations over the past decades, hence providing more robustness and reducing uncertainties on the short timescales. The combination of such improvements may imply that ice-sheet models are now capable of reproducing Antarctic mass changes at short timescales. Therefore, future work may focus on investigating the interactions of the AIS with its environment at decadal timescales as well as regional spatial scales. This would allow, notably, to identify the drivers of mass changes at such spatio-temporal scales, both over hindcasts of the past decades and short-term projections. Nevertheless, being able to evaluate such short-term and regional projections requires reliable and detailed time series of observational data, and this especially at regional (i.e., basin) scales (Nilsson et al., 2022; Rignot et al., 2019). Luckily, the amount of such detailed accurate observations is growing continually. In the future, applying model calibration with detailed observations from longer time periods will allow for increasingly more robust projections.

BIBLIOGRAPHY

Abram, N. J., Mulvaney, R., Wolff, E., Triest, J., Kipfstuhl, S., Trusel, L. D., Vimeux, F., Fleet, L., and Arrowsmith, C. (2013). Acceleration of snow melt in an Antarctic Peninsula ice core during the twentieth century. *Nature Geoscience*, 6, 404–411, https://doi.org/10.1038/ngeo1787. URL https://www.documentation.ird.fr/hor/{PAR}00010586.

Adhikari, S., Ivins, E. R., Larour, E., Seroussi, H., Morlighem, M., and Nowicki, S. (2014). Future Antarctic bed topography and its implications for ice sheet dynamics. *Solid Earth*, 5, 569–584, https://doi.org/https://doi.org/10.5194/se-5-569-2014.

Adusumilli, S., Fricker, H., Medley, B., Padman, L., and Siegfried, M. (2020). Interannual variations in meltwater input to the Southern Ocean from Antarctic ice shelves. *Nature Geoscience*, 13, 1–5, https://doi.org/10.1038/s41561-020-0616-z.

Alley, R. B., Blankenship, D. D., Bentley, C. R., and Rooney, S. (1986). Deformation of till beneath ice stream B, West Antarctica. *Nature*, 322, 57–59.

An, M., Wiens, D. A., Zhao, Y., Feng, M., Nyblade, A. A., Kanao, M., Li, Y., Maggi, A., and Lévêque, J. J. (2015). S-velocity model and inferred Moho topography beneath the Antarctic Plate from Rayleigh waves. *Journal of Geophysical Research: Solid Earth*, 120(1), 359–383, https://doi.org/https://doi.org/10.1002/2014JB011332.

Asay-Davis, X. S., Jourdain, N. C., and Nakayama, Y. (2017). Developments in Simulating and Parameterizing Interactions Between the Southern Ocean and the Antarctic Ice Sheet. *Current Climate Change Reports*, 3(4), https://doi.org/10.1007/s40641-017-0071-0. URL https://www.osti.gov/biblio/1537872.

Aschwanden, A., Aðalgeirsdóttir, G., and Khroulev, C. (2013). Hindcasting to measure ice sheet model sensitivity to initial states. *The Cryosphere*, 7(4), 1083–1093, https://doi.org/10.5194/tc-7-1083-2013. URL https://tc.copernicus.org/articles/7/1083/2013/.

Aschwanden, A., Bartholomaus, T. C., Brinkerhoff, D. J., and Truffer, M. (2021). Brief communication: A roadmap towards credible projections of ice sheet contribution to sea level. *The Cryosphere*, 15(12), 5705–5715, https://doi.org/10.5194/tc-15-5705-2021. URL https://tc.copernicus.org/articles/15/5705/2021/.

Bamber, J. L., Westaway, R. M., Marzeion, B., and Wouters, B. (2018). The land ice contribution to sea level during the satellite era. *Environmental Research Letters*, 13(6), 063008, https://doi.org/10.1088/1748-9326/aac2f0. URL https://doi.org/10.1088/1748-9326/aac2f0.

Barletta, V. R., Bevis, M., Smith, B. E., Wilson, T., Brown, A., Bordoni, A., Willis, M., Khan, S. A., Rovira-Navarro, M., Dalziel, I., Smalley, R., Kendrick, E., Konfal, S., Caccamise, D. J., Aster, R. C., Nyblade, A., and Wiens, D. A. (2018). Observed rapid bedrock uplift in Amundsen Sea Embayment promotes ice-sheet stability. *Science*, 360(6395), 1335–1339, https://doi.org/https://doi.org/110.1126/science.aao1447.

Barthel, A., Agosta, C., Little, C. M., Hattermann, T., Jourdain, N. C., Goelzer, H., Nowicki, S., Seroussi, H., Straneo, F., and Bracegirdle, T. J. (2020). CMIP5 model selection for ISMIP6 ice sheet model forcing: Greenland and Antarctica. *The Cryosphere*, 14(3), 855–879, https://doi.org/10.5194/tc-14-855-2020. URL https://tc.copernicus.org/articles/14/855/2020/.

Bassis, J. N., Berg, B., Crawford, A. J., and Benn, D. I. (2021). Transition to marine ice cliff instability controlled by ice thickness gradients and velocity. *Science*, 372(6548), 1342–1344, https://doi.org/10.1126/science.abf6271. URL https://www.science.org/doi/abs/10.1126/science.abf6271.

Bassis, J. N. and Ultee, L. (2019). A Thin Film Viscoplastic Theory for Calving Glaciers: Toward a Bound on the Calving Rate of Glaciers. *Journal of Geophysical Research: Earth Surface*, 124(8), 2036–2055, https://doi.org/https://doi.org/10.1029/2019JF005160. URL https://agupubs.onlinelibrary.wiley.com/doi/abs/10.1029/2019JF005160.

Bassis, J. N. and Walker, C. C. (2012). Upper and lower limits on the stability of calving glaciers from the yield strength envelope of ice. *Proceedings: Mathematical, Physical and Engineering Sciences*, 468(2140), 913–931. URL http://www.jstor.org/stable/41511043.

Beckmann, A. and Goosse, H. (2003). A parameterization of ice shelf-ocean interaction for climate models . *Ocean Modelling*, 5(2), 157 – 170, https://doi.org/10.1016/S1463-5003(02)00019-7.

Bell, R., Banwell, A., Trusel, L., and Kingslake, J. (2018). Antarctic surface hydrology and impacts on ice-sheet mass balance. *Nature Climate Change*, 8(12), 1044–1052, https://doi.org/10.1038/s41558-018-0326-3.

Bell, R. E., Chu, W., Kingslake, J., Das, I., Tedesco, M., Tinto, K. J., Zappa, C. J., Frezzotti, M., Boghosian, A., and Lee, W. S. (2017). Antarctic ice shelf potentially stabilized by export of meltwater in surface river. *Nature*, 544(7650), 344–348, https://doi.org/10.1038/nature22048.

Benn, D. I., Cowton, T., Todd, J., and Luckman, A. (2017). Glacier Calving in Greenland. *Current Climate Change Reports*, 3(4), 282–290, https://doi.org/10.1007/s40641-017-0070-1. URL https://doi.org/10.1007%2Fs40641-017-0070-1.

Bennett, M. R. (2003). Ice streams as the arteries of an ice sheet: their mechanics, stability and significance. *Earth-Science Reviews*, 61(3-4), 309–339, https://doi.org/10.1016/s0012-8252(02)00130-7. URL https://doi.org/10.1016%2Fs0012-8252%2802%2900130-7.

Bentsen, M., Bethke, I., Debernard, J. B., Iversen, T., Kirkevåg, A., Seland, Ø., Drange, H., Roelandt, C., Seierstad, I. A., Hoose, C., and Kristjánsson, J. E. (2013). The Norwegian Earth System Model, NorESM1-M – Part 1: Description and basic evaluation of the physical climate. *Geoscientific Model Development*, 6(3), 687–720, https://doi.org/10.5194/gmd-6-687-2013. URL https://gmd.copernicus.org/articles/6/687/2013/.

Berdahl, M., Leguy, G., Lipscomb, W. H., Urban, N. M., and Hoffman, M. J. (2022). Exploring ice sheet model sensitivity to ocean thermal forcing using the Community Ice Sheet Model

(CISM). *The Cryosphere Discussions*, 2022, 1–38, https://doi.org/10.5194/tc-2022-156. URL https://tc.copernicus.org/preprints/tc-2022-156/.

Bernales, J., Rogozhina, I., and Thomas, M. (2017). Melting and freezing under Antarctic ice shelves from a combination of ice-sheet modelling and observations. *Journal of Glaciology*, 63(240), 731–744, https://doi.org/10.1017/jog.2017.42.

Bindschadler, R., Choi, H., Wichlacz, A., Bingham, R., Bohlander, J., Brunt, K., Corr, H., Drews, R., Fricker, H., Hall, M., Hindmarsh, R., Kohler, J., Padman, L., Rack, W., Rotschky, G., Urbini, S., Vornberger, P., and Young, N. (2011). Getting around antarctica: new high-resolution mappings of the grounded and freely-floating boundaries of the antarctic ice sheet created for the international polar year. *The Cryosphere*, 5(3), 569–588, https://doi.org/10.5194/tc-5-569-2011. URL https://tc.copernicus.org/articles/5/569/2011/.

Blackburn, T., Edwards, G., Tulaczyk, S., Scudder, M., Piccione, G., Hallet, B., McLean, N., Zachos, J., Cheney, B., and Babbe, J. (2020). Ice retreat in Wilkes Basin of East Antarctica during a warm interglacial. *Nature*, 583, 554–559, https://doi.org/10.1038/s41586-020-2484-5.

Bracegirdle, T. J., Krinner, G., Tonelli, M., Haumann, F. A., Naughten, K. A., Rackow, T., Roach, L. A., and Wainer, I. (2020). Twenty first century changes in antarctic and southern ocean surface climate in cmip6. *Atmospheric Science Letters*, 21(9), e984, https://doi.org/https://doi.org/10.1002/asl.984. URL https://rmets.onlinelibrary.wiley.com/doi/abs/10.1002/asl.984.

Brondex, J., Gagliardini, O., Gillet-Chaulet, F., and Durand, G. (2017). Sensitivity of grounding line dynamics to the choice of the friction law. *Journal of Glaciology*, 63(241), 854–866, https://doi.org/10.1017/jog.2017.51. URL https://doi.org/10.1017%2Fjog.2017.51.

Brondex, J., Gillet-Chaulet, F., and Gagliardini, O. (2019). Sensitivity of centennial mass loss projections of the amundsen basin to the friction law. *The Cryosphere*, 13(1), 177–195, https://doi.org/10.5194/tc-13-177-2019. URL https://tc.copernicus.org/articles/13/177/2019/.

Bronselaer, B., Winton, M., Griffies, S., Hurlin, W., Rodgers, K., Sergienko, O., Ronald, S., and Russell, J. (2018). Change in future climate due to Antarctic meltwater. *Nature*, 564, https://doi.org/10.1038/s41586-018-0712-z.

Brotchie, J. F. and Silvester, R. (1969). On Crustal Flexure. *Journal of Geophysical Research*, 74(22), 5240–5252, https://doi.org/https://doi.org/10.1029/JB074i022p05240.

Budd, W. F., Keage, P. L., and Blundy, N. A. (1979). Empirical Studies of Ice Sliding. *Journal of Glaciology*, 23(89), 157–170, https://doi.org/10.3189/S0022143000029804.

Bueler, E. and Brown, J. (2009). Shallow shelf approximation as a "sliding law" in a thermomechanically coupled ice sheet model. *Journal of Geophysical Research: Earth Surface*, 114(F3), https://doi.org/https://doi.org/10.1029/2008JF001179.

Bulthuis, K., Arnst, M., Sun, S., and Pattyn, F. (2019). Uncertainty quantification of the multi-centennial response of the Antarctic ice sheet to climate change. *The Cryosphere*, 13(4), 1349–1380, https://doi.org/https://doi.org/10.5194/tc-13-1349-2019.

Burgard, C., Jourdain, N. C., Reese, R., Jenkins, A., and Mathiot, P. (2022). An assessment of basal melt parameterisations for Antarctic ice shelves. *The Cryosphere Discussions*, 2022, 1–56, https://doi.org/10.5194/tc-2022-32. URL https://tc.copernicus.org/preprints/tc-2022-32/.

Calov, R. and Greve, R. (2005). A semi-analytical solution for the positive degree-day model with stochastic temperature variations. *Journal of Glaciology*, 51.

Chambers, C., Greve, R., Obase, T., Saito, F., and Abe-Ouchi, A. (2021). Mass loss of the Antarctic ice sheet until the year 3000 under a sustained late-21st-century climate. *Journal of Glaciology*, (pp. 1–13)., https://doi.org/10.1017/jog.2021.124.

Chang, W., Applegate, P. J., Haran, M., and Keller, K. (2014). Probabilistic calibration of a Greenland Ice Sheet model using spatially resolved synthetic observations: toward projections of ice mass loss with uncertainties. *Geoscientific Model Development*, 7(5), 1933–1943, https://doi.org/10.5194/gmd-7-1933-2014. URL https://gmd.copernicus.org/articles/7/1933/2014/.

Chen, B., Haeger, C., Kaban, M. K., and Petrunin, A. G. (2017). Variations of the effective elastic thickness reveal tectonic fragmentation of the Antarctic lithosphere. *Tectonophysics*, 746, 412 – 424, https://doi.org/https://doi.org/10.1016/j.tecto.2017.06.012.

Church, J., Clark, P., Cazenave, A., Gregory, J., Jevrejeva, S., Levermann, A., Merrifield, M., Milne, G., Nerem, R., Nunn, P., Payne, A., Pfeffer, W., Stammer, D., and Unnikrishnan, A. (2013). Sea level change. In V. B. Stocker, T.F., D. Qin, G.-K. Plattner, M. Tignor, S.K. Allen, J. Boschung, A. Nauels, Y. Xia and P. Midgley (Eds.), *Climate Change 2013: The Physical Science Basis. Contribution of Working Group I to the Fifth Assessment Report of the Intergovernmental Panel on Climate Change*, (pp. 1137–1216). Cambridge, United Kingdom and New York, NY, USA.: Cambridge University Press, cambridge edition, https://doi.org/https://doi.org/10.1017/CB09781107415315.026.

Clark, P., He, F., Golledge, N., Mitrovica, J., Dutton, A., Hoffman, J., and Dendy, S. (2020). Oceanic forcing of penultimate deglacial and last interglacial sea-level rise. *Nature*, 577, 660–664, https://doi.org/10.1038/s41586-020-1931-7.

Clerc, F., Minchew, B. M., and Behn, M. D. (2019). Marine Ice Cliff Instability Mitigated by Slow Removal of Ice Shelves. *Geophysical Research Letters*, 46(21), 12108–12116, https://doi.org/https://doi.org/10.1029/2019GL084183. URL https://agupubs.onlinelibrary.wiley.com/doi/abs/10.1029/2019GL084183.

Collins, M., Knutti, R., Arblaster, J., Dufresne, J.-L., Fichefet, T., Friedlingstein, P., Gao, X., Gutowski, W. J., Johns, T., Krinner, G., Shongwe, M., Tebaldi, C., Weaver, A. J., and Wehner, M. (2013). *Long-term climate change: Projections, commitments and irreversibility*, In T. F. Stocker, D. Qin, G.-K. Plattner, M. Tignor, S. K. Allen, J. Doschung, A. Nauels, Y. Xia, V. Bex, and P. M. Midgley (Eds.), *Climate Change 2013: The Physical Science Basis. Contribution of Working Group I to the Fifth Assessment Report of the Intergovernmental Panel on Climate Change*, (pp. 1029–1136). Cambridge University Press: Cambridge, UK, https://doi.org/10.1017/CBO9781107415324.024.

Cornford, S. L., Seroussi, H., Asay-Davis, X. S., Gudmundsson, G. H., Arthern, R., Borstad, C., Christmann, J., Dias dos Santos, T., Feldmann, J., Goldberg, D., Hoffman, M. J., Humbert, A., Kleiner, T., Leguy, G., Lipscomb, W. H., Merino, N., Durand, G., Morlighem, M., Pollard, D., Rückamp, M., Williams, C. R., and Yu, H. (2020). Results of the third Marine Ice Sheet Model Intercomparison Project (MISMIP+). *The Cryosphere*, 14(7), 2283–2301, https://doi.org/10.5194/tc-14-2283-2020. URL https://tc.copernicus.org/articles/14/2283/2020/.

Coulon, V., Bulthuis, K., Whitehouse, P. L., Sun, S., Haubner, K., Zipf, L., and Pattyn, F. (2021). Contrasting Response of West and East Antarctic Ice Sheets to Glacial Isostatic Adjustment. *Journal of Geophysical Research: Earth Surface*, 126(7), e2020JF006003, https://doi.org/

https://doi.org/10.1029/2020JF006003. URL https://agupubs.onlinelibrary.wiley.com/doi/abs/10.1029/2020JF006003.

Crawford, A. J., Benn, D. I., Todd, J., Åström, J. A., Bassis, J. N., and Zwinger, T. (2021). Marine ice-cliff instability modeling shows mixed-mode ice-cliff failure and yields calving rate parameterization. *Nature Communications*, 12(1), https://doi.org/10.1038/s41467-021-23070-7. URL https://doi.org/10.1038%2Fs41467-021-23070-7.

Cuffey, K. M. and Paterson, W. S. B. (2010). *The physics of glaciers*. Academic Press.

de Boer, B., Stocchi, P., and van de Wal, R. S. W. (2014). A fully coupled 3-D ice-sheet–sea-level model: algorithm and applications. *Geoscientific Model Development*, 7(5), 2141–2156, https://doi.org/https://doi.org/10.5194/gmd-7-2141-2014.

de Boer, B., Stocchi, P., Whitehouse, P. L., and van de Wal, R. S. (2017). Current state and future perspectives on coupled ice-sheet – sea-level modelling. *Quaternary Science Reviews*, 169, 13–28, https://doi.org/https://doi.org/10.1016/j.quascirev.2017.05.013.

DeConto, R., Pollard, D., Alley, R., Velicogna, I., Gasson, E., Gomez, N., Sadai, S., Condron, A., Gilford, D., Ashe, E., Kopp, R., Li, D., and Dutton, A. (2021). The Paris Climate Agreement and future sea-level rise from Antarctica. *Nature*, 593, 83–89, https://doi.org/10.1038/s41586-021-03427-0.

DeConto, R. M. and Pollard, D. (2016). Contribution of Antarctica to past and future sea-level rise. *Nature*, 531, 591–597, https://doi.org/https://doi.org/10.1038/nature17145.

Depoorter, M. A., Bamber, J. L., Griggs, J. A., Lenaerts, J. T. M., Ligtenberg, S. R. M., van den Broeke, M. R., and Moholdt, G. (2013). Calving fluxes and basal melt rates of Antarctic ice shelves. *Nature*, 502(7469), 89–92.

Dowdeswell, J. A., Batchelor, C. L., Montelli, A., Ottesen, D., Christie, F. D. W., Dowdeswell, E. K., and Evans, J. (2020). Delicate seafloor landforms reveal past Antarctic grounding-line retreat of kilometers per year. *Science*, 368(6494), 1020–1024, https://doi.org/10.1126/science.aaz3059. URL https://www.science.org/doi/abs/10.1126/science.aaz3059.

Dunmire, D., Lenaerts, J. T. M., Datta, R. T., and Gorte, T. (2022). Antarctic surface climate and surface mass balance in the community earth system model version 2 (1850–2100). *The Cryosphere Discussions*, 2022, 1–28, https://doi.org/10.5194/tc-2022-52. URL https://tc.copernicus.org/preprints/tc-2022-52/.

Durand, G., Gagliardini, O., Zwinger, T., Meur, E. L., and Hindmarsh, R. C. (2009). Full Stokes modeling of marine ice sheets: influence of the grid size. *Annals of Glaciology*, 50(52), 109–114, https://doi.org/10.3189/172756409789624283.

Dutrieux, P., Rydt, J. D., Jenkins, A., Holland, P. R., Ha, H. K., Lee, S. H., Steig, E. J., Ding, Q., Abrahamsen, E. P., and Schröder, M. (2014). Strong Sensitivity of Pine Island Ice-Shelf Melting to Climatic Variability. *Science*, 343(6167), 174–178, https://doi.org/10.1126/science.1244341.

Edwards, T. L., Brandon, M. A., Durand, G., Edwards, N. R., Golledge, N. R., Holden, P. B., Nias, I. J., Payne, A. J., Ritz, C., and Wernecke, A. (2019). Revisiting Antarctic ice loss due to marine ice-cliff instability. *Nature*, 566, 58–64, https://doi.org/https://doi.org/10.1038/s41586-019-0901-4.

Edwards, T. L., Fettweis, X., Gagliardini, O., Gillet-Chaulet, F., Goelzer, H., Gregory, J. M., Hoffman, M., Huybrechts, P., Payne, A. J., Perego, M., Price, S., Quiquet, A., and Ritz, C. (2014). Probabilistic parameterisation of the surface mass balance–elevation feedback in regional climate model simulations of the Greenland ice sheet. *The Cryosphere*, 8(1), 181–194, https://doi.org/10.5194/tc-8-181-2014. URL https://tc.copernicus.org/articles/8/181/2014/.

Edwards, T. L., Nowicki, S., Marzeion, B., Hock, R., Goelzer, H., Seroussi, H., Jourdain, N. C., Slater, D., Turner, F., Smith, C. J., McKenna, C. M., Simon, E., Abe-Ouchi, A., Gregory, J. M., Larour, E., Lipscomb, W. H., Payne, A. J., Shepherd, A., Agosta, C., Alexander, P., Albrecht, T., Anderson, B., Asay-Davis, X., Aschwanden, A., Barthel, A., Bliss, A., Calov, R., Chambers, C., Champollion, N., Choi, Y., Cullather, R., Cuzzone, J., Dumas, C., Felikson, D., Fettweis, X., Fujita, K., Galton-Fenzi, B. K., Gladstone, R., Golledge, N. R., Greve, R., Hattermann, T., Hoffman, M. J., Humbert, A., Huss, M., Huybrechts, P., Immerzeel, W., Kleiner, T., Kraaijenbrink, P., Le clec'h, S., Lee, V., Leguy, G. R., Little, C. M., Lowry, D. P., Malles, J.-H., Martin, D. F., Maussion, F., Morlighem, M., O'Neill, J. F., Nias, I., Pattyn, F., Pelle, T., Price, S., Quiquet, A., Radić, V., Reese, R., Rounce, D. R., Ruckamp, M., Sakai, A., Shafer, C., Schlegel, N.-J., Shannon, S., Smith, R. S., Straneo, F., Sun, S., Tarasov, L., Trusel, L. D., Breedam, J. V., van de Wal, R., van den Broeke, M., Winkelmann, R., Zekollari, H., Zhao, C., Zhang, T., and Zwinger, T. (2021). Projected land ice contributions to 21st century sea level rise. *Nature*, 593, 74–82, https://doi.org/10.1038/s41586-021-03302-y.

Engelhardt, H. F. and Kamb, B. (1997). Basal hydraulic system of a West Antarctic ice stream: constraints from borehole observations. *Journal of Glaciology*, 43, 207–230.

Farrell, W. E. and Clark, J. A. (1976). On Postglacial Sea Level. *Geophysical Journal of the Royal Astronomical Society*, 46(3), 647–667, https://doi.org/https://doi.org/10.1111/j.1365-246X.1976.tb01252.x.

Favier, L., Durand, G., Cornford, S. L., Gudmundsson, G. H., Gagliardini, O., Gillet-Chaulet, F., Zwinger, T., Payne, A. J., and Le Brocq, A. M. (2014). Retreat of Pine Island Glacier controlled by marine ice-sheet instability. *Nature Climate Change*, 4, 117–121, https://doi.org/https://doi.org/10.1038/nclimate2094.

Favier, L., Jourdain, N. C., Jenkins, A., Merino, N., Durand, G., Gagliardini, O., Gillet-Chaulet, F., and Mathiot, P. (2019). Assessment of sub-shelf melting parameterisations using the ocean–ice-sheet coupled model nemo(v3.6)–elmer/ice(v8.3). *Geoscientific Model Development*, 12(6), 2255–2283, https://doi.org/10.5194/gmd-12-2255-2019. URL https://gmd.copernicus.org/articles/12/2255/2019/.

Fettweis, X., Franco, B., Tedesco, M., van Angelen, J. H., Lenaerts, J. T. M., van den Broeke, M. R., and Gallée, H. (2013). Estimating the greenland ice sheet surface mass balance contribution to future sea level rise using the regional atmospheric climate model mar. *The Cryosphere*, 7(2), 469–489, https://doi.org/10.5194/tc-7-469-2013. URL https://tc.copernicus.org/articles/7/469/2013/.

Fox-Kemper, B., Hewitt, H., Xiao, C., Aðalgeirsdóttir, G., Drijfhout, S., Edwards, T., Golledge, N., Hemer, M., Kopp, R., Krinner, G., Mix, A., Notz, D., Nowicki, S., Nurhati, I., Ruiz, L., Sallée, J.-B., Slangen, A., and Yu, Y. (2021). *Ocean, Cryosphere and Sea Level Change*, In V. Masson-Delmotte, P. Zhai, A. Pirani, S. Connors, C. Péan, S. Berger, N. Caud, Y. Chen, L. Goldfarb, M. Gomis, M. Huang, K. Leitzell, E. Lonnoy, J. Matthews, T. Maycock, T. Waterfield, O. Yelekçi, R. Yu, and B. Zhou (Eds.), *Climate Change 2021: The Physical Science*

Basis. Contribution of Working Group I to the Sixth Assessment Report of the Intergovernmental Panel on Climate Change, (pp. 1211–1362). Cambridge University Press: Cambridge, United Kingdom and New York, NY, USA, https://doi.org/10.1017/9781009157896.011.

Fretwell, P., Pritchard, H. D., Vaughan, D. G., Bamber, J. L., Barrand, N. E., Bell, R., Bianchi, C., Bingham, R. G., Blankenship, D. D., Casassa, G., Catania, G., Callens, D., Conway, H., Cook, A. J., Corr, H. F. J., Damaske, D., Damm, V., Ferraccioli, F., Forsberg, R., Fujita, S., Gim, Y., Gogineni, P., Griggs, J. A., Hindmarsh, R. C. A., Holmlund, P., Holt, J. W., Jacobel, R. W., Jenkins, A., Jokat, W., Jordan, T., King, E. C., Kohler, J., Krabill, W., Riger-Kusk, M., Langley, K. A., Leitchenkov, G., Leuschen, C., Luyendyk, B. P., Matsuoka, K., Mouginot, J., Nitsche, F. O., Nogi, Y., Nost, O. A., Popov, S. V., Rignot, E., Rippin, D. M., Rivera, A., Roberts, J., Ross, N., Siegert, M. J., Smith, A. M., Steinhage, D., Studinger, M., Sun, B., Tinto, B. K., Welch, B. C., Wilson, D., Young, D. A., Xiangbin, C., and Zirizzotti, A. (2013). Bedmap2: Improved ice bed, surface and thickness datasets for Antarctica. *The Cryosphere*, 7, 375–393, https://doi.org/https://doi.org/10.5194/tc-7-375-2013.

Frieler, K., Clark, P., He, F., Buizert, C., Reese, R., Ligtenberg, S., Van den Broeke, M., Winkelmann, R., and Levermann, A. (2015). Consistent evidence of increasing antarctic accumulation with warming. *Nature Climate Change*, 5, https://doi.org/10.1038/nclimate2574.

Fürst, J. J., Durand, G., Gillet-Chaulet, F., Tavard, L., Rankl, M., Braun, M. H., and Gagliardini, O. (2016). The safety band of Antarctic ice shelves. *Nature Climate Change*, 6, 479–482.

Fyke, J., Sergienko, O., Löfverström, M., Price, S., and Lenaerts, J. T. M. (2018). An overview of interactions and feedbacks between ice sheets and the earth system. *Reviews of Geophysics*, 56(2), 361–408, https://doi.org/https://doi.org/10.1029/2018RG000600. URL https://agupubs.onlinelibrary.wiley.com/doi/abs/10.1029/2018RG000600.

Gagliardini, O., Cohen, D., Råback, P., and Zwinger, T. (2007). Correction to "Finite-element modeling of subglacial cavities and related friction law". *Journal of Geophysical Research*, 112(F4), https://doi.org/10.1029/2007jf000911. URL https://doi.org/10.1029%2F2007jf000911.

Garbe, J., Albrecht, T., Levermann, A., Donges, J., and Winkelmann, R. (2020). The hysteresis of the Antarctic Ice Sheet. *Nature*, 585, 538–544, https://doi.org/https://doi.org/10.1038/s41586-020-2727-5.

Gardner, A. S., Moholdt, G., Scambos, T., Fahnstock, M., Ligtenberg, S., van den Broeke, M., and Nilsson, J. (2018). Increased west antarctic and unchanged east antarctic ice discharge over the last 7 years. *The Cryosphere*, 12(2), 521–547, https://doi.org/10.5194/tc-12-521-2018. URL https://tc.copernicus.org/articles/12/521/2018/.

Gilbert, E. and Kittel, C. (2021). Surface Melt and Runoff on Antarctic Ice Shelves at 1.5°C, 2°C, and 4°C of Future Warming. *Geophysical Research Letters*, 48(8), e2020GL091733, https://doi.org/https://doi.org/10.1029/2020GL091733. URL https://agupubs.onlinelibrary.wiley.com/doi/abs/10.1029/2020GL091733.

Gilford, D. M., Ashe, E. L., DeConto, R. M., Kopp, R. E., Pollard, D., and Rovere, A. (2020). Could the last interglacial constrain projections of future antarctic ice mass loss and sea-level rise? *Journal of Geophysical Research: Earth Surface*, 125(10), e2019JF005418, https://doi.org/https://doi.org/10.1029/2019JF005418. URL https://agupubs.onlinelibrary.wiley.com/doi/abs/10.1029/2019JF005418.

Gladstone, R. M., Warner, R. C., Galton-Fenzi, B. K., Gagliardini, O., Zwinger, T., and Greve, R. (2017). Marine ice sheet model performance depends on basal sliding physics and sub-shelf melting. *The Cryosphere*, 11(1), 319–329, https://doi.org/10.5194/tc-11-319-2017. URL https://tc.copernicus.org/articles/11/319/2017/.

Goelzer, H., Coulon, V., Pattyn, F., de Boer, B., and van de Wal, R. (2020). Brief communication: On calculating the sea-level contribution in marine ice-sheet models. *The Cryosphere*, 14(3), 833–840, https://doi.org/10.5194/tc-14-833-2020.

Goelzer, H., Nowicki, S., Edwards, T., Beckley, M., Abe-Ouchi, A., Aschwanden, A., Calov, R., Gagliardini, O., Gillet-Chaulet, F., Golledge, N. R., Gregory, J., Greve, R., Humbert, A., Huybrechts, P., Kennedy, J. H., Larour, E., Lipscomb, W. H., Le clec'h, S., Lee, V., Morlighem, M., Pattyn, F., Payne, A. J., Rodehacke, C., Rückamp, M., Saito, F., Schlegel, N., Seroussi, H., Shepherd, A., Sun, S., van de Wal, R., and Ziemen, F. A. (2018). Design and results of the ice sheet model initialisation experiments initmip-greenland: an ismip6 intercomparison. *The Cryosphere*, 12(4), 1433–1460, https://doi.org/10.5194/tc-12-1433-2018. URL https://tc.copernicus.org/articles/12/1433/2018/.

Golledge, N., Keller, E., Gomez, N., Naughten, K., Bernales, J., Trusel, L., and Edwards, T. (2019). Global environmental consequences of twenty-first-century ice-sheet melt. *Nature*, 566, 65–72, https://doi.org/10.1038/s41586-019-0889-9.

Golledge, N. R., Kowalewski, D. E., Naish, T. R., Levy, R. H., Fogwill, C. J., and Gasson, E. G. W. (2015). The multi-millennial Antarctic commitment to future sea-level rise. *Nature*, 526(7573), 421–425, https://doi.org/https://doi.org/10.1038/nature15706.

Gomez, N., Latychev, K., and Pollard, D. (2018). A Coupled Ice Sheet–Sea Level Model Incorporating 3D Earth Structure: Variations in Antarctica during the Last Deglacial Retreat. *Journal of Climate*, 31(10), 4041–4054, https://doi.org/https://doi.org/10.1175/JCLI-D-17-0352.1.

Gomez, N., Pollard, D., and Holland, D. (2015). Sea-level feedback lowers projections of future Antarctic Ice-Sheet mass loss. *Nature Communications*, 6, 1–8, https://doi.org/https://doi.org/10.1038/ncomms9798.

Gomez, N., Pollard, D., and Mitrovica, J. X. (2013). A 3-D coupled ice sheet – sea level model applied to Antarctica through the last 40 ky. *Earth and Planetary Science Letters*, 384, 88–99, https://doi.org/https://doi.org/10.1016/j.epsl.2013.09.042.

Gomez, N., Pollard, D., Mitrovica, J. X., Huybers, P., and Clark, P. U. (2012). Evolution of a coupled marine ice sheet–sea level model. *Journal of Geophysical Research: Earth Surface*, 117(F1), https://doi.org/https://doi.org/10.1029/2011JF002128.

Goosse, H., Crespin, E., de Montety, A., Mann, M. E., Renssen, H., and Timmermann, A. (2010). Reconstructing surface temperature changes over the past 600 years using climate model simulations with data assimilation. *Journal of Geophysical Research: Atmospheres*, 115(D9), https://doi.org/https://doi.org/10.1029/2009JD012737. URL https://agupubs.onlinelibrary.wiley.com/doi/abs/10.1029/2009JD012737.

Graham, A. G. C., Wåhlin, A., Hogan, K. A., Nitsche, F. O., Heywood, K. J., Totten, R. L., Smith, J. A., Hillenbrand, C.-D., Simkins, L. M., Anderson, J. B., Wellner, J. S., and Larter, R. D. (2022). Rapid retreat of Thwaites Glacier in the pre-satellite era. *Nature Geoscience*, https://doi.org/10.1038/s41561-022-01019-9. URL https://doi.org/10.1038%2Fs41561-022-01019-9.

Gregory, J., Griffies, S., Hughes, C., Lowe, J., Church, J., Fukimori, I., Gomez, N., Kopp, R., Landerer, F., Le Cozannet, G., Ponte, R., Stammer, D., Tamisiea, M., and Wal, R. (2019). Concepts and terminology for sea level: Mean, variability and change, both local and global. *Surveys in Geophysics*, 40, https://doi.org/10.1007/s10712-019-09525-z.

Gudmundsson, G. H. (2013). Ice-shelf buttressing and the stability of marine ice sheets. *The Cryosphere*, 7(2), 647–655, https://doi.org/10.5194/tc-7-647-2013. URL https://tc.copernicus.org/articles/7/647/2013/.

Gudmundsson, G. H., Paolo, F. S., Adusumilli, S., and Fricker, H. A. (2019). Instantaneous antarctic ice sheet mass loss driven by thinning ice shelves. *Geophysical Research Letters*, 46(23), 13903–13909, https://doi.org/https://doi.org/10.1029/2019GL085027. URL https://agupubs.onlinelibrary.wiley.com/doi/abs/10.1029/2019GL085027.

Han, D. and Wahr, J. (1989). Post-glacial rebound analysis for a rotating Earth. *Washington DC American Geophysical Union Geophysical Monograph Series*, 49, 1–6, https://doi.org/10.1029/GM049p0001.

Haseloff, M. and Sergienko, O. V. (2018). The effect of buttressing on grounding line dynamics. *Journal of Glaciology*, 64(245), 417–431, https://doi.org/https://doi.org/10.1017/jog.2018.30.

Hausfather, Z. and Peters, G. (2020). Emissions – the 'business as usual' story is misleading. *Nature*, 577, 618–620, https://doi.org/10.1038/d41586-020-00177-3.

Hay, C. C., Lau, H. C., Gomez, N., Austermann, J., Powell, E., Mitrovica, J. X., Latychev, K., and Wiens, D. A. (2017). Sea level fingerprints in a region of complex earth structure: The case of WAIS. *Journal of Climate*, 30(6), 1881–1892, https://doi.org/https://doi.org/10.1175/JCLI-D-16-0388.1.

Heeszel, D. S., Wiens, D. A., Anandakrishnan, S., Aster, R. C., Dalziel, I. W., Huerta, A. D., Nyblade, A. A., Wilson, T. J., and Winberry, J. P. (2016). Upper mantle structure of central and West Antarctica from array analysis of Rayleigh wave phase velocities. *Journal of Geophysical Research: Solid Earth*, 121(3), 1758–1775, https://doi.org/https://doi.org/10.1002/2015JB012616.

Hellmer, H. H., Kauker, F., Timmermann, R., Determann, J., and Rae, J. (2012). Twenty-first-century warming of a large Antarctic ice-shelf cavity by a redirected coastal current. *Nature*, 485(7397), 225–228, https://doi.org/10.1038/nature11064. URL https://doi.org/10.1038%2Fnature11064.

Hellmer, H. H., Kauker, F., Timmermann, R., and Hattermann, T. (2017). The Fate of the Southern Weddell Sea Continental Shelf in a Warming Climate. *Journal of Climate*, 30(12), 4337 – 4350, https://doi.org/10.1175/JCLI-D-16-0420.1. URL https://journals.ametsoc.org/view/journals/clim/30/12/jcli-d-16-0420.1.xml.

Herraiz-Borreguero, L. and Garabato, A. C. N. (2022). Poleward shift of circumpolar deep water threatens the east antarctic ice sheet. *Nature Climate Change*, 12(8), 728–734, https://doi.org/10.1038/s41558-022-01424-3. URL https://doi.org/10.1038%2Fs41558-022-01424-3.

Hersbach, H., Bell, B., Berrisford, P., Hirahara, S., Horányi, A., Muñoz-Sabater, J., Nicolas, J., Peubey, C., Radu, R., Schepers, D., Simmons, A., Soci, C., Abdalla, S., Abellan, X., Balsamo, G., Bechtold, P., Biavati, G., Bidlot, J., Bonavita, M., De Chiara, G., Dahlgren, P., Dee, D., Diamantakis, M., Dragani, R., Flemming, J., Forbes, R., Fuentes, M., Geer, A., Haimberger, L., Healy, S., Hogan, R. J., Hólm, E., Janisková, M., Keeley, S., Laloyaux, P., Lopez, P., Lupu, C., Radnoti, G., de Rosnay, P., Rozum, I., Vamborg, F., Villaume, S., and Thépaut, J.-N. (2020). The ERA5 global reanalysis. *Quarterly Journal of the Royal Meteorological Society*, 146(730), 1999–2049, https://doi.org/https://doi.org/10.1002/qj.3803. URL https://rmets.onlinelibrary.wiley.com/doi/abs/10.1002/qj.3803.

Hill, E. A., Rosier, S. H. R., Gudmundsson, G. H., and Collins, M. (2021). Quantifying the potential future contribution to global mean sea level from the filchner–ronne basin, antarctica. *The Cryosphere*, 15(10), 4675–4702, https://doi.org/10.5194/tc-15-4675-2021. URL https://tc.copernicus.org/articles/15/4675/2021/.

Hindmarsh, R. (2018). Chapter 18 - ice sheet and glacier modelling. In J. Menzies and J. J. van der Meer (Eds.), *Past Glacial Environments (Second Edition)*, (pp. 607–663). Elsevier, second edition edition, https://doi.org/https://doi.org/10.1016/B978-0-08-100524-8.00019-1, URL https://www.sciencedirect.com/science/article/pii/B9780081005248000191.

Hindmarsh, R. C. A. (1999). On the numerical computation of temperature in an ice sheet. *J. Glaciol.*, 45(151), 568–574.

Holland, P. R., Bracegirdle, T. J., Dutrieux, P., Jenkins, A., and Steig, E. J. (2019). West antarctic ice loss influenced by internal climate variability and anthropogenic forcing. *Nature Geoscience*, 12(9), 718–724, https://doi.org/10.1038/s41561-019-0420-9. URL https://doi.org/10.1038%2Fs41561-019-0420-9.

Holland, P. R., Jenkins, A., and Holland, D. M. (2008). The response of ice shelf basal melting to variations in ocean temperature. *Journal of Climate*, 21(11).

Hubbard, B., Luckman, A., Ashmore, D. W., Bevan, S., Kulessa, B., Munneke, P. K., Philippe, M., Jansen, D., Booth, A., Sevestre, H., Tison, J.-L., O'Leary, M., and Rutt, I. (2016). Massive subsurface ice formed by refreezing of ice-shelf melt ponds. *Nature Communications*, 7(1), https://doi.org/10.1038/ncomms11897. URL https://doi.org/10.1038%2Fncomms11897.

Huybrechts, P. and de Wolde, J. (1999). The Dynamic Response of the Greenland and Antarctic Ice Sheets to Multiple-Century Climatic Warming. *Journal of Climate*, 12(8), 2169–2188. URL http://www.jstor.org/stable/26244561.

Huybrechts, P., Payne, A., and The EISMINT Intercomparison Group (1996). The EISMINT benchmarks for testing ice–sheet models. *Ann. Glaciol.*, 23, 1–12.

IPCC (2021). *Climate Change 2021: The Physical Science Basis. Contribution of Working Group I to the Sixth Assessment Report of the Intergovernmental Panel on Climate Change*, volume In Press. Cambridge, United Kingdom and New York, NY, USA: Cambridge University Press, https://doi.org/10.1017/9781009157896.

Janssens, I. and Huybrechts, P. (2000). The treatment of meltwater retention in Mass-balance parameterisation of the Greenland Ice Sheet. *Annals of Glaciology*, 31, 133–140, https://doi.org/10.3189/172756400781819941.

Jenkins, A. (1991). A one-dimensional model of ice shelf-ocean interaction. *Journal of Geophysical Research: Oceans*, 96(C11), 20671–20677, https://doi.org/10.1029/91JC01842. URL https://agupubs.onlinelibrary.wiley.com/doi/abs/10.1029/91JC01842.

Jenkins, A., Shoosmith, D., Dutrieux, P., Jacobs, S., Kim, T. W., Lee, S. H., Ha, H. K., and Stammerjohn, S. (2018). West antarctic ice sheet retreat in the amundsen sea driven by decadal oceanic variability. *Nature Geoscience*, 11(10), 733–738, https://doi.org/10.1038/s41561-018-0207-4. URL https://doi.org/10.1038%2Fs41561-018-0207-4.

Joughin, I., Shean, D. E., Smith, B. E., and Floricioiu, D. (2020). A decade of variability on Jakobshavn Isbræ: ocean temperatures pace speed through influence on mélange rigidity. *The Cryosphere*, 14(1), 211–227, https://doi.org/10.5194/tc-14-211-2020. URL https://tc.copernicus.org/articles/14/211/2020/.

Joughin, I., Smith, B. E., and Medley, B. (2014). Marine Ice Sheet Collapse Potentially Under Way for the Thwaites Glacier Basin, West Antarctica. *Science*, 344(6185), 735–738, https://doi.org/https://doi.org/10.1126/science.1249055.

Jourdain, N. C., Asay-Davis, X., Hattermann, T., Straneo, F., Seroussi, H., Little, C. M., and Nowicki, S. (2020). A protocol for calculating basal melt rates in the ISMIP6 Antarctic ice sheet projections. *The Cryosphere*, 14(9), 3111–3134, https://doi.org/10.5194/tc-14-3111-2020. URL https://tc.copernicus.org/articles/14/3111/2020/.

Kachuck, S. B., Martin, D. F., Bassis, J. N., and Price, S. F. (2020). Rapid Viscoelastic Deformation Slows Marine Ice Sheet Instability at Pine Island Glacier. *Geophysical Research Letters*, 47(10), e2019GL086446, https://doi.org/https://doi.org/10.1029/2019GL086446.

Kaufmann, G., Wu, P., and Ivins, E. R. (2005). Lateral viscosity variations beneath Antarctica and their implications on regional rebound motions and seismotectonics. *Journal of Geodynamics*, 39(2), 165–181, https://doi.org/https://doi.org/10.1016/j.jog.2004.08.009.

Kazmierczak, E., Sun, S., Coulon, V., and Pattyn, F. (2022). Subglacial hydrology modulates basal sliding response of the Antarctic ice sheet to climate forcing. *The Cryosphere Discussions*, 2022, 1–24, https://doi.org/10.5194/tc-2022-53. URL https://tc.copernicus.org/preprints/tc-2022-53/.

Khan, S. A., Sasgen, I., Bevis, M., van Dam, T., Bamber, J. L., Wahr, J., Willis, M., Kjær, K. H., Wouters, B., Helm, V., Csatho, B., Fleming, K., Bjørk, A. A., Aschwanden, A., Knudsen, P., and Munneke, P. K. (2016). Geodetic measurements reveal similarities between post–last glacial maximum and present-day mass loss from the greenland ice sheet. *Science Advances*, 2(9), e1600931, https://doi.org/10.1126/sciadv.1600931. URL https://www.science.org/doi/abs/10.1126/sciadv.1600931.

Kim, B.-H., Seo, K.-W., Eom, J., Chen, J., and Wilson, C. (2020). Antarctic ice mass variations from 1979 to 2017 driven by anomalous precipitation accumulation. *Scientific Reports*, 10, https://doi.org/10.1038/s41598-020-77403-5.

Kingslake, J., Ely, J., Das, I., and Bell, R. (2017). Widespread movement of meltwater onto and across Antarctic ice shelves. *Nature*, 544, 349–352, https://doi.org/10.1038/nature22049.

Kingslake, J., Scherer, R., Albrecht, T., Coenen, J., Powell, R., Reese, R., Stansell, N., Tulaczyk, S., Wearing, M., and Whitehouse, P. (2018). Extensive retreat and re-advance of the west antarctic ice sheet during the holocene. *Nature.*, 558(7710), 430–434, https://doi.org/https://doi.org/10.1038/s41586-018-0208-x.

Kirsch, A. (2011). *An Introduction to the Mathematical Theory of Inverse Problems*. Springer New York, https://doi.org/10.1007/978-1-4419-8474-6.

Kittel, C., Amory, C., Agosta, C., Jourdain, N. C., Hofer, S., Delhasse, A., Doutreloup, S., Huot, P.-V., Lang, C., Fichefet, T., and Fettweis, X. (2021). Diverging future surface mass balance between the Antarctic ice shelves and grounded ice sheet. *The Cryosphere*, 15(3), 1215–1236, https://doi.org/10.5194/tc-15-1215-2021. URL https://tc.copernicus.org/articles/15/1215/2021/.

Konrad, H., Sasgen, I., Klemann, V., Thoma, M., Grosfeld, K., and Martinec, Z. (2016). Sensitivity of grounding-line dynamics to viscoelastic deformation of the solid-earth in an idealized scenario. *Polarforschung*, 85(2), 89–99, https://doi.org/https://doi.org/10.2312/polfor.2016.005.

Konrad, H., Sasgen, I., Pollard, D., and Klemann, V. (2015). Potential of the solid-Earth response for limiting long-term West Antarctic Ice Sheet retreat in a warming climate. *Earth and Planetary Science Letters*, 432, 254–264, https://doi.org/https://doi.org/10.1016/j.epsl.2015.10.008.

Konrad, H., Thoma, M., Sasgen, I., Klemann, V., Grosfeld, K., Barbi, D., and Martinec, Z. (2014). The Deformational Response of a Viscoelastic Solid Earth Model Coupled to a Thermomechanical Ice Sheet Model. *Surveys in Geophysics*, 35(6), 1441–1458, https://doi.org/https://doi.org/10.2312/polfor.2016.005.

Kopp, R. E., DeConto, R. M., Bader, D. A., Hay, C. C., Radley, M., Kulp, S., Oppenheimer, M., Pollard, D., and Strauss, B. H. (2017). Implications of ice-shelf hydrofracturing and ice-cliff collapse mechanisms for sea-level projections. *Pnas*, (pp. 1–26).

Kopp, R. E., Kemp, A. C., Bittermann, K., Horton, B. P., Donnelly, J. P., Gehrels, W. R., Hay, C. C., Mitrovica, J. X., Morrow, E. D., and Rahmstorf, S. (2016). Temperature-driven global sea-level variability in the Common Era. *Proceedings of the National Academy of Sciences*, 113(11), E1434–E1441, https://doi.org/10.1073/pnas.1517056113. URL https://www.pnas.org/doi/abs/10.1073/pnas.1517056113.

Kreuzer, M., Reese, R., Huiskamp, W. N., Petri, S., Albrecht, T., Feulner, G., and Winkelmann, R. (2021). Coupling framework (1.0) for the PISM (1.1.4) ice sheet model and the MOM5 (5.1.0) ocean model via the PICO ice shelf cavity model in an Antarctic domain. *Geoscientific Model Development*, 14(6), 3697–3714, https://doi.org/10.5194/gmd-14-3697-2021. URL https://gmd.copernicus.org/articles/14/3697/2021/.

Kuipers Munneke, P., Ligtenberg, S. R., Van Den Broeke, M. R., and Vaughan, D. G. (2014). Firn air depletion as a precursor of Antarctic ice-shelf collapse. *Journal of Glaciology*, 60(220), 205–214, https://doi.org/10.3189/2014JoG13J183.

Lai, C.-Y., Kingslake, J., Wearing, M., Chen, P.-H., Gentine, P., Li, H., Spergel, J., and Wessem, J. M. (2020). Vulnerability of Antarctica's ice shelves to meltwater-driven fracture. *Nature*, 584, 574–578, https://doi.org/10.1038/s41586-020-2627-8.

Larour, E., Seroussi, H., Adhikari, S., Ivins, E., Caron, L., Morlighem, M., and Schlegel, N. (2019). Slowdown in antarctic mass loss from solid earth and sea-level feedbacks. *Science*, 364(6444), https://doi.org/https://doi.org/10.1126/science.aav7908.

Lazeroms, W. M. J., Jenkins, A., Gudmundsson, G. H., and van de Wal, R. S. W. (2018). Modelling present-day basal melt rates for Antarctic ice shelves using a parametrization of buoyant meltwater plumes. *The Cryosphere*, 12(1), 49–70, https://doi.org/10.5194/tc-12-49-2018. URL https://tc.copernicus.org/articles/12/49/2018/.

Lazeroms, W. M. J., Jenkins, A., Rienstra, S. W., and van de Wal, R. S. W. (2019). An Analytical Derivation of Ice-Shelf Basal Melt Based on the Dynamics of Meltwater Plumes. *Journal of Physical Oceanography*, 49(4), 917 – 939, https://doi.org/10.1175/JPO-D-18-0131.1. URL https://journals.ametsoc.org/view/journals/phoc/49/4/jpo-d-18-0131.1.xml.

Le clec'h, S., Charbit, S., Quiquet, A., Fettweis, X., Dumas, C., Kageyama, M., Wyard, C., and Ritz, C. (2019). Assessment of the greenland ice sheet–atmosphere feedbacks for the next century with a regional atmospheric model coupled to an ice sheet model. *The Cryosphere*, 13(1), 373–395, https://doi.org/10.5194/tc-13-373-2019. URL https://tc.copernicus.org/articles/13/373/2019/.

Le Meur, E. and Huybrechts, P. (1996). A comparison of different ways of dealing with isostasy: examples from modelling the Antarctic ice sheet during the last glacial cycle. *Annals of Glaciology*, 23, 309–317, https://doi.org/https://doi.org/10013/epic.12717.d001.

Lenaerts, J. T. M., Medley, B., van den Broeke, M. R., and Wouters, B. (2019). Observing and Modeling Ice Sheet Surface Mass Balance. *Reviews of Geophysics*, 57(2), 376–420, https://doi.org/https://doi.org/10.1029/2018RG000622. URL https://agupubs.onlinelibrary.wiley.com/doi/abs/10.1029/2018RG000622.

Lenaerts, J. T. M., Vizcaíno, M., Fyke, J. G., van Kampenhout, L., and van den Broeke, M. R. (2016). Present-day and future Antarctic ice sheet climate and surface mass balance in the Community Earth System Model. *Climate Dynamics*, 47, 1367–1381.

Lenton, T. M., Held, H., Kriegler, E., Hall, J. W., Lucht, W., Rahmstorf, S., and Schellnhuber, H. J. (2008). Tipping elements in the Earth's climate system. *Proceedings of the National Academy of Sciences*, 105(6), 1786–1793, https://doi.org/10.1073/pnas.0705414105. URL https://www.pnas.org/doi/abs/10.1073/pnas.0705414105.

Levermann, A. and Winkelmann, R. (2016). A simple equation for the melt elevation feedback of ice sheets. *The Cryosphere*, 10(4), 1799–1807, https://doi.org/10.5194/tc-10-1799-2016. URL https://tc.copernicus.org/articles/10/1799/2016/.

Levermann, A., Winkelmann, R., Albrecht, T., Goelzer, H., Golledge, N. R., Greve, R., Huybrechts, P., Jordan, J., Leguy, G., Martin, D., Morlighem, M., Pattyn, F., Pollard, D., Quiquet, A., Rodehacke, C., Seroussi, H., Sutter, J., Zhang, T., Van Breedam, J., Calov, R., DeConto, R., Dumas, C., Garbe, J., Gudmundsson, G. H., Hoffman, M. J., Humbert, A., Kleiner, T., Lipscomb, W. H., Meinshausen, M., Ng, E., Nowicki, S. M. J., Perego, M., Price, S. F., Saito, F., Schlegel, N.-J., Sun, S., and van de Wal, R. S. W. (2020). Projecting Antarctica's contribution to future sea level rise from basal ice shelf melt using linear response functions of 16 ice sheet models (LARMIP-2). *Earth System Dynamics*, 11(1), 35–76, https://doi.org/10.5194/esd-11-35-2020. URL https://esd.copernicus.org/articles/11/35/2020/.

Lewis, E. L. and Perkin, R. G. (1986). Ice pumps and their rates. *Journal of Geophysical Research*, 91, 11756–11762.

Lhermitte, S., Sun, S., Shuman, C., Wouters, B., Pattyn, F., Wuite, J., Berthier, E., and Nagler, T. (2020). Damage accelerates ice shelf instability and mass loss in Amundsen Sea Embayment. *Proceedings of the National Academy of Sciences*, 117(40), 24735–24741, https://doi.org/10.1073/pnas.1912890117. URL https://www.pnas.org/doi/abs/10.1073/pnas.1912890117.

Lipscomb, W. H., Leguy, G. R., Jourdain, N. C., Asay-Davis, X., Seroussi, H., and Nowicki, S. (2021). ISMIP6-based projections of ocean-forced Antarctic Ice Sheet evolution using the Community Ice Sheet Model. *The Cryosphere*, 15(2), 633–661, https://doi.org/10.5194/tc-15-633-2021. URL https://tc.copernicus.org/articles/15/633/2021/.

Little, C. M. and Urban, N. M. (2016). CMIP5 temperature biases and 21st century warming around the Antarctic coast. *Annals of Glaciology*, 57(73), 69–78, https://doi.org/10.1017/aog.2016.25.

Liu, Y., Moore, J. C., Cheng, X., Gladstone, R. M., Bassis, J. N., Liu, H., Wen, J., and Hui, F. (2015). Ocean-driven thinning enhances iceberg calving and retreat of antarctic ice shelves. *Proceedings of the National Academy of Sciences*, 112(11), 3263–3268, https://doi.org/10.1073/pnas.1415137112. URL https://www.pnas.org/doi/abs/10.1073/pnas.1415137112.

Lliboutry, L. (1979). A critical review of analytical approximate solutions for steady state velocities and temperatures in cold ice-sheets. *Zeitschrift für Gletscherkunde und Glazialgeologie*, 35(2), 135–148.

Lloyd, A. J., Wiens, D. A., Zhu, H., Tromp, J., Nyblade, A. A., Aster, R. C., Hansen, S. E., Dalziel, I. W. D., Wilson, T., Ivins, E. R., and O'Donnell, J. P. (2020). Seismic Structure of the Antarctic Upper Mantle Imaged with Adjoint Tomography. *Journal of Geophysical Research: Solid Earth*, 125(3), https://doi.org/https://doi.org/10.1029/2019JB017823.

Loeppky, J. L., Sacks, J., and Welch, W. J. (2009). Choosing the Sample Size of a Computer Experiment: A Practical Guide. *Technometrics*, 51(4), 366–376, https://doi.org/10.1198/TECH.2009.08040. URL https://doi.org/10.1198/TECH.2009.08040.

Lowry, D., Krapp, M., Golledge, N., and Alevropoulos-Borrill, A. (2021). The influence of emissions scenarios on future Antarctic ice loss is unlikely to emerge this century. *Communications Earth & Environment*, 2, https://doi.org/10.1038/s43247-021-00289-2.

Lowry, D. P., Golledge, N. R., Bertler, N. A., Jones, R. S., McKay, R., and Stutz, J. (2020). Geologic controls on ice sheet sensitivity to deglacial climate forcing in the ross embayment, antarctica. *Quaternary Science Advances*, 1, 100002, https://doi.org/https://doi.org/10.1016/j.qsa.2020.100002. URL https://www.sciencedirect.com/science/article/pii/S2666033420300022.

Ma, Y., Gagliardini, O., Ritz, C., Gillet-Chaulet, F., Durand, G., and Montagnat, M. (2010). Enhancement factors for grounded ice and ice shelves inferred from an anisotropic ice-flow model. *Journal of Glaciology*, 56, 805–812, https://doi.org/10.3189/002214310794457209.

Magand, O., Frezzotti, M., Pourchet, M., Stenni, B., Genoni, L., and Fily, M. (2004). Climate variability along latitudinal and longitudinal transects in East Antarctica. *Annals of Glaciology*, 39, 351–358, https://doi.org/10.3189/172756404781813961.

Maris, M. N. A., de Boer, B., Ligtenberg, S. R. M., Crucifix, M., van de Berg, W. J., and Oerlemans, J. (2014). Modelling the evolution of the Antarctic ice sheet since the last interglacial. *The Cryosphere*, 8, 1347–1360, https://doi.org/https://doi.org/10.5194/tc-8-1347-2014.

Martin, M. A., Winkelmann, R., Haseloff, M., Albrecht, T., Bueler, E., Khroulev, C., and Levermann, A. (2011). The potsdam parallel ice sheet model (pism-pik) part 2: Dynamic equilibrium simulation of the antarctic ice sheet. *The Cryosphere*, 5(3), 727–740, https://doi.org/10.5194/tc-5-727-2011.

Martin, P. J. and Peel, D. A. (1978). The Spatial Distribution of 10 m Temperatures in the Antarctic Peninsula. *Journal of Glaciology*, 20(83), 311–317, https://doi.org/10.3189/S0022143000013861.

Martín-Español, A., Zammit-Mangion, A., Clarke, P. J., Flament, T., Helm, V., King, M. A., Luthcke, S. B., Petrie, E., Rémy, F., Schön, N., Wouters, B., and Bamber, J. L. (2016). Spatial and temporal Antarctic Ice Sheet mass trends, glacio-isostatic adjustment, and surface processes from a joint inversion of satellite altimeter, gravity, and GPS data. *Journal of Geophysical Research: Earth Surface*, 121(2), 182–200, https://doi.org/https://doi.org/10.1002/2015JF003550. URL https://agupubs.onlinelibrary.wiley.com/doi/abs/10.1002/2015JF003550.

Matsuoka, K., Hindmarsh, R. C., Moholdt, G., Bentley, M. J., Pritchard, H. D., Brown, J., Conway, H., Drews, R., Durand, G., Goldberg, D., Hattermann, T., Kingslake, J., Lenaerts, J. T., Martín, C., Mulvaney, R., Nicholls, K. W., Pattyn, F., Ross, N., Scambos, T., and Whitehouse, P. L. (2015). Antarctic ice rises and rumples: Their properties and significance for ice-sheet dynamics and evolution. *Earth-Science Reviews*, 150, 724–745, https://doi.org/https://doi.org/10.1016/j.earscirev.2015.09.004.

McKay, D. I. A., Staal, A., Abrams, J. F., Winkelmann, R., Sakschewski, B., Loriani, S., Fetzer, I., Cornell, S. E., Rockström, J., and Lenton, T. M. (2022). Exceeding 1.5°C global warming could trigger multiple climate tipping points. *Science*, 377(6611), https://doi.org/10.1126/science.abn7950. URL https://doi.org/10.1126%2Fscience.abn7950.

Medley, B. and Thomas, E. (2019). Increased snowfall over the antarctic ice sheet mitigated twentieth-century sea-level rise. *Nature Climate Change*, 9, https://doi.org/10.1038/s41558-018-0356-x.

Meehl, G. A., Senior, C. A., Eyring, V., Flato, G., Lamarque, J.-F., Stouffer, R. J., Taylor, K. E., and Schlund, M. (2020). Context for interpreting equilibrium climate sensitivity and transient climate response from the CMIP6 Earth system models. *Science Advances*, 6(26), eaba1981, https://doi.org/10.1126/sciadv.aba1981. URL https://www.science.org/doi/abs/10.1126/sciadv.aba1981.

Mengel, M. and Levermann, A. (2014). Ice plug prevents irreversible discharge from East Antarctica. *Nature Climate Change*, 4(6), 451–455, https://doi.org/10.1038/nclimate2226. URL https://doi.org/10.1038%2Fnclimate2226.

Mercer, J. H. (1978). West Antarctic ice sheet and CO2 greenhouse effect: a threat of disaster. *Nature*, 271, 321–325, https://doi.org/https://doi.org/10.1038/271321a0.

Mikkelsen, T. B., Grinsted, A., and Ditlevsen, P. (2018). Influence of temperature fluctuations on equilibrium
ice sheet volume. *The Cryosphere*, 12(1), 39–47, https://doi.org/10.5194/tc-12-39-2018. URL https://tc.copernicus.org/articles/12/39/2018/.

Milillo, P., Rignot, E., Rizzoli, P., Scheuchl, B., Mouginot, J., Bueso-Bello, J. L., Prats-Iraola, P., and Dini, L. (2022). Rapid glacier retreat rates observed in west antarctica. *Nature Geoscience*, 15(1), 48–53, https://doi.org/10.1038/s41561-021-00877-z. URL https://doi.org/10.1038%2Fs41561-021-00877-z.

Milne, Glenn, A. and Mitrovica, Jerry, X. (1998). Postglacial sea-level change on a rotating Earth. *Geophysical Journal International*, 133(1), 1–19, https://doi.org/https://doi.org/10.1046/j.1365-246X.1998.1331455.x.

Minchew, B. and Joughin, I. (2020). Toward a universal glacier slip law. *Science*, 368(6486), 29–30, https://doi.org/10.1126/science.abb3566. URL https://doi.org/10.1126%2Fscience.abb3566.

Mitrovica, J. X., Gomez, N., Morrow, E., Hay, C., Latychev, K., and Tamisiea, M. E. (2011). On the robustness of predictions of sea level fingerprints. *Geophysical Journal International*, 187(2), 729–742, https://doi.org/10.1111/j.1365-246x.2011.05090.x. URL https://doi.org/10.1111%2Fj.1365-246x.2011.05090.x.

Mitrovica, J. X., Tamisiea, M. E., Davis, J. L., and Milne, G. A. (2001). Recent mass balance of polar ice sheets inferred from patterns of global sea-level change. *Nature*, 409, 1026–1029, https://doi.org/https://doi.org/10.1038/35059054.

Moon, T., Scambos, T., Abdalati, W., Ahlstrøm, A. P., Bindschadler, R., Gambill, J., Heimbach, P., Hock, R., Langley, K., Miller, I., and Truffer, M. (2020). Ending a sea of confusion: Insights and opportunities in sea-level change communication. *Environment: Science and Policy for Sustainable Development*, 62(5), 4–15, https://doi.org/10.1080/00139157.2020.1791627. URL https://doi.org/10.1080/00139157.2020.1791627.

Morelli, A. and Danesi, S. (2004). Seismological imaging of the Antarctic continental lithosphere: A review. *Global and Planetary Change*, 42(1-4), 155–165, https://doi.org/https://doi.org/10.1016/j.gloplacha.2003.12.005.

Morlighem, M., Rignot, E., Binder, T., Blankenship, D., Drews, R., Eagles, G., Eisen, O., Ferraccioli, F., Forsberg, R., Fretwell, P., Goel, V., Greenbaum, J. S., Gudmundsson, H., Guo, J., Helm, V., Hofstede, C., Howat, I., Humbert, A., Jokat, W., Karlsson, N. B., Lee, W. S., Matsuoka, K., Millan, R., Mouginot, J., Paden, J., Pattyn, F., Roberts, J., Rosier, S., Ruppel, A., Seroussi, H., and Smith, E. C. (2020). Deep glacial troughs and stabilizing ridges unveiled beneath the margins of the Antarctic ice sheet. *Nature Geoscience*, https://doi.org/https://doi.org/10.1038/s41561-019-0510-8.

Morlighem, M., Seroussi, H., Larour, E., and Rignot, E. (2013). Inversion of basal friction in Antarctica using exact and incomplete adjoints of a higher-order model. *Journal of Geophysical Research: Earth Surface*, 118(3), 1746–1753, https://doi.org/10.1002/jgrf.20125. URL https://doi.org/10.1002%2Fjgrf.20125.

Mottram, R., Hansen, N., Kittel, C., van Wessem, J. M., Agosta, C., Amory, C., Boberg, F., van de Berg, W. J., Fettweis, X., Gossart, A., van Lipzig, N. P. M., van Meijgaard, E., Orr, A., Phillips, T., Webster, S., Simonsen, S. B., and Souverijns, N. (2021). What is the surface mass balance of Antarctica? An intercomparison of regional climate model estimates. *The Cryosphere*, 15(8), 3751–3784, https://doi.org/10.5194/tc-15-3751-2021. URL https://tc.copernicus.org/articles/15/3751/2021/.

Munneke, K., Picard, G., Van den Broeke, M., Lenaerts, J., and Meijgaard, E. (2012). Insignificant change in Antarctic snowmelt volume since 1979. *Geophys. Res. Lett*, 39, https://doi.org/10.1029/2011GL050207.

Naughten, K., Meissner, K., Galton-Fenzi, B., England, M., Timmermann, R., and Hellmer, H. (2018). Future Projections of Antarctic Ice Shelf Melting Based on CMIP5 Scenarios. *Journal of Climate*, 31, https://doi.org/10.1175/JCLI-D-17-0854.1.

Nias, I. J., Cornford, S. L., Edwards, T. L., Gourmelen, N., and Payne, A. J. (2019). Assessing uncertainty in the dynamical ice response to ocean warming in the amundsen sea embayment, west antarctica. *Geophysical Research Letters*, 46(20), 11253–11260, https://doi.org/https://doi.org/10.1029/2019GL084941. URL https://agupubs.onlinelibrary.wiley.com/doi/abs/10.1029/2019GL084941.

Nicholls, R. J., Hinkel, J., Lincke, D., and van der Pol, T. (2019). Global Investment Costs for Coastal Defense Through the 21st Century. *World Bank Policy Research Working Paper Series*.

Nield, G. A., Barletta, V. R., Bordoni, A., King, M. A., Whitehouse, P. L., Clarke, P. J., Domack, E., Scambos, T. A., and Berthier, E. (2014). Rapid bedrock uplift in the Antarctic Peninsula explained by viscoelastic response to recent ice unloading. *Earth and Planetary Science Letters*, 397, 32–41, https://doi.org/https://doi.org/10.1016/j.epsl.2014.04.019.

Nield, G. A., Whitehouse, P. L., Wal, W. V. D., Blank, B., Donnell, P. O., and Stuart, G. W. (2018). The impact of lateral variations in lithospheric thickness on glacial isostatic adjustment in West Antarctica. *Geophysical Journal International*, 214, 811–824, https://doi.org/https://doi.org/10.1093/gji/ggy158.

Nilsson, J., Gardner, A. S., and Paolo, F. S. (2022). Elevation change of the antarctic ice sheet: 1985 to 2020. *Earth System Science Data*, 14(8), 3573–3598, https://doi.org/10.5194/essd-14-3573-2022. URL https://doi.org/10.5194%2Fessd-14-3573-2022.

Nowicki, S., Goelzer, H., Seroussi, H., Payne, A. J., Lipscomb, W. H., Abe-Ouchi, A., Agosta, C., Alexander, P., Asay-Davis, X. S., Barthel, A., Bracegirdle, T. J., Cullather, R., Felikson, D., Fettweis, X., Gregory, J. M., Hattermann, T., Jourdain, N. C., Kuipers Munneke, P., Larour, E., Little, C. M., Morlighem, M., Nias, I., Shepherd, A., Simon, E., Slater, D., Smith, R. S., Straneo, F., Trusel, L. D., van den Broeke, M. R., and van de Wal, R. (2020). Experimental protocol for sea level projections from ISMIP6 stand-alone ice sheet models. *The Cryosphere*, 14(7), 2331–2368, https://doi.org/10.5194/tc-14-2331-2020. URL https://tc.copernicus.org/articles/14/2331/2020/.

Nowicki, S. M. J., Payne, A., Larour, E., Seroussi, H., Goelzer, H., Lipscomb, W., Gregory, J., Abe-Ouchi, A., and Shepherd, A. (2016). Ice sheet model intercomparison project (ismip6) contribution to cmip6. *Geoscientific Model Development*, 9(12), 4521–4545, https://doi.org/10.5194/gmd-9-4521-2016. URL https://gmd.copernicus.org/articles/9/4521/2016/.

Oerlemans, J. (1981). Some basic experiments with a vertically-integrated ice sheet model. *Tellus*, 33(1), 1–11, https://doi.org/10.1111/j.2153-3490.1981.tb01726.x. URL https://doi.org/10.1111%2Fj.2153-3490.1981.tb01726.x.

Olbers, D. and Hellmer, H. (2010). A box model of circulation and melting in ice shelf caverns. *Ocean Dynamics*, 60(1), 141–153, https://doi.org/10.1007/s10236-009-0252-z.

Oppenheimer, M., Glavovic, B., Hinkel, J., Roderik, v., Magnan, A., Abd-Elgawad, A., Rongshu, C., Cifuentes, M., Robert, D., Ghosh, T., Hay, J., Ben, M., Meyssignac, B., Sebesvari, Z., A.J., S., Dangendorf, S., and Frederikse, T. (2019). *Sea Level Rise and Implications for Low Lying Islands, Coasts and Communities*, In *The Ocean and Cryosphere in a Changing Climate: Special Report of the Intergovernmental Panel on Climate Change*. Cambridge University Press.

Oreskes, N., Shrader-Frechette, K., and Belitz, K. (1994). Verification, Validation, and Confirmation of Numerical Models in the Earth Sciences. *Science*, 263(5147), 641–646, https://doi.org/10.1126/science.263.5147.641. URL https://doi.org/10.1126%2Fscience.263.5147.641.

O'Hagan, A. (2006). Bayesian analysis of computer code outputs: A tutorial. *Reliability Engineering & System Safety*, 91(10), 1290–1300, https://doi.org/https://doi.org/10.1016/j.ress.2005.11.025. URL https://www.sciencedirect.com/science/article/pii/S0951832005002383.

Pan, L., Powell, E. M., Latychev, K., Mitrovica, J. X., Creveling, J. R., Gomez, N., Hoggard, M. J., and Clark, P. U. (2021). Rapid postglacial rebound amplifies global sea level rise following west antarctic ice sheet collapse. *Science Advances*, 7(18), https://doi.org/10.1126/sciadv.abf7787. URL https://doi.org/10.1126/sciadv.abf7787.

Paolo, F., Padman, L., Fricker, H., Adusumilli, S., Howard, S., and Siegfried, M. (2018). Response of Pacific-sector Antarctic ice shelves to the El Niño/Southern Oscillation. *Nature Geoscience*, 1, https://doi.org/10.1038/s41561-017-0033-0.

Paolo, F. S., Fricker, H. A., and Padman, L. (2015). Volume loss from Antarctic ice shelves is accelerating. *Science*, 348(6232), 327–331, https://doi.org/10.1126/science.aaa0940. URL https://www.science.org/doi/abs/10.1126/science.aaa0940.

Pappa, F., Ebbing, J., Ferraccioli, F., and van der Wal, W. (2019). Modeling Satellite Gravity Gradient Data to Derive Density, Temperature, and Viscosity Structure of the Antarctic Lithosphere. *Journal of Geophysical Research: Solid Earth*, 124(11), 12053–12076, https://doi.org/https://doi.org/10.1029/2019JB017997.

Parizek, B. R., Christianson, K., Anandakrishnan, S., Alley, R. B., Walker, R. T., Edwards, R. A., Wolfe, D. S., Bertini, G. T., Rinehart, S. K., Bindschadler, R. A., and Nowicki, S. M. J. (2013). Dynamic (in)stability of thwaites glacier, west antarctica. *Journal of Geophysical Research: Earth Surface*, 118(2), 638–655, https://doi.org/https://doi.org/10.1002/jgrf.20044. URL https://agupubs.onlinelibrary.wiley.com/doi/abs/10.1002/jgrf.20044.

Pattyn, F. (2017). Sea-level response to melting of Antarctic ice shelves on multi-centennial timescales with the fast Elementary Thermomechanical Ice Sheet model (f.ETISh v1.0). *Cryosphere*, 11, 1–28, https://doi.org/https://doi.org/10.5194/tc-11-1-2017.

Pattyn, F. (2018). The paradigm shift in Antarctic ice sheet modelling. *Nature Communications*, 9, https://doi.org/10.1038/s41467-018-05003-z.

Pattyn, F., Favier, L., Sun, S., and Durand, G. (2017). Progress in Numerical Modeling of Antarctic Ice-Sheet Dynamics. *Current Climate Change Reports*, 3(3), 174–184, https://doi.org/https://doi.org/10.1007/s40641-017-0069-7.

Pattyn, F. and Morlighem, M. (2020). The uncertain future of the Antarctic Ice Sheet. *Science*, 367(6484), 1331–1335, https://doi.org/10.1126/science.aaz5487. URL https://www.science.org/doi/abs/10.1126/science.aaz5487.

Pattyn, F., Perichon, L., Durand, G., Favier, L., Gagliardini, O., Hindmarsh, R. C., Zwinger, T., Albrecht, T., Cornford, S., Docquier, D., and et al. (2013). Grounding-line migration in plan-view marine ice-sheet models: results of the ice2sea MISMIP3d intercomparison. *Journal of Glaciology*, 59(215), 410–422, https://doi.org/10.3189/2013JoG12J129.

Pattyn, F., Ritz, C., Hanna, E., Asay-Davis, X., DeConto, R., Durand, G., Favier, L., Fettweis, X., Goelzer, H., Golledge, N., Munneke, P., Lenaerts, J., Nowicki, S., Payne, A., Robinson, A., Seroussi, H., Trusel, L., and Van den Broeke, M. (2018). The Greenland and Antarctic ice sheets under 1.5 °C global warming. *Nature Climate Change*, 8, https://doi.org/10.1038/s41558-018-0305-8.

Pattyn, F., Schoof, C., Perichon, L., Hindmarsh, R. C. A., Bueler, E., de Fleurian, B., Durand, G., Gagliardini, O., Gladstone, R., Goldberg, D., Gudmundsson, G. H., Huybrechts, P., Lee, V., Nick, F. M., Payne, A. J., Pollard, D., Rybak, O., Saito, F., and Vieli, A. (2012). Results of the marine ice sheet model intercomparison project, mismip. *The Cryosphere*, 6(3), 573–588, https://doi.org/10.5194/tc-6-573-2012. URL https://tc.copernicus.org/articles/6/573/2012/.

Paxman, G. J. G., Austermann, J., and Hollyday, A. (2022). Total isostatic response to the complete unloading of the greenland and antarctic ice sheets. *Scientific Reports*, 12(1), https://doi.org/10.1038/s41598-022-15440-y. URL https://doi.org/10.1038%2Fs41598-022-15440-y.

Payne, A., Nowicki, S., Abe-Ouchi, A., Agosta, C., Alexander, P., Albrecht, T., Asay-Davis, X., Aschwanden, A., Barthel, A., Bracegirdle, T., Calov, R., Chambers, C., Choi, Y., Cullather, R., Cuzzone, J., Dumas, C., Edwards, T., Felikson, D., Fettweis, X., and Zwinger, T. (2021). Future sea level change under cmip5 and cmip6 scenarios from the greenland and antarctic ice sheets. *Geophysical Research Letters*, 48, https://doi.org/10.1029/2020GL091741.

Payne, A. J., Huybrechts, P., Abe-Ouchi, A., Calov, R., Fastook, J. L., Greve, R., Marshall, S. J., Marsiat, I., Ritz, C., Tarasov, L., and Thomassen, M. (2000). Results from the EISMINT model intercomparsion: the effects of thermomechanical coupling. *J. Glaciol.*, 46(153), 227–238.

Pelle, T., Morlighem, M., and Bondzio, J. H. (2019). Brief communication: PICOP, a new ocean melt parameterization under ice shelves combining PICO and a plume model. *The Cryosphere*, 13(3), 1043–1049, https://doi.org/10.5194/tc-13-1043-2019. URL https://tc.copernicus.org/articles/13/1043/2019/.

Pelletier, C., Fichefet, T., Goosse, H., Haubner, K., Helsen, S., Huot, P.-V., Kittel, C., Klein, F., Le clec'h, S., van Lipzig, N. P. M., Marchi, S., Massonnet, F., Mathiot, P., Moravveji, E., Moreno-Chamarro, E., Ortega, P., Pattyn, F., Souverijns, N., Van Achter, G., Vanden Broucke, S., Vanhulle, A., Verfaillie, D., and Zipf, L. (2022). PARASO, a circum-Antarctic fully coupled ice-sheet–ocean–sea-ice–atmosphere–land model involving f.ETISh1.7, NEMO3.6, LIM3.6, COSMO5.0 and CLM4.5. *Geoscientific Model Development*, 15(2), 553–594, https://doi.org/10.5194/gmd-15-553-2022. URL https://gmd.copernicus.org/articles/15/553/2022/.

Pollard, D., Chang, W., Haran, M., Applegate, P., and DeConto, R. (2016). Large ensemble modeling of the last deglacial retreat of the West Antarctic Ice Sheet: Comparison of simple and advanced statistical techniques. *Geoscientific Model Development*, 9(5), 1697–1723, https://doi.org/https://doi.org/10.5194/gmd-9-1697-2016.

Pollard, D. and DeConto, R. M. (2009). Modelling West Antarctic ice sheet growth and collapse through the past five million years. *Nature*, 458(7236), 329–332, https://doi.org/https://doi.org/10.1038/nature07809.

Pollard, D. and DeConto, R. M. (2012a). A simple inverse method for the distribution of basal sliding coefficients under ice sheets , applied to Antarctica. *The Cryosphere*, 6, 953–971, https://doi.org/https://doi.org/10.5194/tc-6-953-2012.

Pollard, D. and DeConto, R. M. (2012b). Description of a hybrid ice sheet-shelf model , and application to Antarctica. *Geoscientific Model Development*, 5, 1273–1295, https://doi.org/https://doi.org/10.5194/gmd-5-1273-2012.

Pollard, D. and DeConto, R. M. (2020). Improvements in one-dimensional grounding-line parameterizations in an ice-sheet model with lateral variations (PSUICE3D v2.1). *Geoscientific Model Development*, 13(12), 6481–6500, https://doi.org/https://doi.org/10.5194/gmd-13-6481-2020.

Pollard, D., DeConto, R. M., and Alley, R. B. (2015). Potential Antarctic Ice Sheet retreat driven by hydrofracturing and ice cliff failure. *Earth and Planetary Science Letters*, 412, 112–121, https://doi.org/https://doi.org/10.1016/j.epsl.2014.12.035.

Pollard, D., Gomez, N., and Deconto, R. M. (2017). Variations of the antarctic ice sheet in a coupled ice sheet-earth-sea level model: Sensitivity to viscoelastic earth properties. *Journal of Geophysical Research: Earth Surface*, 122(11), 2124–2138, https://doi.org/https://doi.org/10.1002/2017JF004371.

Previdi, M. and Polvani, L. M. (2016). Anthropogenic impact on antarctic surface mass balance, currently masked by natural variability, to emerge by mid-century. *Environmental Research Letters*, 11(9), 094001, https://doi.org/10.1088/1748-9326/11/9/094001. URL https://doi.org/10.1088/1748-9326/11/9/094001.

Quiquet, A., Dumas, C., Ritz, C., Peyaud, V., and Roche, D. M. (2018). The GRISLI ice sheet model (version 2.0): calibration and validation for multi-millennial changes of the antarctic ice sheet. *Geoscientific Model Development*, 11(12), 5003–5025, https://doi.org/https://doi.org/10.5194/gmd-11-5003-2018.

Raftery, A. E., Zimmer, A. S., Frierson, D. M. W., Startz, R., and Liu, P. (2017). Less Than 2 °C Warming by 2100 Unlikely. *Nature climate change*, 7, 637 – 641.

Reeh, N. (1989). Parameterization of melt rate and surface temperature on the greenland ice sheet. *Polarforschung*, 59(3), 113–128.

Reeh, N. (1991). Parameterization of melt rate and surface temperature in the greenland ice sheet. *Polarforschung.*, 59(3).

Reese, R., Albrecht, T., Mengel, M., Asay-Davis, X., and Winkelmann, R. (2018a). Antarctic sub-shelf melt rates via PICO. *The Cryosphere*, 12(6), 1969–1985, https://doi.org/https://doi.org/10.5194/tc-12-1969-2018. URL https://tc.copernicus.org/articles/12/1969/2018/.

Reese, R., Garbe, J., Hill, E. A., Urruty, B., Naughten, K. A., Gagliardini, O., Durand, G., Gillet-Chaulet, F., Chandler, D., Langebroek, P. M., and Winkelmann, R. (2022). The stability of present-day antarctic grounding lines – part b: Possible commitment of regional collapse under current climate. *The Cryosphere Discussions*, 2022, 1–33, https://doi.org/10.5194/tc-2022-105. URL https://tc.copernicus.org/preprints/tc-2022-105/.

Reese, R., Gudmundsson, G. H., Levermann, A., and Winkelmann, R. (2018b). The far reach of ice-shelf thinning in Antarctica. *Nature Climate Change*, 8, 53–57.

Reese, R., Levermann, A., Albrecht, T., Seroussi, H., and Winkelmann, R. (2020). The role of history and strength of the oceanic forcing in sea level projections from antarctica with the parallel ice sheet model. *The Cryosphere*, 14(9), 3097–3110, https://doi.org/10.5194/tc-14-3097-2020. URL https://tc.copernicus.org/articles/14/3097/2020/.

Reijmer, C. H., van den Broeke, M. R., Fettweis, X., Ettema, J., and Stap, L. B. (2012). Refreezing on the greenland ice sheet: a comparison of parameterizations. *The Cryosphere*, 6(4), 743–762, https://doi.org/10.5194/tc-6-743-2012. URL https://tc.copernicus.org/articles/6/743/2012/.

Rignot, E., Jacobs, S., Mouginot, J., and Scheuchl, B. (2013). Ice-Shelf Melting Around Antarctica. *Science*, 341(6143), 266–270, https://doi.org/10.1126/science.1235798. URL https://www.science.org/doi/abs/10.1126/science.1235798.

Rignot, E., Mouginot, J., Morlighem, M., Seroussi, H., and Scheuchl, B. (2014). Widespread, rapid grounding line retreat of pine island, thwaites, smith, and kohler glaciers, west antarctica, from 1992 to 2011. *Geophysical Research Letters*, 41(10), 3502–3509, https://doi.org/https://doi.org/10.1002/2014GL060140. URL https://agupubs.onlinelibrary.wiley.com/doi/abs/10.1002/2014GL060140.

Rignot, E., Mouginot, J., and Scheuchl, B. (2011). Ice flow of the antarctic ice sheet. *Science*, 333(6048), 1427–1430.

Rignot, E., Mouginot, J., Scheuchl, B., van den Broeke, M., van Wessem, M. J., and Morlighem, M. (2019). Four decades of Antarctic Ice Sheet mass balance from 1979–2017. *Proceedings of the National Academy of Sciences*, 116(4), 1095–1103, https://doi.org/https://doi.org/10.1073/pnas.1812883116.

Rintoul, S. R., Silvano, A., Pena-Molino, B., van Wijk, E., Rosenberg, M., Greenbaum, J. S., and Blankenship, D. D. (2016). Ocean heat drives rapid basal melt of the totten ice shelf. *Science Advances*, 2(12), https://doi.org/10.1126/sciadv.1601610. URL https://doi.org/10.1126%2Fsciadv.1601610.

Ritsema, J., Deuss, A., van Heijst, H. J., and Woodhouse, J. H. (2011). S40RTS: a degree-40 shear-velocity model for the mantle from new Rayleigh wave dispersion, teleseismic traveltime and normal-mode splitting function measurements. *Geophysical Journal International*, 184(3), 1223–1236, https://doi.org/10.1111/j.1365-246X.2010.04884.x. URL https://doi.org/10.1111/j.1365-246X.2010.04884.x.

Ritz, C. (1992). *Un Modèle Thermo-Mèchanique d'Evolution pour le Bassin Glaciaire Antarctique Vostok-Glacier Byrd: Sensibilité aux Valeurs des Paramètres Mal Connus*. PhD Thesis, Univ. J. Fourier.

Ritz, C., Edwards, T. L., Durand, G., Payne, A. J., Peyaud, V., and Hindmarsh, R. C. A. (2015). Potential sea-level rise from Antarctic ice-sheet instability constrained by observations. *Nature*, 528(7580), 115–118, https://doi.org/https://doi.org/10.1038/nature16147.

Ritzwoller, M. H., Shapiro, N. M., Levshin, A. L., and Leahy, G. M. (2001). Crustal and upper mantle structure beneath Antarctica and surrounding oceans. *Journal of Geophysical Research: Solid Earth*, 106(B12), 30645–30670, https://doi.org/https://doi.org/10.1029/2001JB000179.

Robel, A. A., Seroussi, H., and Roe, G. H. (2019). Marine ice sheet instability amplifies and skews uncertainty in projections of future sea-level rise. *Proceedings of the National Academy of Sciences*, 116(30), 14887–14892, https://doi.org/10.1073/pnas.1904822116. URL https://www.pnas.org/doi/abs/10.1073/pnas.1904822116.

Robinson, A., Calov, R., and Ganopolski, A. (2012). Multistability and critical thresholds of the Greenland Ice Sheet. *Nature Climate Change*, 2, 429–432, https://doi.org/10.1038/nclimate1449.

Rodehacke, C. B., Pfeiffer, M., Semmler, T., Gurses, O., and Kleiner, T. (2020). Future sea level contribution from Antarctica inferred from CMIP5 model forcing and its dependence on precipitation ansatz. *Earth System Dynamics*, 11(4), 1153–1194, https://doi.org/10.5194/esd-11-1153-2020. URL https://esd.copernicus.org/articles/11/1153/2020/.

Roussel, M.-L., Lemonnier, F., Genthon, C., and Krinner, G. (2020). Brief communication: Evaluating Antarctic precipitation in ERA5 and CMIP6 against CloudSat observations. *The Cryosphere*, 14(8), 2715–2727, https://doi.org/10.5194/tc-14-2715-2020. URL https://tc.copernicus.org/articles/14/2715/2020/.

Sadai, S., Condron, A., DeConto, R., and Pollard, D. (2020). Future climate response to Antarctic Ice Sheet melt caused by anthropogenic warming. *Science Advances*, 6(39), eaaz1169, https://doi.org/10.1126/sciadv.aaz1169. URL https://www.science.org/doi/abs/10.1126/sciadv.aaz1169.

Scambos, T., Bohlander, J., Shuman, C., and Skvarca, P. (2004). Glacier Acceleration and Thinning after Ice Shelf Collapse in the Larsen B Embayment, Antarctica. *Geophysical Research Letters*, 31, https://doi.org/10.1029/2004GL020670.

Scambos, T., Hulbe, C., Fahnestock, M., and Bohlander, J. (2000). The link between climate warming and ice shelf break-ups in the Antarctic Peninsula. *Journal of Glaciology*, 46, 516–530, https://doi.org/10.3189/172756500781833043.

Schaeffer, A. J. and Lebedev, S. (2013). Global shear speed structure of the upper mantle and transition zone. *Geophysical Journal International*, 194(1), 417–449, https://doi.org/10.1093/gji/ggt095. URL https://doi.org/10.1093%2Fgji%2Fggt095.

Schmidtko, S., Heywood, K. J., Thompson, A. F., and Aoki, S. (2014). Multidecadal warming of Antarctic waters. *Science*, 346(6214), 1227–1231, https://doi.org/https://doi.org/10.1126/science.1256117.

Schoof, C. (2005). The effect of cavitation on glacier sliding. *Proceedings of The Royal Society A: Mathematical, Physical and Engineering Sciences*, 461, 609–627, https://doi.org/10.1098/rspa.2004.1350.

Schoof, C. (2007). Ice sheet grounding line dynamics: Steady states, stability, and hysteresis. *Journal of Geophysical Research: Earth Surface*, 112, 1–19, https://doi.org/https://doi.org/10.1029/2006JF000664.

Schoof, C. and Hewitt, I. (2013). Ice-sheet dynamics. *Annual Review of Fluid Mechanics*, 45(1), 217–239, https://doi.org/10.1146/annurev-fluid-011212-140632. URL https://doi.org/10.1146/annurev-fluid-011212-140632.

Schröder, L., Horwath, M., Dietrich, R., Helm, V., van den Broeke, M. R., and Ligtenberg, S. R. M. (2019). Four decades of antarctic surface elevation changes from multi-mission satellite altimetry. *The Cryosphere*, 13(2), 427–449, https://doi.org/10.5194/tc-13-427-2019. URL https://doi.org/10.5194%2Ftc-13-427-2019.

Schwalm, C. R., Glendon, S., and Duffy, P. B. (2020). RCP8.5 tracks cumulative CO₂ emissions. *Proceedings of the National Academy of Sciences*, 117(33), 19656–19657, https://doi.org/10.1073/pnas.2007117117. URL https://www.pnas.org/doi/abs/10.1073/pnas.2007117117.

Seguinot, J. (2013). Spatial and seasonal effects of temperature variability in a positive degree-day glacier surface mass-balance model. *Journal of Glaciology*, 59(218), 1202–1204, https://doi.org/10.3189/2013JoG13J081.

Seguinot, J. and Rogozhina, I. (2014). Daily temperature variability predetermined by thermal conditions over ice-sheet surfaces. *Journal of Glaciology*, 60(221), 603–605, https://doi.org/10.3189/2014JoG14J036.

Sergienko, O. V. and Wingham, D. J. (2019). Grounding line stability in a regime of low driving and basal stresses. *Journal of Glaciology*, 65(253), 833–849, https://doi.org/https://doi.org/10.1017/jog.2019.53.

Seroussi, H., Nakayama, Y., Larour, E., Menemenlis, D., Morlighem, M., Rignot, E., and Khazendar, A. (2017). Continued retreat of Thwaites Glacier, West Antarctica, controlled by bed topography and ocean circulation. *Geophysical Research Letters*, 44(12), 6191–6199, https://doi.org/https://doi.org/10.1002/2017GL072910. URL https://agupubs.onlinelibrary.wiley.com/doi/abs/10.1002/2017GL072910.

Seroussi, H., Nowicki, S., Payne, A. J., Goelzer, H., Lipscomb, W. H., Abe-Ouchi, A., Agosta, C., Albrecht, T., Asay-Davis, X., Barthel, A., Calov, R., Cullather, R., Dumas, C., Galton-Fenzi, B. K., Gladstone, R., Golledge, N. R., Gregory, J. M., Greve, R., Hattermann, T., Hoffman, M. J., Humbert, A., Huybrechts, P., Jourdain, N. C., Kleiner, T., Larour, E., Leguy, G. R., Lowry, D. P., Little, C. M., Morlighem, M., Pattyn, F., Pelle, T., Price, S. F., Quiquet, A., Reese, R., Schlegel, N.-J., Shepherd, A., Simon, E., Smith, R. S., Straneo, F., Sun, S., Trusel, L. D., Van Breedam, J., van de Wal, R. S. W., Winkelmann, R., Zhao, C., Zhang, T., and Zwinger, T. (2020). ISMIP6 Antarctica: a multi-model ensemble of the Antarctic ice sheet evolution over the 21st century. *The Cryosphere*, 14(9), 3033–3070, https://doi.org/https://doi.org/10.5194/tc-14-3033-2020.

Seroussi, H., Nowicki, S., Simon, E., Abe-Ouchi, A., Albrecht, T., Brondex, J., Cornford, S., Dumas, C., Gillet-Chaulet, F., Goelzer, H., Golledge, N. R., Gregory, J. M., Greve, R., Hoffman, M. J., Humbert, A., Huybrechts, P., Kleiner, T., Larour, E., Leguy, G., Lipscomb, W. H., Lowry, D., Mengel, M., Morlighem, M., Pattyn, F., Payne, A. J., Pollard, D., Price, S. F., Quiquet, A., Reerink, T. J., Reese, R., Rodehacke, C. B., Schlegel, N.-J., Shepherd, A., Sun, S., Sutter, J., Van Breedam, J., van de Wal, R. S. W., Winkelmann, R., and Zhang, T. (2019). initMIP-Antarctica: an ice sheet model initialization experiment of ISMIP6. *The Cryosphere*, 13(5), 1441–1471, https://doi.org/https://doi.org/10.5194/tc-13-1441-2019.

Shapiro, N. M. and Ritzwoller, M. H. (2004). Inferring surface heat flux distributions guided by a global seismic model : particular application to Antarctica. *Earth and Planetary Science Letters*, 223, 213–224, https://doi.org/https://doi.org/10.1016/j.epsl.2004.04.011.

Shepherd, A., Ivins, E., Rignot, E., Smith, B., van den Broeke, M., Velicogna, I., Whitehouse, P., Briggs, K., Joughin, I., Krinner, G., Nowicki, S., Payne, T., Scambos, T., Schlegel, N., A, G., Agosta, C., Ahlstrøm, A., Babonis, G., Barletta, V., Blazquez, A., Bonin, J., Csatho, B., Cullather, R., Felikson, D., Fettweis, X., Forsberg, R., Gallee, H., Gardner, A., Gilbert, L., Groh, A., Gunter, B., Hanna, E., Harig, C., Helm, V., Horvath, A., Horwath, M., Khan, S., K. Kjeldsen, K., Konrad, H., Langen, P., Lecavalier, B., Loomis, B., Luthcke, S., McMillan, M., Melini, D., Mernild, S., Mohajerani, Y., Moore, P., Mouginot, J., Moyano, G., Muir, A., Nagler, T., Nield, G., Nilsson, J., Noel, B., Otosaka, I., E. Pattle, M., Peltier, W., Pie, N., Rietbroek, R., Rott, H., Sandberg-Sørensen, L., Sasgen, I., Save, H., Scheuchl, B., Schrama, E., Schröder, L., Seo, K.-W., Simonsen, S., Slater, T., Spada, G., Sutterley, T., Talpe, M., Tarasov, L., van de Berg, W., van der Wal, W., van Wessem, M., Dutt Vishwakarma, B., Wiese, D., and Wouters, B. (2018). Mass balance of the Antarctic Ice Sheet from 1992 to 2017. *Nature*, 558(7709), 219–222, https://doi.org/10.1038/s41586-018-0179-y.

Siahaan, A., Smith, R., Holland, P., Jenkins, A., Gregory, J. M., Lee, V., Mathiot, P., Payne, T., Ridley, J., and Jones, C. (2021). The antarctic contribution to 21st century sea-level rise predicted by the uk earth system model with an interactive ice sheet. *The Cryosphere Discussions*, 2021, 1–42, https://doi.org/10.5194/tc-2021-371. URL https://tc.copernicus.org/preprints/tc-2021-371/.

Silvano, A., Rintoul, S. R., Peña-Molino, B., Hobbs, W. R., van Wijk, E., Aoki, S., Tamura, T., and Williams, G. D. (2018). Freshening by glacial meltwater enhances melting of ice shelves and reduces formation of antarctic bottom water. *Science Advances*, 4(4), https://doi.org/10.1126/sciadv.aap9467. URL https://doi.org/10.1126%2Fsciadv.aap9467.

Smith, B., Fricker, H. A., Gardner, A. S., Medley, B., Nilsson, J., Paolo, F. S., Holschuh, N., Adusumilli, S., Brunt, K., Csatho, B., Harbeck, K., Markus, T., Neumann, T., Siegfried, M. R., and Zwally, H. J. (2020). Pervasive ice sheet mass loss reflects competing ocean and atmosphere processes. *Science*, 368(6496), 1239–1242, https://doi.org/10.1126/science.aaz5845. URL https://www.science.org/doi/abs/10.1126/science.aaz5845.

Stokes, C. R., Abram, N. J., Bentley, M. J., Edwards, T. L., England, M. H., Foppert, A., Jamieson, S. S. R., Jones, R. S., King, M. A., Lenaerts, J. T. M., Medley, B., Miles, B. W. J., Paxman, G. J. G., Ritz, C., van de Flierdt, T., and Whitehouse, P. L. (2022). Response of the east antarctic ice sheet to past and future climate change. *Nature*, 608(7922), 275–286, https://doi.org/10.1038/s41586-022-04946-0. URL https://doi.org/10.1038%2Fs41586-022-04946-0.

Stuart, A. M. (2010). Inverse problems: A bayesian perspective. *Acta Numerica*, 19, 451–559, https://doi.org/10.1017/s0962492910000061.

Sun, S., Pattyn, F., Simon, E. G., Albrecht, T., Cornford, S., Calov, R., Dumas, C., Gillet-Chaulet, F., Goelzer, H., Golledge, N. R., and et al. (2020). Antarctic ice sheet response to sudden and sustained ice-shelf collapse (ABUMIP). *Journal of Glaciology*, 66(260), 891–904, https://doi.org/https://doi.org/10.1017/jog.2020.67.

Swain, C. J. and Kirby, J. F. (2021). Effective elastic thickness map reveals subglacial structure of east antarctica. *Geophysical Research Letters*, 48(4), e2020GL091576, https://doi.org/https://doi.org/10.1029/2020GL091576. URL https://agupubs.onlinelibrary.wiley.com/doi/abs/10.1029/2020GL091576.

Tarantola, A. (2005). *Inverse Problem Theory and Methods for Model Parameter Estimation*. Society for Industrial and Applied Mathematics, https://doi.org/10.1137/1.9780898717921.

Tarasov, L. and Peltier, W. R. (1999). Impact of thermomechanical ice sheet coupling on a model of the 100 kyr ice age cycle. *Journal of Geophysical Research: Atmospheres*, 104(D8), 9517–9545, https://doi.org/https://doi.org/10.1029/1998JD200120. URL https://agupubs.onlinelibrary.wiley.com/doi/abs/10.1029/1998JD200120.

the PISM authors (2022). Pism, a parallel ice sheet model: User's manual. URL http://www.pism.io/docs/manual.

Thomas, E. R., van Wessem, J. M., Roberts, J., Isaksson, E., Schlosser, E., Fudge, T. J., Vallelonga, P., Medley, B., Lenaerts, J., Bertler, N., van den Broeke, M. R., Dixon, D. A., Frezzotti, M., Stenni, B., Curran, M., and Ekaykin, A. A. (2017). Regional Antarctic snow accumulation over the past 1000 years. *Climate of the Past*, 13(11), 1491–1513, https://doi.org/10.5194/cp-13-1491-2017. URL https://cp.copernicus.org/articles/13/1491/2017/.

Thomas, R. H. (1979). The Dynamics of Marine Ice Sheets. *Journal of Glaciology*, 24(90), 167–177, https://doi.org/10.3189/S0022143000014726.

Thomas, R. H. and Bentley, C. R. (1978). A Model for Holocene Retreat of the West Antarctic Ice Sheet. *Quaternary Research*, 10(2), 150–170, https://doi.org/https://doi.org/10.1016/0033-5894(78)90098-4.

Timmermann, R. and Hellmer, H. (2013). Southern Ocean warming and increased ice shelf basal melting in the twenty-first and twenty-second centuries based on coupled ice-ocean finite-element modelling. *Ocean Dynamics*, 63, 1011–1026, https://doi.org/10.1007/s10236-013-0642-0.

Trusel, L., Frey, K., Das, S., Karnauskas, K., Munneke, P., Meijgaard, E., and Van den Broeke, M. (2015). Divergent trajectories of Antarctic surface melt under two twenty-first-century climate scenarios. *Nature Geoscience*, 8, https://doi.org/10.1038/ngeo2563.

Tsai, C.-Y., Forest, C., and Pollard, D. (2020). The role of internal climate variability in projecting Antarctica's contribution to future sea-level rise. *Climate Dynamics*, 55, https://doi.org/10.1007/s00382-020-05354-8.

Tsai, C.-Y., Forest, C. E., and Pollard, D. (2017). Assessing the contribution of internal climate variability to anthropogenic changes in ice sheet volume. *Geophysical Research Letters*, 44(12), 6261–6268, https://doi.org/https://doi.org/10.1002/2017GL073443. URL https://agupubs.onlinelibrary.wiley.com/doi/abs/10.1002/2017GL073443.

Tsai, V., Stewart, A., and Thompson, A. (2015). Marine ice-sheet profiles and stability under coulomb basal conditions. *Journal of Glaciology*, 61, 205–215, https://doi.org/10.3189/2015JoG14J221.

Urruty, B., Hill, E. A., Reese, R., Garbe, J., Gagliardini, O., Durand, G., Gillet-Chaulet, F., Gudmundsson, G. H., Winkelmann, R., Chekki, M., Chandler, D., and Langebroek, P. M. (2022). The stability of present-day antarctic grounding lines – part a: No indication of marine ice sheet instability in the current geometry. *The Cryosphere Discussions*, 2022, 1–34, https://doi.org/10.5194/tc-2022-104. URL https://tc.copernicus.org/preprints/tc-2022-104/.

van de Wal, R. and Oerlemans, J. (1994). An energy balance model for the Greenland ice sheet. *Global and Planetary Change*, 9(1), 115–131, https://doi.org/https://doi.org/10.1016/0921-8181(94)90011-6. URL https://www.sciencedirect.com/science/article/pii/0921818194900116, greenland ice margin experiment (GIMEx).

van den Berg, J., van de Wal, R. S., Milne, G. A., and Oerlemans, J. (2008). Effect of isostasy on dynamical ice sheet modeling: A case study for Eurasia. *Journal of Geophysical Research: Solid Earth*, 113(5), 1–13, https://doi.org/https://doi.org/10.1029/2007JB004994.

van der Wal, W., Whitehouse, P. L., and Schrama, E. J. (2015). Effect of GIA models with 3D composite mantle viscosity on GRACE mass balance estimates for Antarctica. *Earth and Planetary Science Letters*, 414, 134–143, https://doi.org/https://doi.org/10.1016/j.epsl.2015.01.001.

van Kampenhout, L., Rhoades, A. M., Herrington, A. R., Zarzycki, C. M., Lenaerts, J. T. M., Sacks, W. J., and van den Broeke, M. R. (2019). Regional grid refinement in an earth system model: impacts on the simulated greenland surface mass balance. *The Cryosphere*, 13(6), 1547–1564, https://doi.org/10.5194/tc-13-1547-2019. URL https://tc.copernicus.org/articles/13/1547/2019/.

van Wessem, J. M., van de Berg, W. J., Noël, B. P. Y., van Meijgaard, E., Amory, C., Birnbaum, G., Jakobs, C. L., Krüger, K., Lenaerts, J. T. M., Lhermitte, S., Ligtenberg, S. R. M., Medley, B., Reijmer, C. H., van Tricht, K., Trusel, L. D., van Ulft, L. H., Wouters, B., Wuite, J., and van den Broeke, M. R. (2018). Modelling the climate and surface mass balance of polar ice sheets using RACMO2 – Part 2: Antarctica (1979–2016). *The Cryosphere*, 12(4), 1479–1498, https://doi.org/10.5194/tc-12-1479-2018. URL https://tc.copernicus.org/articles/12/1479/2018/.

van Wessem, J. M. V., Reijmer, C. H., Lenaerts, J. T. M., Berg, W. J. V. D., van den Broeke, M. R. V. D., and van Meijgaard, E. (2014). Updated cloud physics in a regional atmospheric climate model improves the modelled surface energy balance of Antarctica. *The Cryosphere*, 8, 125–135, https://doi.org/https://doi.org/10.5194/tc-8-125-2014.

Verjans, V., Leeson, A. A., Nemeth, C., Stevens, C. M., Kuipers Munneke, P., Noël, B., and van Wessem, J. M. (2020). Bayesian calibration of firn densification models. *The Cryosphere*, 14(9), 3017–3032, https://doi.org/10.5194/tc-14-3017-2020. URL https://tc.copernicus.org/articles/14/3017/2020/.

Vitousek, S., Barnard, P., Fletcher, C., Frazer, N., Erikson, L., and Storlazzi, C. (2017). Doubling of coastal flooding frequency within decades due to sea-level rise. *Scientific Reports*, 7, https://doi.org/10.1038/s41598-017-01362-7.

Wake, L. and Marshall, S. (2015). Assessment of current methods of positive degree-day calculation using in situ observations from glaciated regions. *Journal of Glaciology*, 61(226), 329–344, https://doi.org/10.3189/2015JoG14J116.

Weertman, J. (1957). On the Sliding of Glaciers. *Journal of Glaciology*, 3(21), 33–38, https://doi.org/10.3189/S0022143000024709.

Weertman, J. (1974). Stability of the junction of an ice sheet and an ice shelf. *Journal of Glaciology*, 13, 3–11, https://doi.org/https://doi.org/10.3189/S0022143000023327.

Whitehouse, P. L. (2018). Glacial isostatic adjustment modelling: historical perspectives, recent advances, and future directions. *Earth Surface Dynamics*, 6(2), 401–429, https://doi.org/10.5194/esurf-6-401-2018. URL https://esurf.copernicus.org/articles/6/401/2018/.

Whitehouse, P. L., Bentley, M. J., and Le Brocq, A. M. (2012a). A deglacial model for Antarctica: geological constraints and glaciological modelling as a basis for a new model of Antarctic glacial isostatic adjustment. *Quaternary Science Reviews*, 32, 1 – 24, https://doi.org/https://doi.org/10.1016/j.quascirev.2011.11.016.

Whitehouse, P. L., Bentley, M. J., Milne, G. A., King, M. A., and Thomas, I. D. (2012b). A new glacial isostatic adjustment model for Antarctica: calibrated and tested using observations of relative sea-level change and present-day uplift rates. *Geophysical Journal International*, 190(3), 1464–1482, https://doi.org/https://doi.org/10.1111/j.1365-246X.2012.05557.x.

Whitehouse, P. L., Wiens, D. A., Gomez, N., and King, M. A. (2019). Solid Earth change and the evolution of the Antarctic Ice Sheet. *Nature Communications*, (pp. 1–14)., https://doi.org/https://doi.org/10.1038/s41467-018-08068-y.

Wilson, D., Bertram, R., Needham, E., Flierdt, T., Welsh, K., McKay, R., Mazumder, A., Riesselman, C., Jiménez-Espejo, F., and Escutia, C. (2018). Ice loss from the East Antarctic Ice Sheet during late Pleistocene interglacials. *Nature*, 561, https://doi.org/10.1038/s41586-018-0501-8.

Winkelmann, R., Martin, M. A., Haseloff, M., Albrecht, T., Bueler, E., Khroulev, C., and Levermann, A. (2011). The Potsdam Parallel Ice Sheet Model (PISM-PIK) – Part 1: Model description. *The Cryosphere*, 5(3), 715–726, https://doi.org/10.5194/tc-5-715-2011. URL https://tc.copernicus.org/articles/5/715/2011/.

Wise, M., Dowdeswell, J., Jakobsson, M., and Larter, R. (2017). Evidence of marine ice-cliff instability in Pine Island Bay from iceberg-keel plough marks. *Nature*, 550, 506–510, https://doi.org/10.1038/nature24458.

Wright, A., Wadham, J., Siegert, M., Luckman, A., Kohler, J., and Nuttall, A.-M. (2007). Modeling the refreezing of meltwater as superimposed ice on a high arctic glacier: A comparison of approaches. *Journal of Geophysical Research*, 112, https://doi.org/10.1029/2007JF000818.

Wu, P. and Peltier, W. R. (1984). Pleistocene deglaciation and the earth's rotation: a new analysis. *Geophysical Journal of the Royal Astronomical Society*, 76(3), 753–791, https://doi.org/https://doi.org/10.1111/j.1365-246X.1984.tb01920.x. URL https://onlinelibrary.wiley.com/doi/abs/10.1111/j.1365-246X.1984.tb01920.x.

Yousefi, M., Wan, J., Pan, L., Gomez, N., Latychev, K., Mitrovica, J. X., Pollard, D., and DeConto, R. M. (2022). The influence of the solid earth on the contribution of marine sections of the antarctic ice sheet to future sea-level change. *Geophysical Research Letters*, 49(15), e2021GL097525, https://doi.org/https://doi.org/10.1029/2021GL097525. URL https://agupubs.onlinelibrary.wiley.com/doi/abs/10.1029/2021GL097525.

Zeitz, M., Reese, R., Beckmann, J., Krebs-Kanzow, U., and Winkelmann, R. (2021). Impact of the melt–albedo feedback on the future evolution of the greenland ice sheet with pism-debm-simple. *The Cryosphere*, 15(12), 5739–5764, https://doi.org/10.5194/tc-15-5739-2021. URL https://tc.copernicus.org/articles/15/5739/2021/.

Zhu, J., Poulsen, C. J., and Otto-Bliesner, B. L. (2020). High climate sensitivity in CMIP6 model not supported by paleoclimate. *Nature Climate Change*, 10(5), 378–379.

Zoet, L. K. and Iverson, N. R. (2020). A slip law for glaciers on deformable beds. *Science*, 368(6486), 76–78, https://doi.org/10.1126/science.aaz1183. URL https://doi.org/10.1126%2Fscience.aaz1183.

Zuo, H., Alonso-Balmaseda, M., Mogensen, K., and Tietsche, S. (2018). OCEAN5: The ECMWF Ocean Reanalysis System and its Real-Time analysis component. https://doi.org/10.21957/LA2V0442. URL https://www.ecmwf.int/node/18519.

Zuo, H., Balmaseda, M. A., Tietsche, S., Mogensen, K., and Mayer, M. (2019). The ECMWF operational ensemble reanalysis–analysis system for ocean and sea ice: a description of the system and assessment. *Ocean Science*, 15(3), 779–808, https://doi.org/10.5194/os-15-779-2019. URL https://os.copernicus.org/articles/15/779/2019/.

Zweck, C. and Huybrechts, P. (2005). Modeling of the northern hemisphere ice sheets during the last glacial cycle and glaciological sensitivity. *Journal of Geophysical Research: Atmospheres*, 110(D7), https://doi.org/https://doi.org/10.1029/2004JD005489. URL https://agupubs.onlinelibrary.wiley.com/doi/abs/10.1029/2004JD005489.

APPENDIX A

SUPPLEMENTARY INFORMATION FOR CHAPTER 3

JOURNAL OF GEOPHYSICAL RESEARCH

Supporting Information for "Contrasting response of West and East Antarctic ice sheets to Glacial Isostatic Adjustment"

Violaine Coulon[1], Kevin Bulthuis[2], Pippa L. Whitehouse[3], Sainan Sun[1],

Konstanze Haubner[1], Lars Zipf[1], Frank Pattyn[1]

[1]Laboratoire de Glaciologie, Université Libre de Bruxelles, Brussels, Belgium

[2]Jet Propulsion Laboratory, California Institute of technology, Pasadena, CA, USA

[3]Department of Geography, Durham University, Durham, UK DH1 3LE

Contents of this file

1. Text S1
2. Figures S1 to S19

Introduction

The following supporting information provides

1. a review of some elements of plate bending theory relevant for GIA models in glaciology and the derivation of the ELRA model for a spatially-varying flexural rigidity (Text S1)

2. additional figures concerning (i) the local sea level calculation (Fig. S1), (ii) WRMS of the predicted uplift rates obtained using specific ice-loading histories (Figs. S2–S3), (iii) the relative sea-level changes observed under RCP 8.5 (Fig. S4), (iv) the behavior of *non-plausible* ensemble members compared to the overall spread of the ensemble (Fig. S5), (v) the behavior of the UNIBED simulation under the four RCP scenarios (Fig. S6), (vi) the behavior of control simulations under various GIA configurations (Figs. S7–S9), (vii) results from the sensitivity analysis of AIS future behavior to GIA processes for different marine basins (Figs. S10–S14), (viii) the ice thickness changes of the UNIBED experiment with a fixed geoid under the four RCP scenarios at various snapshots (Figs. S15–S18), and (iv) uplift rates predicted by the ensemble of 2000 Monte Carlo simulations at 2100 CE (Fig. S19).

Text S1.

Derivation of the ELRA model with a spatially-varying flexural rigidity

In this section, we provide a formal derivation of the ELRA model with a spatially-varying flexural rigidity (equation (7) in the main manuscript). The derivation of the ELRA model can be carried out based on the plate bending theory (Van Wees & Cloetingh, 1994; Ventsel & Krauthammer, 2001). In this context, the equilibrium vertical displacement of the lithosphere in response to an ice loading is described as the equilibrium vertical displacement of a horizontal linear elastic plate subject to a transverse load. In order to represent the viscous asthenosphere underneath the lithosphere, it is also assumed that this plate lies on a viscous substratum. Most of our derivation is based on Ventsel and Krauthammer (2001) but we also refer the reader to Garcia, Sandwell, and Luttrell (2014) for complementary information.

We first present the equation for the equilibrium vertical displacement of an elastic plate with constant thickness (section 1) and its extension to a plate lying on a viscous substratum (section 2). We then present their extensions to an elastic plate with spatially-varying thickness (sections 3 and 4).

1. Plate with constant thickness

Let us a consider a thin rectangular plate (which represents the lithosphere in the case of the ELRA model) with constant thickness h (and infinite horizontal dimension). The mechanical properties of the plate are given by its Young's modulus E and its Poisson's ratio ν (both properties are assumed to be constant). The plate is subjected to a transverse load p (the ice and ocean loadings in the case of the ELRA model), which is a function of the horizontal position $\boldsymbol{x} = (x, y)$ i.e. $p = p(\boldsymbol{x})$. Let $w = w(\boldsymbol{x})$ be the normal displacement of the plate (also called the deflection). For a thin rectangular plate, it is assumed that the shear strains ϵ_{xz} and ϵ_{xy} and the normal strain ϵ_{xx} are negligible, where we denoted the strain tensor by ϵ. In this context and using Hooke's law in linear elasticity (the plate is assumed to behave like a linear elastic material), the components σ_{xy}, σ_{xx}, and σ_{xy} of the stress tensor are given by

$$\sigma_{xx} = \tfrac{E}{1-\nu^2}(\epsilon_{xx} + \nu\epsilon_{yy}), \tag{1}$$

$$\sigma_{yy} = \tfrac{E}{1-\nu^2}(\epsilon_{yy} + \nu\epsilon_{xx}), \tag{2}$$

$$\sigma_{xy} = \tfrac{1}{2}G\epsilon_{xy}, \tag{3}$$

where $G = \frac{E}{2(1+\nu)}$ is the shear modulus. In the context of thin rectangular plates (see equation (2.1) in Ventsel and Krauthammer (2001)), these stress components can be written as

$$\sigma_{xx} = -\tfrac{Ez}{1-\nu^2}(\tfrac{\partial^2 w}{\partial x^2} + \nu\tfrac{\partial^2 w}{\partial y^2}), \tag{4}$$

$$\sigma_{yy} = -\tfrac{Ez}{1-\nu^2}(\tfrac{\partial^2 w}{\partial y^2} + \nu\tfrac{\partial^2 w}{\partial x^2}), \tag{5}$$

$$\sigma_{xy} = -\tfrac{Ez}{1+\nu}\tfrac{\partial^2 w}{\partial x}\partial y, \tag{6}$$

where the vertical coordinate z is measured from the middle surface of the plate.

The resulting twisting (or torsion) moments M_{xx} and M_{yy} and bending moment M_{xy} (equal to M_{yx}) are given by

$$M_{xx} = \int_{-h/2}^{h/2} \sigma_{xx} z dz = -D\left(\frac{\partial^2 w}{\partial x^2} + \nu\frac{\partial^2 w}{\partial y^2}\right), \tag{7}$$

$$M_{yy} = \int_{-h/2}^{h/2} \sigma_{xy} z dz = -D\left(\frac{\partial^2 w}{\partial y^2} + \nu\frac{\partial^2 w}{\partial x^2}\right), \tag{8}$$

$$M_{xy} = \int_{-h/2}^{h/2} \sigma_{xy} z dz = -D(1-\nu)\frac{\partial^2 w}{\partial x \partial y}, \tag{9}$$

where

$$D = \frac{Eh^3}{12(1-\nu^2)} \tag{10}$$

is the *flexural rigidity of the plate.*

Writing the equilibrium of forces and moments for the plate (see equations (2.19)–(2.21) in Ventsel and Krauthammer (2001)), it can be shown that the twisting and bending moments satisfy the following differential equation (see equation (2.23) in Ventsel and Krauthammer (2001)):

$$\frac{\partial^2 M_{xx}}{\partial x^2} + 2\frac{\partial^2 M_{xy}}{\partial x \partial y} + \frac{\partial^2 M_{yy}}{\partial y^2} = -p. \tag{11}$$

Substituting equations (7)–(9) into equation (11) gives the following partial differential equation for the deflection w:

$$\frac{\partial^2}{\partial x^2}\left(-D\left(\frac{\partial^2 w}{\partial x^2} + \nu\frac{\partial^2 w}{\partial y^2}\right)\right) + 2\frac{\partial^2}{\partial x \partial y}\left(-D(1-\nu)\frac{\partial^2 w}{\partial x \partial y}\right) + \frac{\partial^2}{\partial y^2}\left(-D\left(\frac{\partial^2 w}{\partial y^2} + \nu\frac{\partial^2 w}{\partial x^2}\right)\right) = -p, \tag{12}$$

or as D is assumed to be constant and ν is constant

$$-D\left(\frac{\partial^4 w}{\partial x^4} + 2\nu\frac{\partial^4 w}{\partial x^2 y^2} + \frac{\partial^4 w}{\partial y^4}\right) - 2D(1-\nu)\frac{\partial^4 w}{\partial x^2 y^2} = -p, \tag{13}$$

that is,

$$D\left(\frac{\partial^4 w}{\partial x^4} + 2\frac{\partial^4 w}{\partial x^2 y^2} + \frac{\partial^4 w}{\partial y^4}\right) \equiv D\nabla_{\boldsymbol{x}}^4 w = p. \tag{14}$$

2. Plate with constant thickness on a viscous substratum

We consider now that the plate (lithosphere) in section 1 lies on a viscous substratum (the asthenosphere) with density ρ_{a}. In this case, we must account for the buoyancy force (which depends on the vertical displacement w) that the lithosphere experiences in the underlying viscous substratum. The buoyancy force acts to reduce the exerted load p by an amount $\rho_{\mathrm{a}} g w$ (hydrostatic pressure of the asthenosphere). Then, equation (14) writes in the presence of a viscous substratum as

$$D\nabla_{\boldsymbol{x}}^4 w + \rho_{\mathrm{a}} g w = p. \tag{15}$$

This equation is simply the equation for the deflection of the lithosphere in the ELRA model (equation (1) in the main manuscript).

For a general applied load p, a solution to the linear partial differential equation (15) can be established using a superposition principle. Indeed, the Green's function for the linear differential operator $D\nabla_{\boldsymbol{x}}^4 + \rho_{\mathrm{a}} g$ writes as (Hertz, 1884; Nadai, 1963)

$$G(\boldsymbol{x}) = -\frac{L^2}{2\pi D} \mathrm{kei}\left(\frac{\|\boldsymbol{x}\|}{L}\right), \tag{16}$$

where kei denotes the zeroth-order Kelvin function and $L = \sqrt[4]{D/(\rho_{\mathrm{a}} g)}$ is the so-called radius of relative stiffness (or flexural length scale), which determines the non-locality of the plate displacement. Using the superposition principle, the solution to the linear partial differential equation (15) can be expressed as

$$w(\boldsymbol{x}) = G(\boldsymbol{x}) * p(\boldsymbol{x}) = \int_{\mathbb{R}^2} -\frac{L^2}{2\pi D} \mathrm{kei}\left(\frac{\|\boldsymbol{x} - \boldsymbol{x}'\|}{L}\right) p(\boldsymbol{x}') d\boldsymbol{x}', \tag{17}$$

where $*$ denotes the convolution operator. The use of this Green's function provides an efficient way to solve for the deflection of the lithosphere due to ice loading in numerical ice-sheet models (see for instance (Pattyn, 2017; Pollard & DeConto, 2012)).

3. Plate with spatially-varying thickness

Let us consider in this section a thin rectangular plate having a spatially-varying thickness $h = h(\boldsymbol{x})$ (and infinite horizontal dimension). As in section 1, the plate is assumed to behave as a linear elastic material with constant Young's modulus E and Poisson's ratio ν. The plate is subjected to a transverse load $p = p(\boldsymbol{x})$ that induces a deflection $w = w(\boldsymbol{x})$ of the plate. Following section 3.8 in Ventsel and Krauthammer (2001), we assume that the thickness varies gradually and there is no abrupt variation in thickness so that the expressions for the bending and twisting moments introduced earlier for plates of constant thickness (see equations (7)–(9)) also apply with sufficient accuracy to the case of a thin rectangular plate having a spatially-varying thickness. Please note that in this case, the flexural rigidity D is therefore spatially varying i.e.

$$D = D(\boldsymbol{x}) = \frac{Eh(\boldsymbol{x})^3}{12(1-\nu^2)}. \tag{18}$$

Substituting equations (7)–(9) with the spatially-varying flexural rigidity $D(\boldsymbol{x})$ into equation (11) gives the following partial differential equation for the deflection w:

$$\begin{aligned}\frac{\partial^2}{\partial x^2}\left(-D(\boldsymbol{x})\left(\frac{\partial^2 w}{\partial x^2}+\nu\frac{\partial^2 w}{\partial y^2}\right)\right)+2\frac{\partial^2}{\partial x \partial y}\left(-D(\boldsymbol{x})(1-\nu)\frac{\partial^2 w}{\partial x \partial y}\right)\\+\frac{\partial^2}{\partial y^2}\left(-D(\boldsymbol{x})\left(\frac{\partial^2 w}{\partial y^2}+\nu\frac{\partial^2 w}{\partial x^2}\right)\right)=-p,\end{aligned} \tag{19}$$

where we have highlighted the dependence of D on the horizontal position $\boldsymbol{x}$. Please note that although this equation is identical to equation (12), it cannot be reduced to the simple equation (14) due to the fact that the spatially-varying flexural rigidity $D(\boldsymbol{x})$ cannot be simply drawn out of the derivatives. Arranging the different terms in equation (19) (using Leibniz rule for derivation), one obtains the following equation for the deflection of a plate having a spatially-varying flexural rigidity (see equation (3.83) in Ventsel and

Krauthammer (2001)):

$$
\begin{aligned}
&D\nabla_{\boldsymbol{x}}^4 w + 2\frac{\partial D}{\partial x}\frac{\partial}{\partial x}(\nabla_{\boldsymbol{x}}^2 w) + 2\frac{\partial D}{\partial y}\frac{\partial}{\partial y}(\nabla_{\boldsymbol{x}}^2 w) + \nabla_{\boldsymbol{x}}^2 D(\nabla_{\boldsymbol{x}}^2 w) \\
&-(1-\nu)\left(\frac{\partial^2 D}{\partial x^2}\frac{\partial^2 w}{\partial y^2} - 2\frac{\partial^2 D}{\partial x \partial y}\frac{\partial^2 w}{\partial x \partial y} + \frac{\partial^2 D}{\partial y^2}\frac{\partial^2 w}{\partial x^2}\right) = p.
\end{aligned}
\tag{20}
$$

Please note that in the latter equation, the Poisson's ratio of the plate appears explicitly in the equation. Also, this equation involves both the gradient of the flexural rigidity (through its first derivatives) and the curvature of the flexural rigidity (through its second derivatives). All the terms in equation (20) involving derivatives of the flexural rigidity are nil when the plate has a constant thickness and therefore a constant flexural rigidity.

4. Plate with spatially-varying thickness on a viscous substratum

We consider now that the plate (lithosphere) in section 3 lies on a viscous substratum (the asthenosphere) with density ρ_{a}. Similarly to section 2, we must account for the buoyancy force (which depends on the vertical displacement w) that the lithosphere experiences in the underlying viscous substratum. Then, equation (20) writes in the presence of a viscous substratum as

$$
\begin{aligned}
&D\nabla_{\boldsymbol{x}}^4 w + 2\frac{\partial D}{\partial x}\frac{\partial}{\partial x}(\nabla_{\boldsymbol{x}}^2 w) + 2\frac{\partial D}{\partial y}\frac{\partial}{\partial y}(\nabla_{\boldsymbol{x}}^2 w) + \nabla_{\boldsymbol{x}}^2 D(\nabla_{\boldsymbol{x}}^2 w) \\
&-(1-\nu)\left(\frac{\partial^2 D}{\partial x^2}\frac{\partial^2 w}{\partial y^2} - 2\frac{\partial^2 D}{\partial x \partial y}\frac{\partial^2 w}{\partial x \partial y} + \frac{\partial^2 D}{\partial y^2}\frac{\partial^2 w}{\partial x^2}\right) + \rho_{\mathrm{a}} g w = p.
\end{aligned}
\tag{21}
$$

This equation is simply the equation for the equilibrium deflection of the lithosphere in the ELRA model with spatially-varying flexural rigidity (equation (7) in the main manuscript)

Please note that contrary to section 2 and to our knowledge, there exists no Green's function that allows to write the solution to equation (21) as a superposition principle. In this case, equation (21) is solved using numerical methods such as finite-difference methods or finite-element methods.

References

Argus, D. F., Peltier, W. R., Drummond, R., & Moore, A. W. (2014). The Antarctica component of postglacial rebound model ICE-6G_C (VM5a) based on GPS positioning, exposure age dating of ice thicknesses, and relative sea level histories. *Geophysical Journal International*, *198*, 537–563. doi: https://doi.org/10.1093/gji/ggu140

Garcia, E. S., Sandwell, D. T., & Luttrell, K. M. (2014). An iterative spectral solution method for thin elastic plate flexure with variable rigidity. *Geophysical Journal International*, *200*(2), 1012-1028. doi: https://doi.org/10.1093/gji/ggu449

Goelzer, H., Coulon, V., Pattyn, F., de Boer, B., & van de Wal, R. (2020). Brief communication: On calculating the sea-level contribution in marine ice-sheet models. *The Cryosphere*, *14*(3), 833–840. doi: 10.5194/tc-14-833-2020

Hertz, H. (1884). Ueber das gleichgewicht schwimmender elastischer platten. *Annalen der Physik*, *258*(7), 449-455. doi: https://doi.org/10.1002/andp.18842580711

Le Meur, E., & Huybrechts, P. (1996). A comparison of different ways of dealing with isostasy: examples from modelling the Antarctic ice sheet during the last glacial cycle. *Annals of Glaciology*, *23*, 309–317. doi: https://doi.org/10013/epic.12717.d001

Nadai, A. (1963). Theory of flow and fracture of solids. In (Vol. 2). New York, NY: McGraw-Hill Book Company.

Pattyn, F. (2017). Sea-level response to melting of Antarctic ice shelves on multi-centennial timescales with the fast Elementary Thermomechanical Ice Sheet model (f.ETISh v1.0). *Cryosphere*, *11*, 1–28. doi: https://doi.org/10.5194/tc-11-1-2017

Pollard, D., & DeConto, R. M. (2012). Description of a hybrid ice sheet-shelf model , and application to Antarctica. *Geoscientific Model Development*, *5*, 1273–1295. doi:

https://doi.org/10.5194/gmd-5-1273-2012

Van Wees, J. D., & Cloetingh, S. (1994). A finite-difference technique to incorporate spatial variations in rigidity and planar faults into 3-d models for lithospheric flexure. *Geophysical Journal International*, *117*(1), 179-195. doi: https://doi.org/10.1111/j.1365-246X.1994.tb03311.x

Ventsel, E., & Krauthammer, T. (2001). *Thin plates and shells* (1st ed.). Boca Raton: CRC Press. doi: https://doi.org/10.1201/9780203908723

Whitehouse, P. L., Bentley, M. J., & Le Brocq, A. M. (2012). A deglacial model for antarctica: geological constraints and glaciological modelling as a basis for a new model of antarctic glacial isostatic adjustment. *Quaternary Science Reviews*, *32*, 1 - 24. doi: https://doi.org/10.1016/j.quascirev.2011.11.016

Whitehouse, P. L., Bentley, M. J., Milne, G. A., King, M. A., & Thomas, I. D. (2012). A new glacial isostatic adjustment model for antarctica: calibrated and tested using observations of relative sea-level change and present-day uplift rates. *Geophysical Journal International*, *190*(3), 1464-1482. doi: https://doi.org/10.1111/j.1365-246X.2012.05557.x

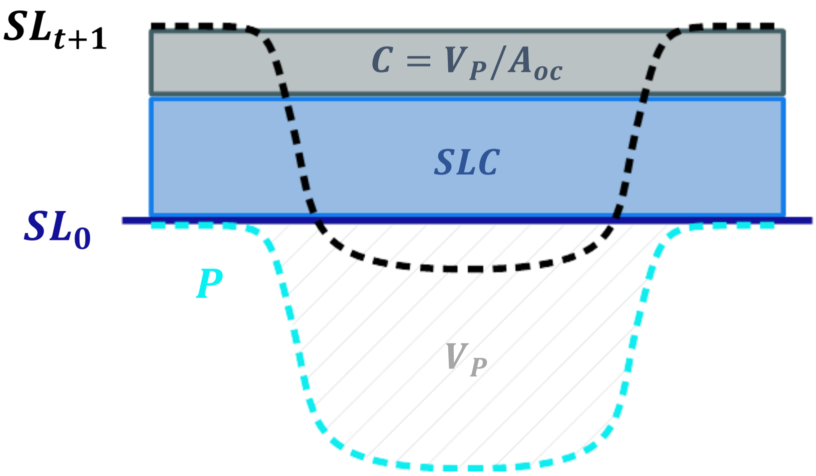

$$SL_{t+1} = SL_0 + P + SLC + C$$

Figure S1. Schematic 2D representation of local sea-level change calculations. Local sea level at time $t+1$, SL_{t+1} (black dashed line), is calculated as the sum of the initial sea surface SL_0 (dark blue solid line), the geoid perturbation P due to mass changes m_G (light blue dashed line), the barystatic sea-level contribution arising from Antarctic ice mass changes (SLC, calculated as in Goelzer et al. (2020)) and a mass conservation term C, which is a spatial constant that must be added to the solution in order to conserve oceanic mass. C is calculated by redistributing the volume change across ocean areas due to P (V_P) over the ocean area A_{oc}.

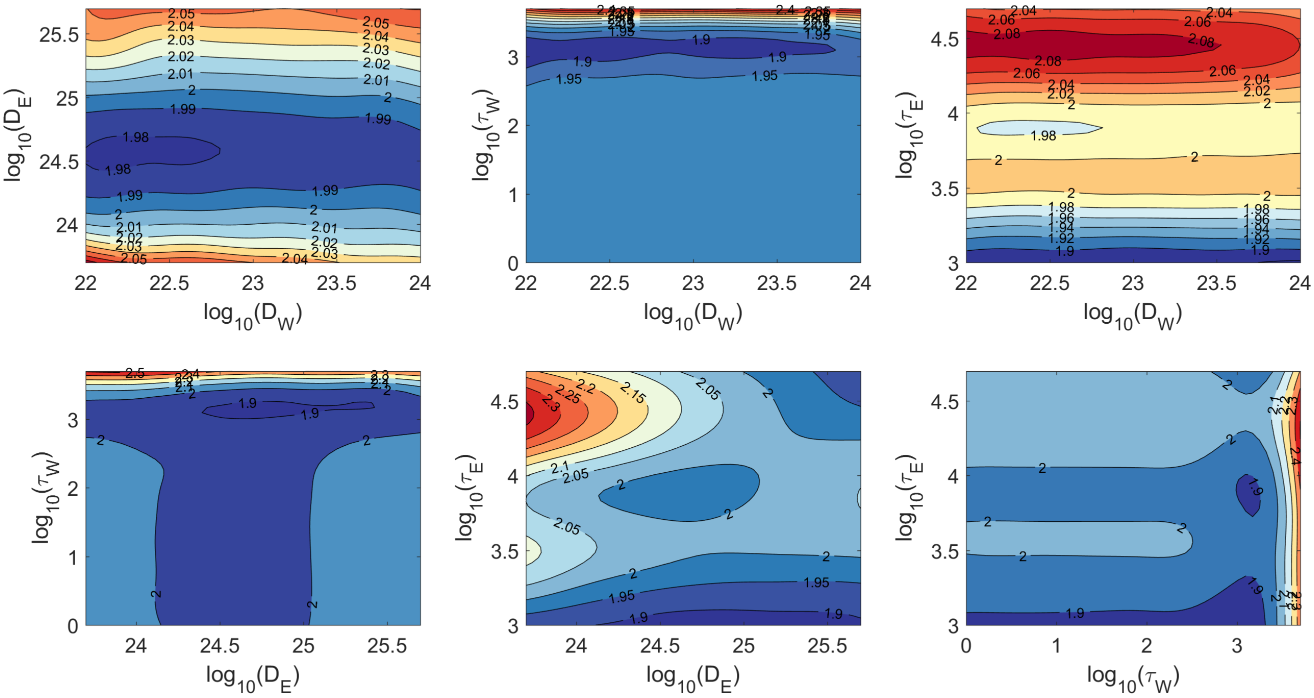

Figure S2. Weighted Root-Mean Square (WRMS, see equation B1) of the predicted uplift rates obtained using W12 ice-loading history (Whitehouse, Bentley, & Le Brocq, 2012) relative to present-day uplift rates (Whitehouse, Bentley, Milne, et al., 2012). As a comparison, predicted uplift rates obtained using uniform ELRA parameters (τ=8000 yr (Argus et al., 2014) and $D = 10^{25}$ N m (Le Meur & Huybrechts, 1996)) give a WRMS of 2.97 mm/yr. Units for D_{E} are N m and units for τ_{E} are years.

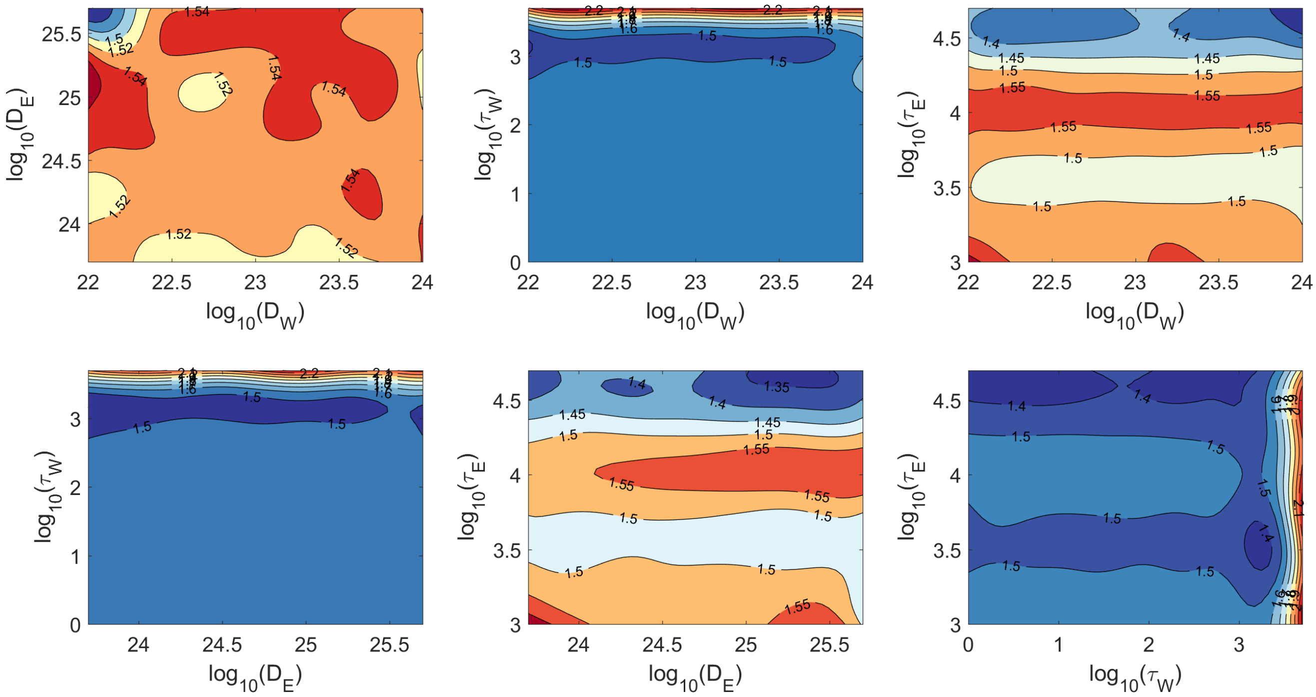

Figure S3. Weighted Root-Mean Square (WRMS, see equation B1) of the predicted uplift rates obtained using ICE-6G ice-loading history (Argus et al., 2014) relative to present-day uplift rates (Whitehouse, Bentley, Milne, et al., 2012). As a comparison, predicted uplift rates obtained using uniform ELRA parameters (τ=4000 yr (Argus et al., 2014) and $D = 10^{25}$ N m (Le Meur & Huybrechts, 1996)) give a WRMS of 2.12 mm/yr. Units for D_{E} are N m and units for τ_{E} are years.

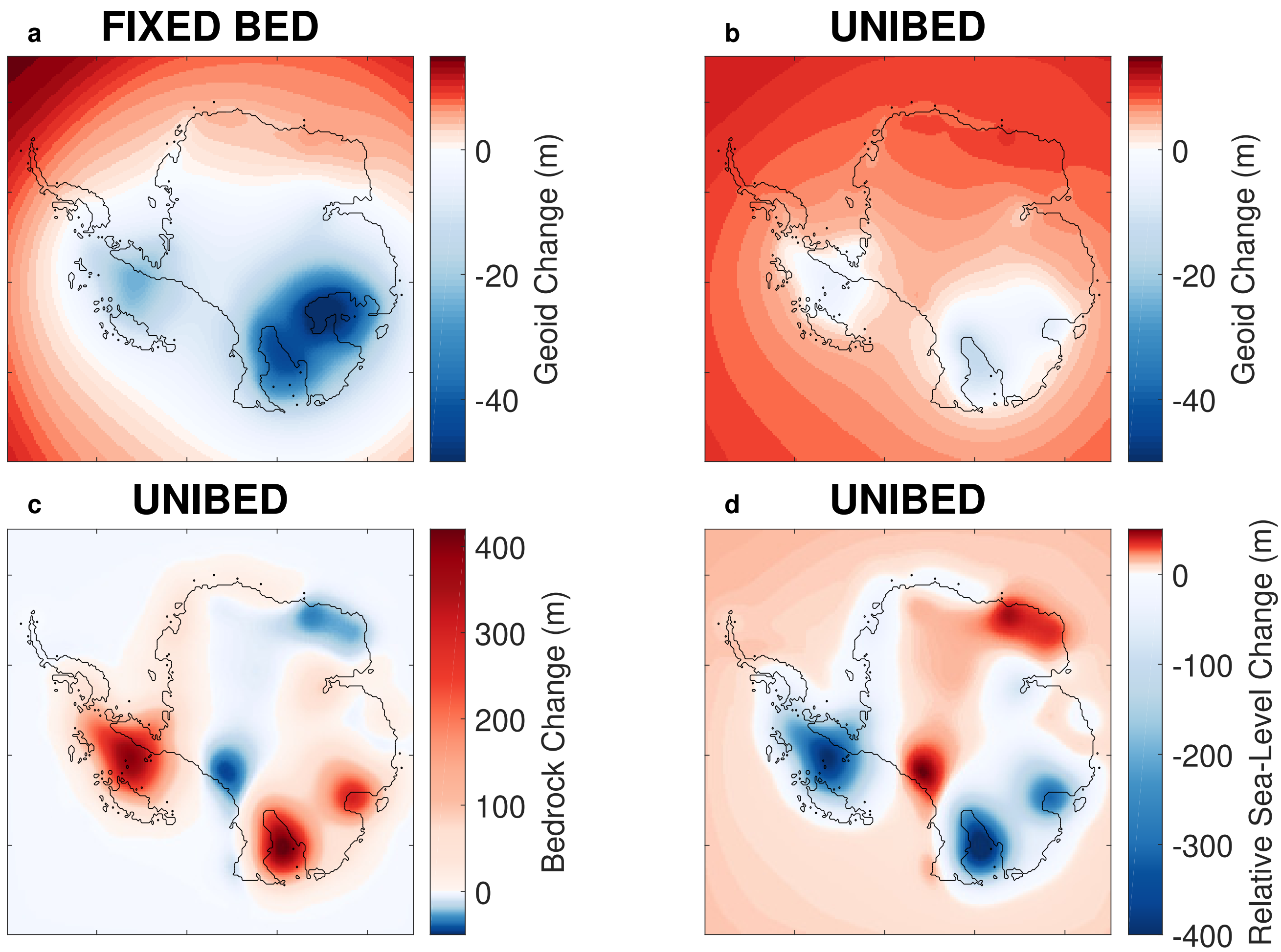

Figure S4. Relative sea-level changes at 7000 CE under RCP 8.5 for a simulation with a fixed bedrock (a), and a simulation where bedrock adjustment is considered (b–d). Relative sea-level changes due to geoid change are displayed in (a–b). Bedrock changes are displayed in (c). Note that relative sea-level changes due to bedrock changes are the opposite of (c). Total relative sea-level changes – i.e. the combination of geoid and bedrock changes – are displayed in (a) for the simulation with a fixed bedrock (FIXED BED) and in (d) for a simulation where bedrock adjustment is considered (UNIBED, with uniform ELRA parameters taken from Le Meur and Huybrechts (1996)). When bedrock adjustment is considered, geoid changes (b) have a smaller contribution to relative sea-level change (d) than bedrock changes (c). In addition, note that the gravitational effect of changes in the distribution of mantle material associated with solid earth deformation counteracts geoid changes due to ice and ocean mass changes, leading to geoid changes of smaller amplitude in (b) than in (a).

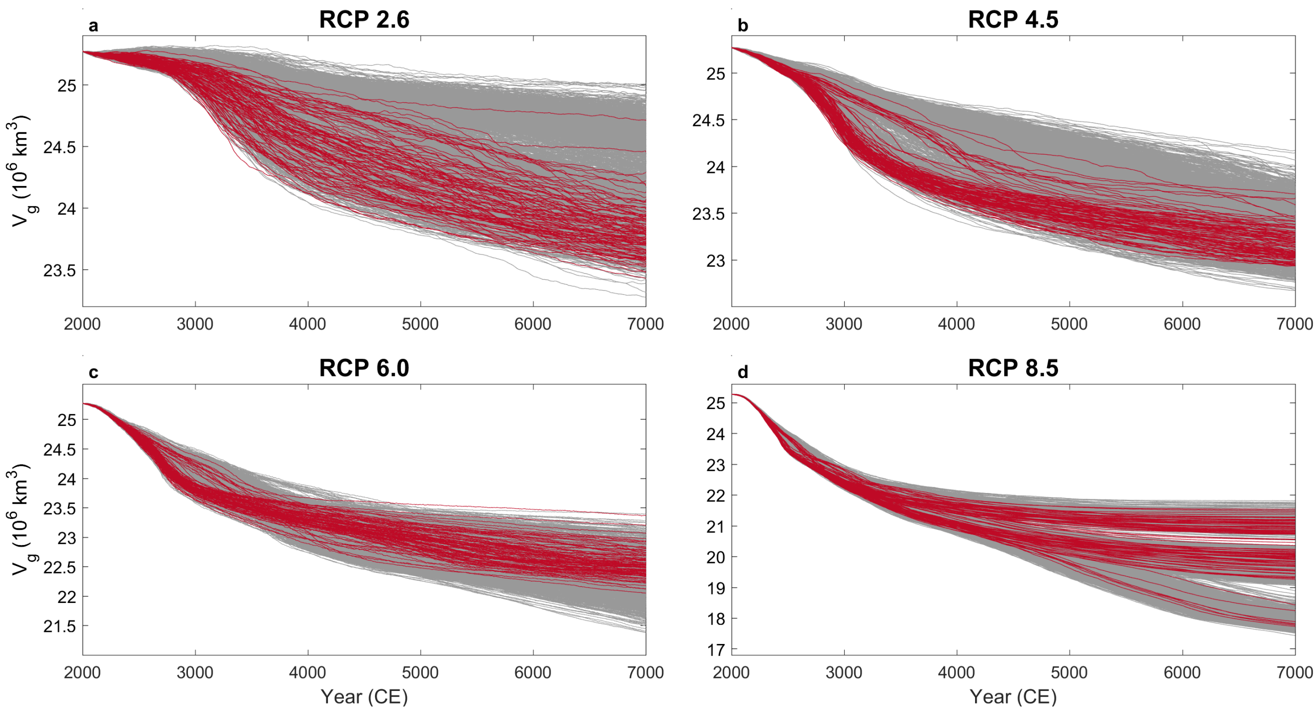

Figure S5. Projections of Antarctic grounded-ice volume (V_g) under RCP 2.6 (a), 4.5 (b), 6.0 (c), and 8.5 (d). Grey lines represent time series of Antarctic grounded-ice volume for the 1900 *plausible* Monte Carlo ensemble members while red line represent those of the 100 *non-plausible* Monte Carlo ensemble members (i.e. either $D_W > D_E$ or $\tau_W > \tau_E$).

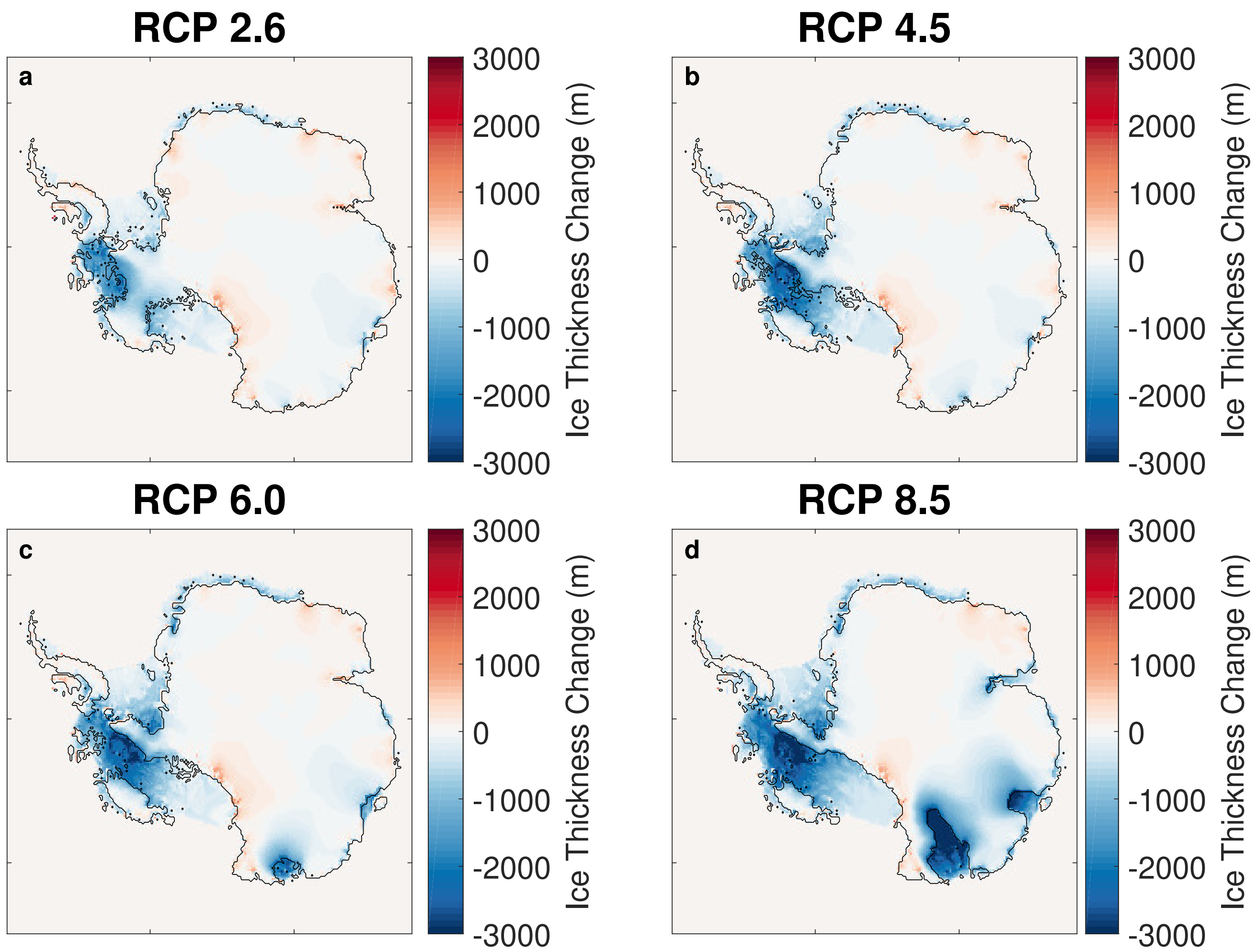

Figure S6. Change in Antarctic ice thickness at 7000 CE for the UNIBED simulations (with uniform ELRA parameters taken from Le Meur & Huybrechts, 1996) under (a) RCP 2.6, (b) RCP 4.5, (c) RCP 6.0, and (d) RCP 8.5.

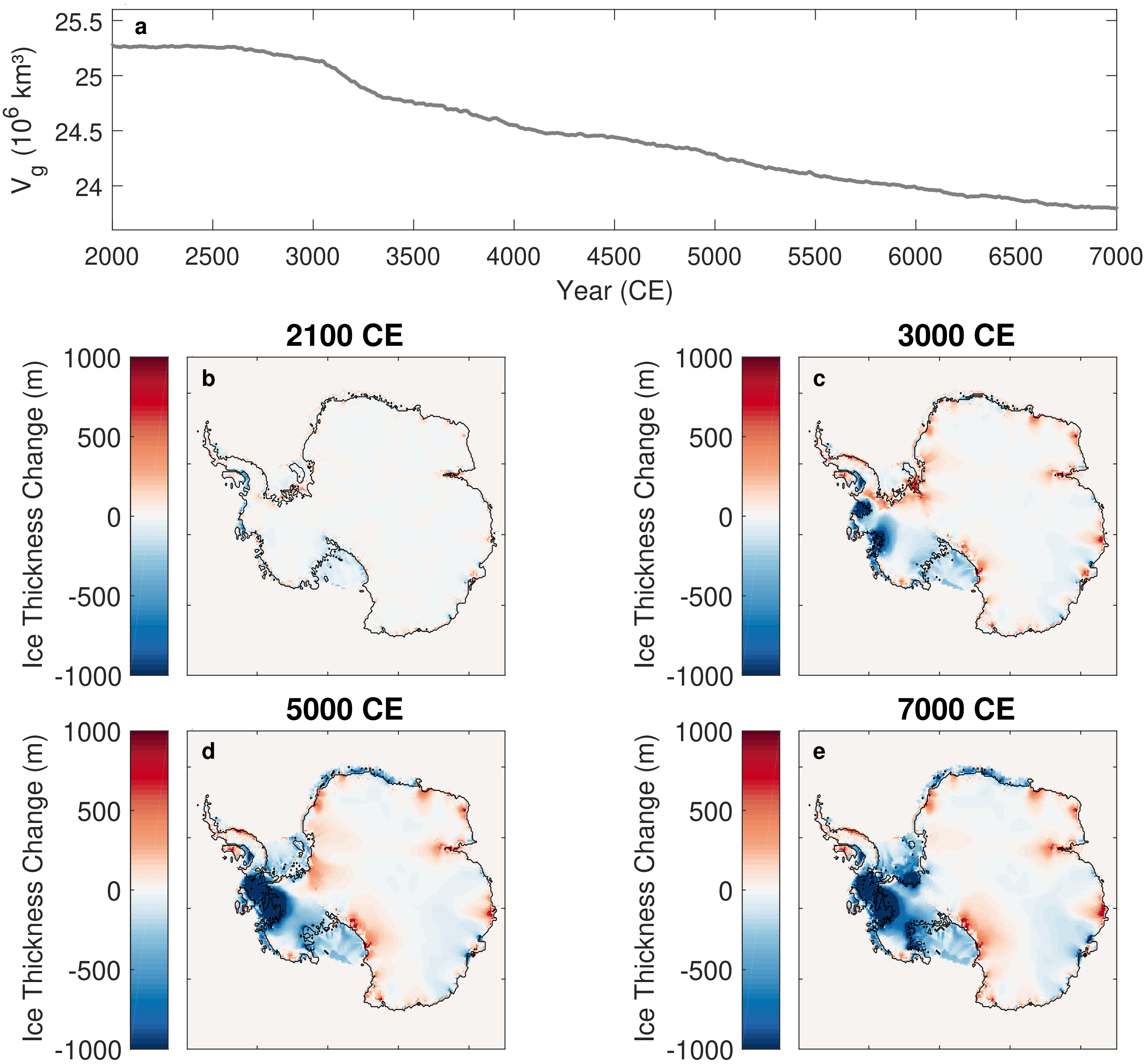

Figure S7. Evolution of Antarctic grounded-ice volume V_g (a) and ice thickness change at 2100 CE (b), 3000 CE (c), 5000 CE (d), and 7000 CE (e) for a control NOGIA (bedrock and geoid are fixed) simulation under constant present-day climate (no climatic perturbation).

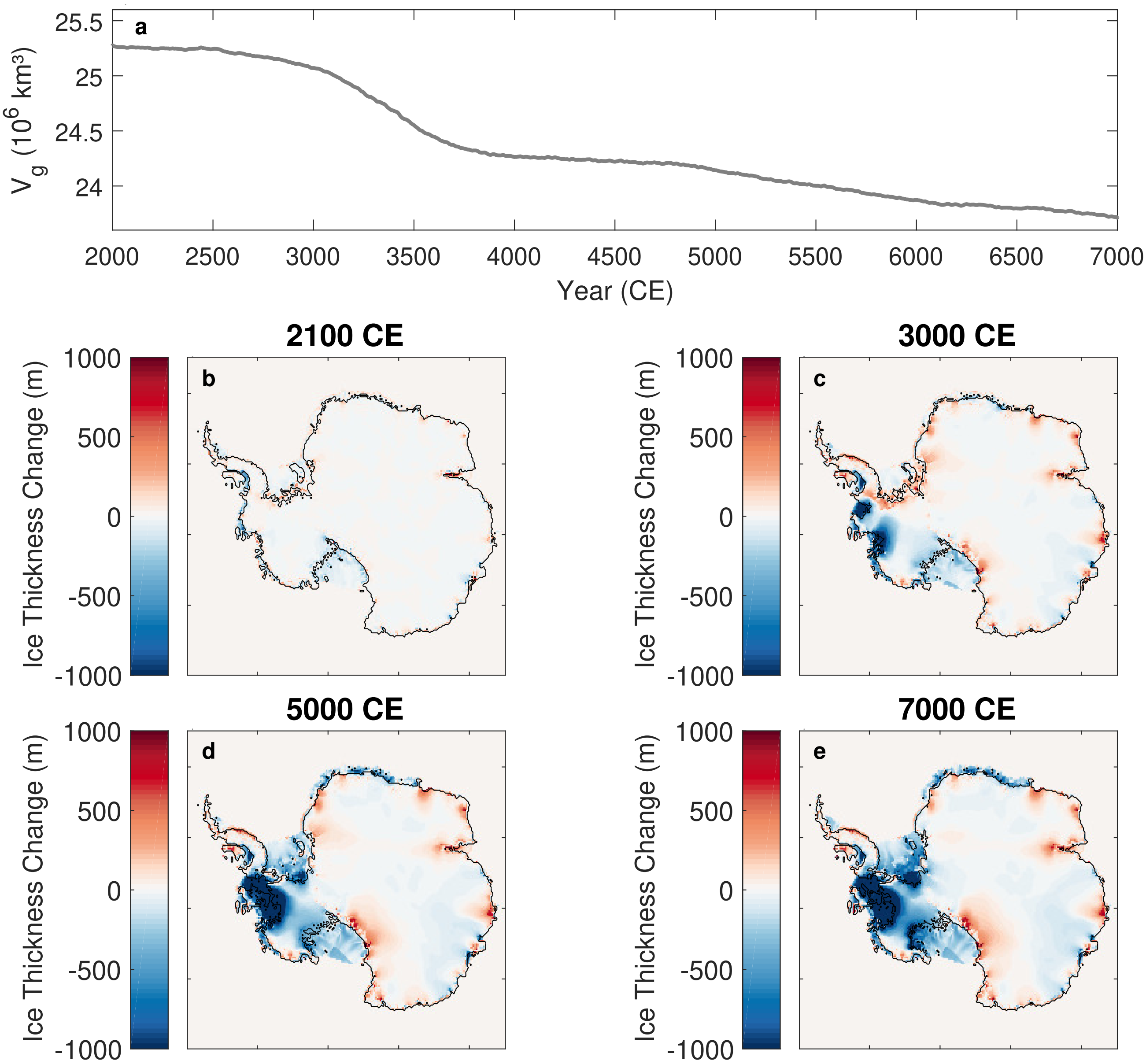

Figure S8. Evolution of Antarctic grounded-ice volume V_g (a) and ice thickness change at 2100 CE (b), 3000 CE (c), 5000 CE (d), and 7000 CE (e) for a control simulation under constant present-day climate (no climatic perturbation) for which uniform ELRA parameters (UNIBED) from Le Meur and Huybrechts (1996) are considered.

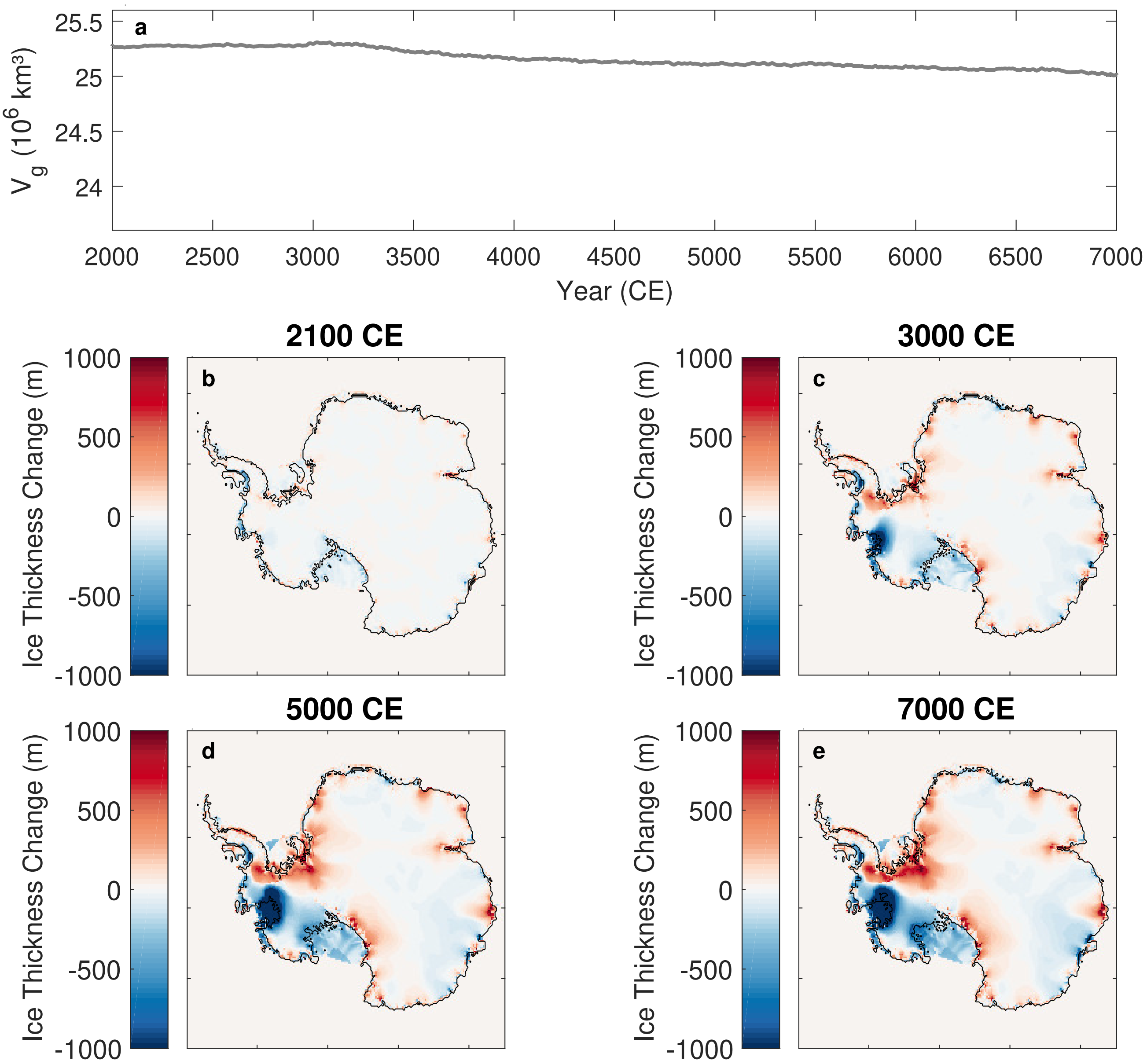

Figure S9. Evolution of Antarctic grounded-ice volume V_g (a) and ice thickness change at 2100 CE (b), 3000 CE (c), 5000 CE (d), and 7000 CE (e) for a control simulation under constant present-day climate (no climatic perturbation) for which median values of the ELRA parameters are considered.

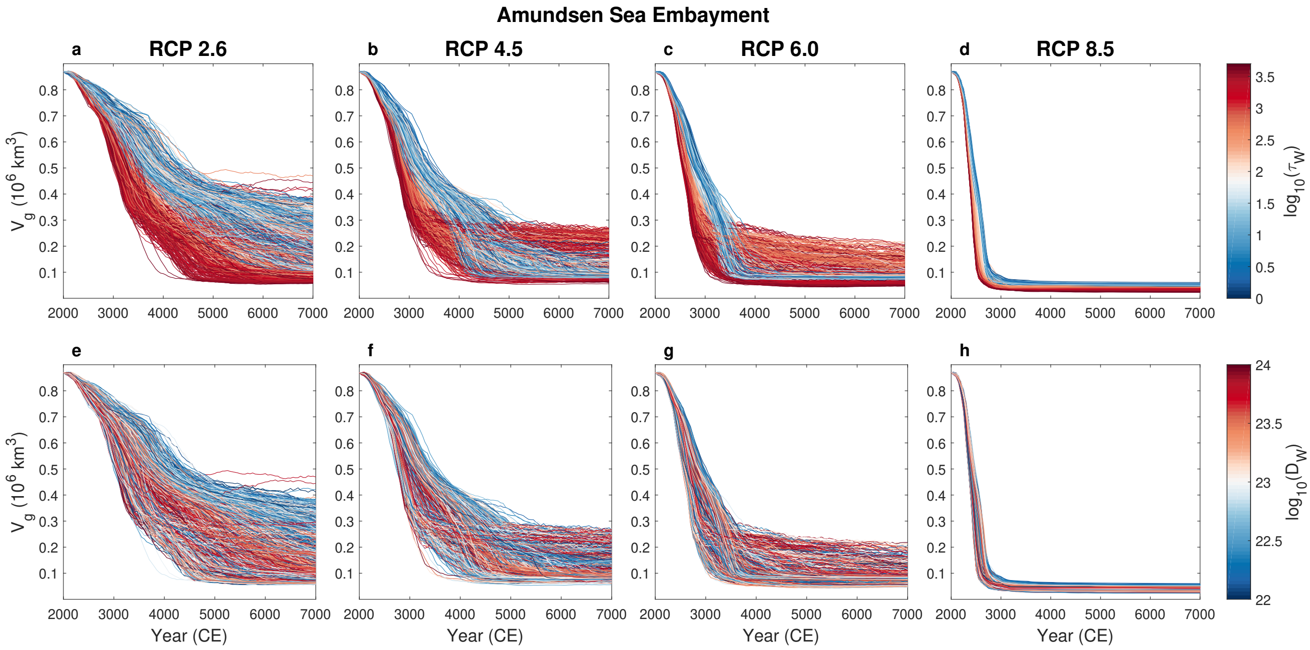

Figure S10. Evolution of Amundsen Sea Embayment grounded-ice volume under RCP 2.6 (a, e), 4.5 (b, f), 6.0 (c, g), and 8.5 (e, h) for 2000 Monte Carlo samples from the parameter space. Time-series of the ensemble are color-coded by values of (a–d) $\log_{10}(\tau_W)$ and (e–h) $\log_{10}(D_W)$. Units for D_W are N m and units for τ_W are years.

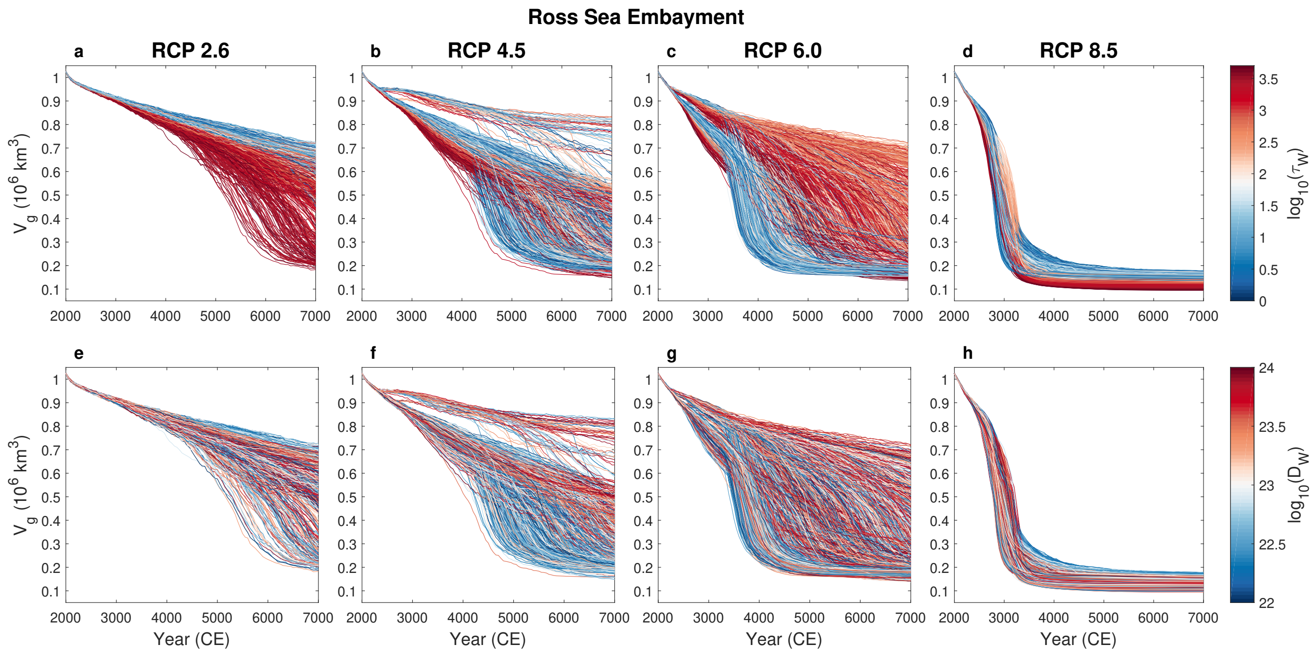

Figure S11. Evolution of Ross Sea Embayment grounded-ice volume (V_g) under RCP 2.6 (a, e), 4.5 (b, f), 6.0 (c, g), and 8.5 (e, h) for 2000 Monte Carlo samples from the parameter space. Time-series of the ensemble are color-coded by values of (a–d) $\log_{10}(\tau_\mathrm{W})$ and (e–h) $\log_{10}(D_\mathrm{W})$. Units for D_W are N m and units for τ_W are years.

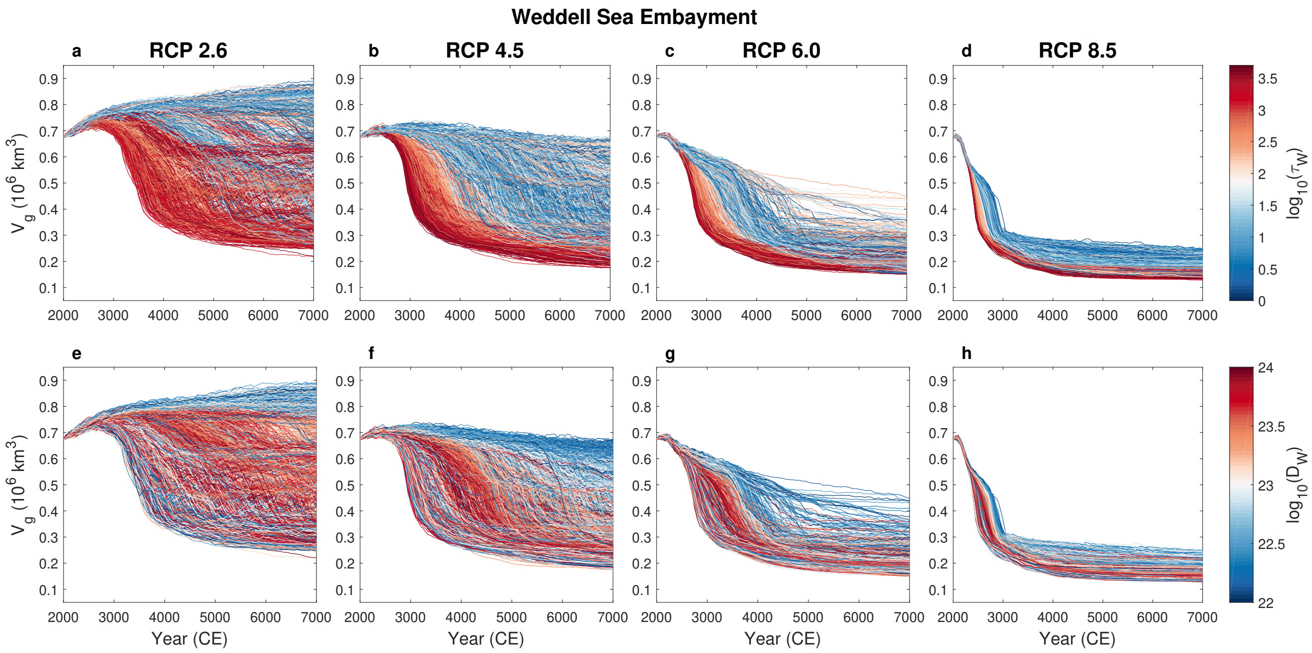

Figure S12. Evolution of Weddell Sea Embayment grounded-ice volume (V_g) under RCP 2.6 (a, e), 4.5 (b, f), 6.0 (c, g), and 8.5 (e, h) for 2000 Monte Carlo samples from the parameter space. Time-series of the ensemble are color-coded by values of (a–d) $\log_{10}(\tau_{\mathrm{W}})$ and (e–h) $\log_{10}(D_{\mathrm{W}})$. Units for D_{W} are N m and units for τ_{W} are years.

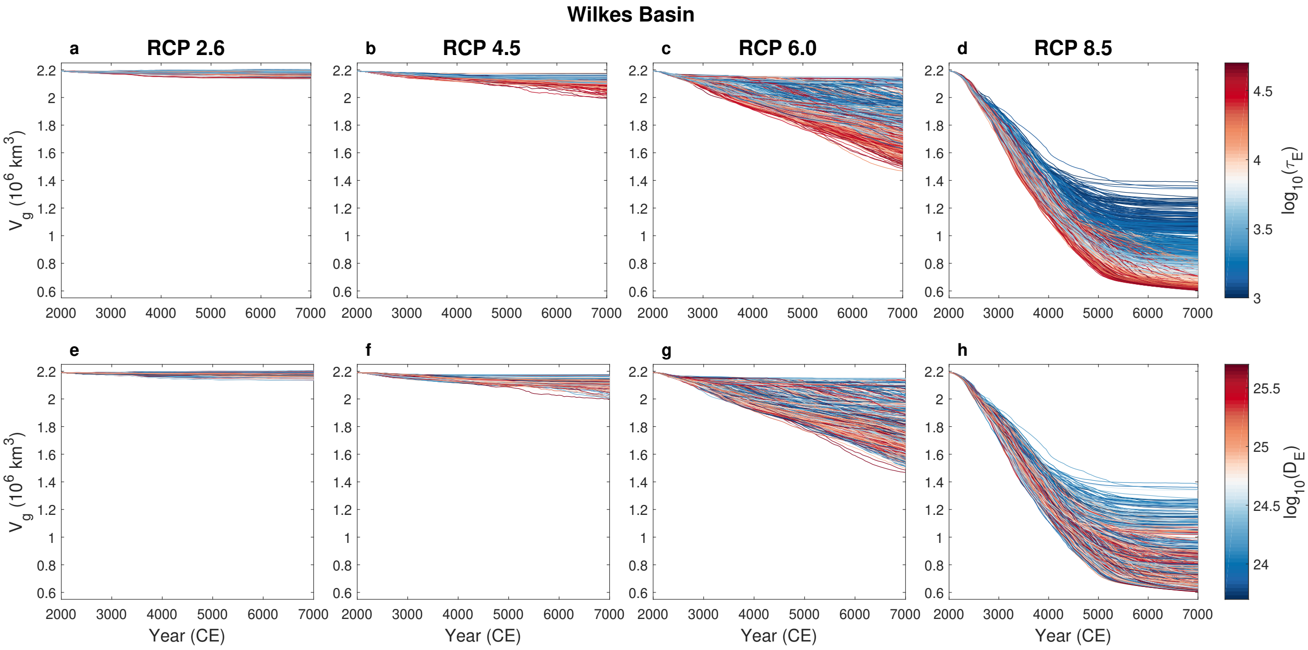

Figure S13. Evolution of Wilkes Basin grounded-ice volume (V_g) under RCP 2.6 (a, e), 4.5 (b, f), 6.0 (c, g), and 8.5 (e, h) for 2000 Monte Carlo samples from the parameter space. Time-series of the ensemble are color-coded by values of (a–d) $\log_{10}(\tau_{\mathrm{E}})$ and (e–h) $\log_{10}(D_{\mathrm{E}})$. Units for D_{E} are N m and units for τ_{E} are years.

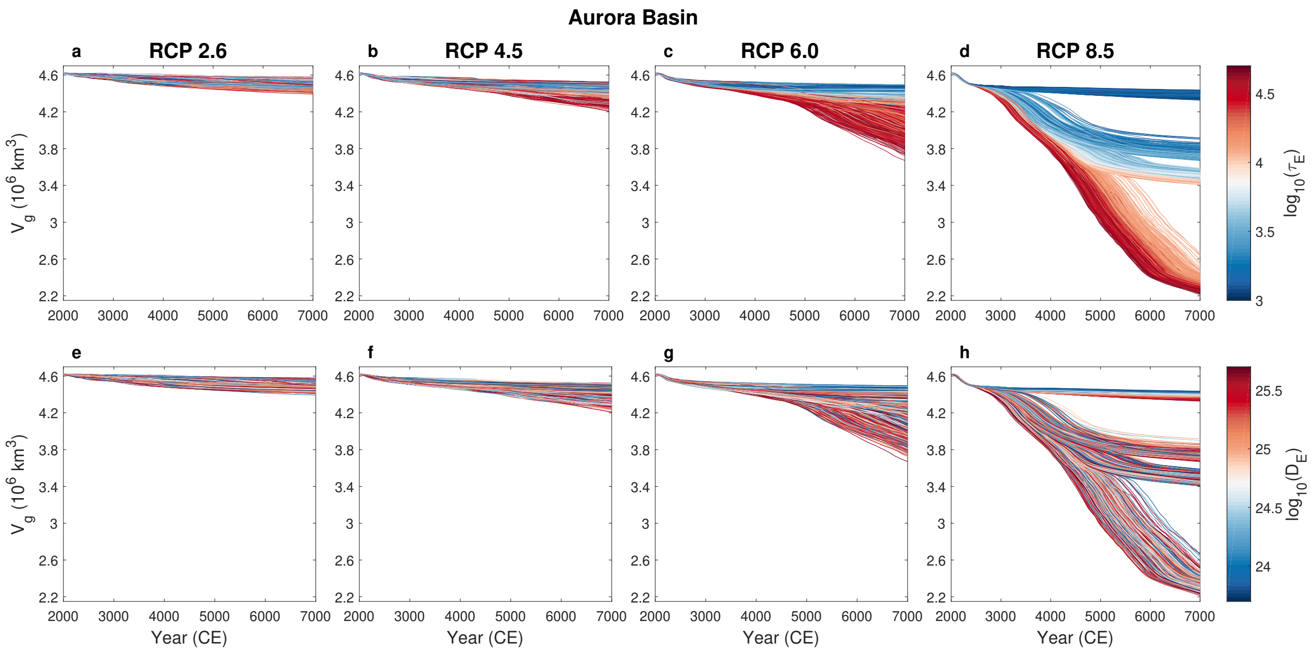

Figure S14. Evolution of Aurora Basin grounded-ice volume (V_g) under RCP 2.6 (a, e), 4.5 (b, f), 6.0 (c, g), and 8.5 (e, h) for 2000 Monte Carlo samples from the parameter space. Time-series of the ensemble are color-coded by values of (a–d) $\log_{10}(\tau_{\mathrm{E}})$ and (e–h) $\log_{10}(D_{\mathrm{E}})$. Units for D_{E} are N m and units for τ_{E} are years.

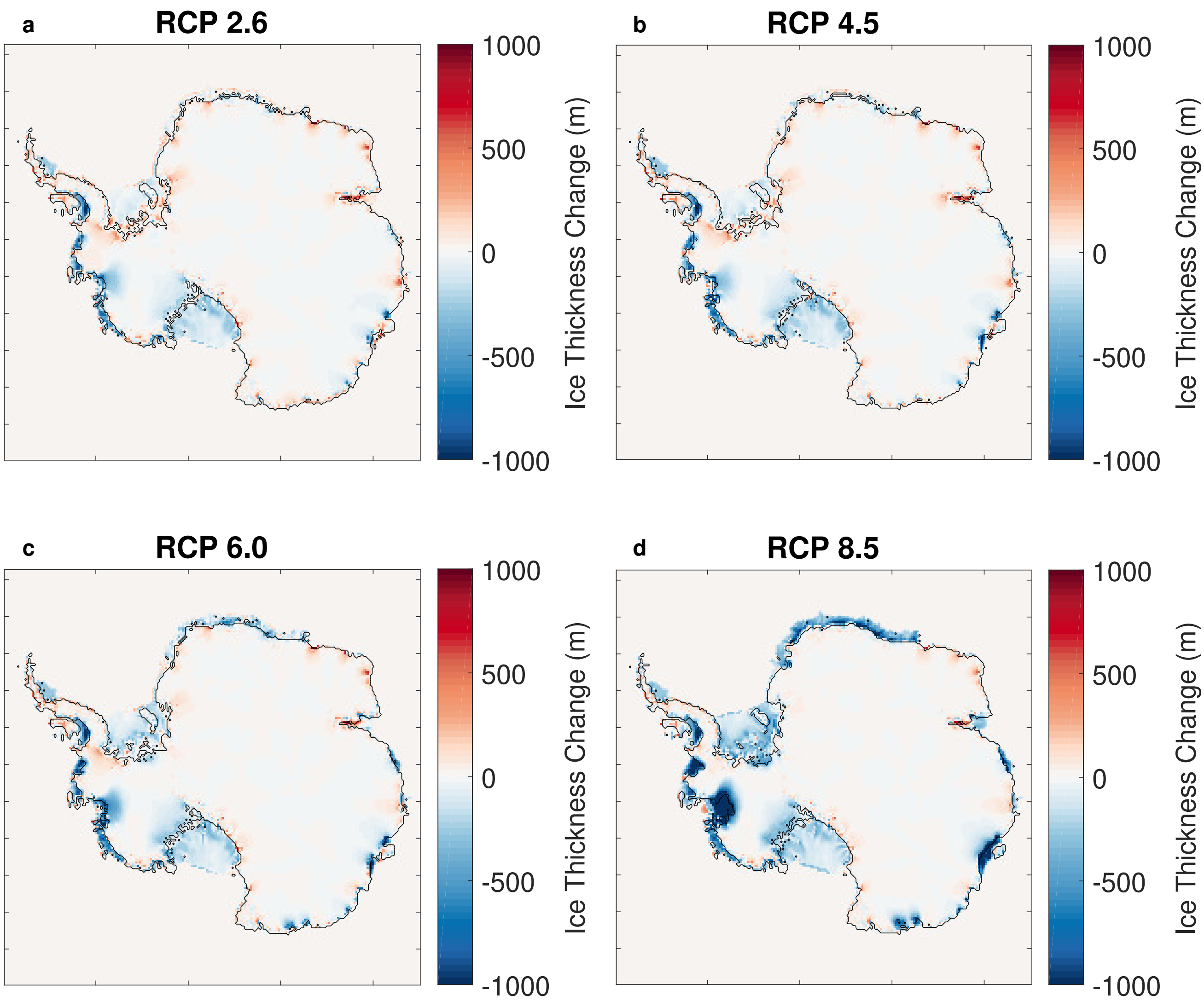

Figure S15. Ice thickness change at 2300 CE under RCP (a) 2.6, (b) 4.5, (c) 6.0, and (d) 8.5 for a simulation with uniform ELRA parameters (UNIBED) taken from Le Meur and Huybrechts (1996) and for which only bedrock adjustment is considered, i.e. gravitationally-consistent sea-level changes are not included.

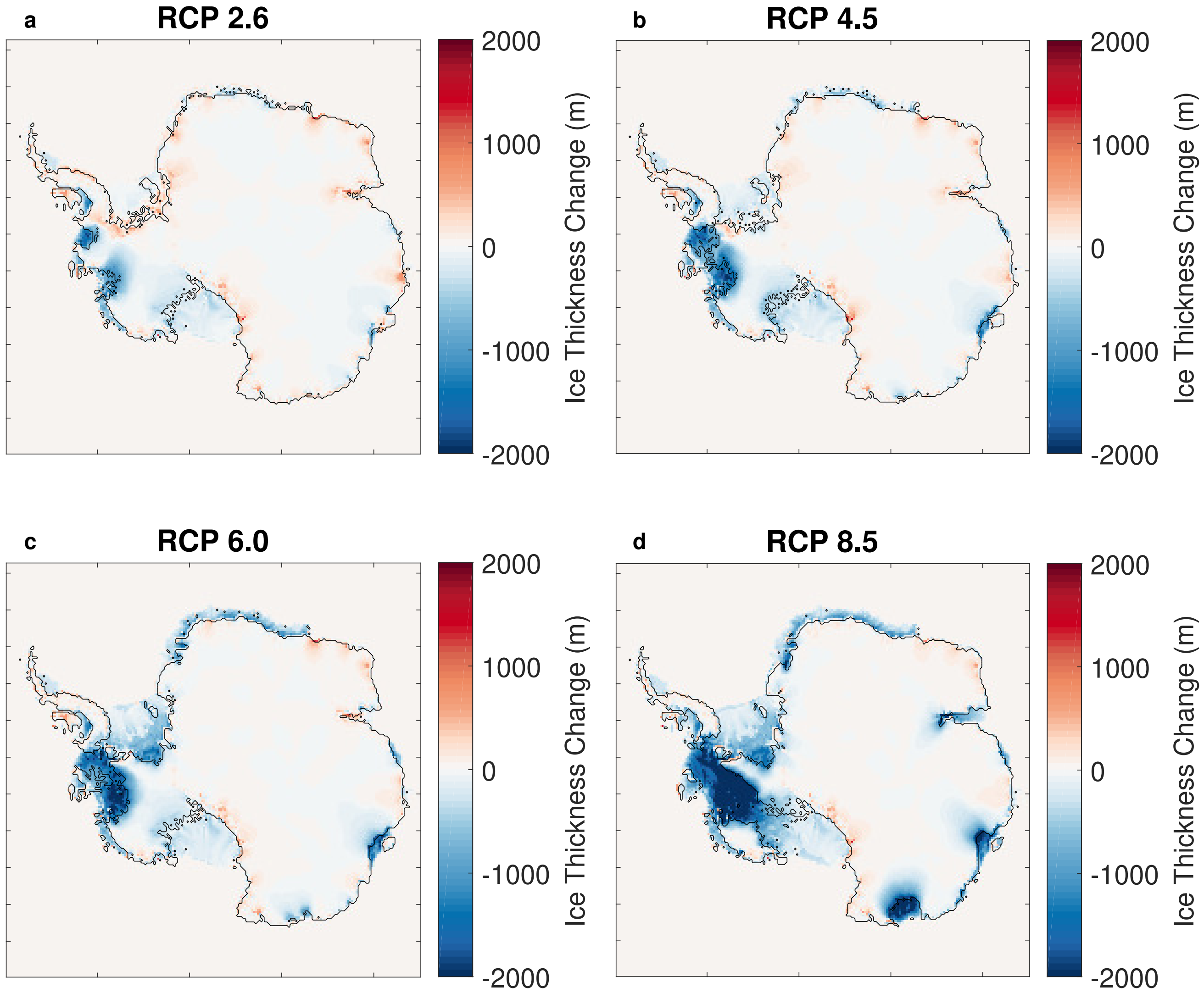

Figure S16. Ice thickness change at 3000 CE under RCP (a) 2.6, (b) 4.5, (c) 6.0, and (d) 8.5 for a simulation with uniform ELRA parameters (UNIBED) taken from Le Meur and Huybrechts (1996) and for which only bedrock adjustment is considered, i.e. gravitationally-consistent sea-level changes are not included.

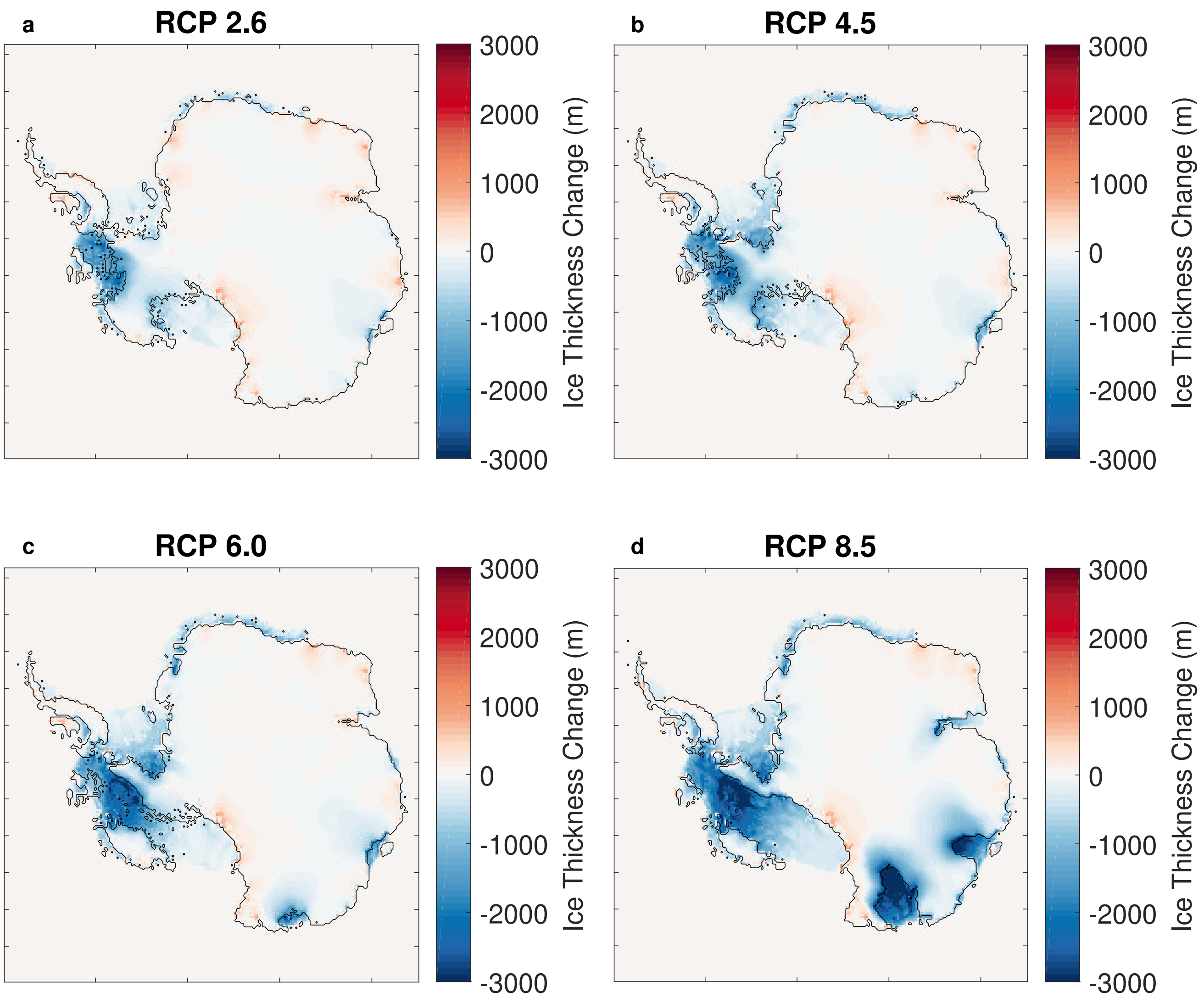

Figure S17. Ice thickness change at 5000 CE under RCP (a) 2.6, (b) 4.5, (c) 6.0, and (d) 8.5 for a simulation with uniform ELRA parameters (UNIBED) taken from Le Meur and Huybrechts (1996) and for which only bedrock adjustment is considered, i.e. gravitationally-consistent sea-level changes are not included.

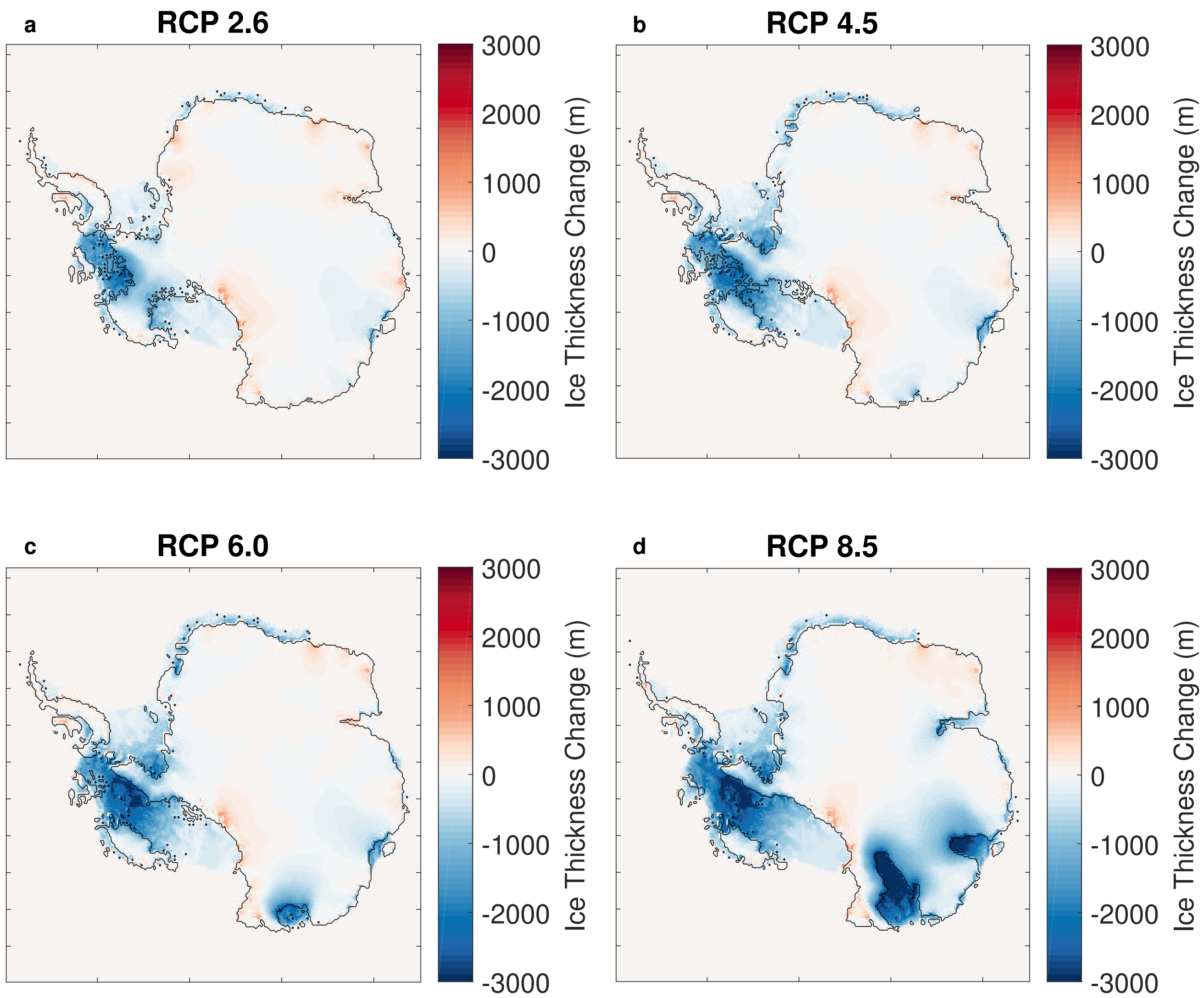

Figure S18. Ice thickness change at 7000 CE under RCP (a) 2.6, (b) 4.5, (c) 6.0, and (d) 8.5 for a simulation with uniform ELRA parameters (UNIBED) taken from Le Meur and Huybrechts (1996) and for which only bedrock adjustment is considered, i.e. gravitationally-consistent sea-level changes are not included.

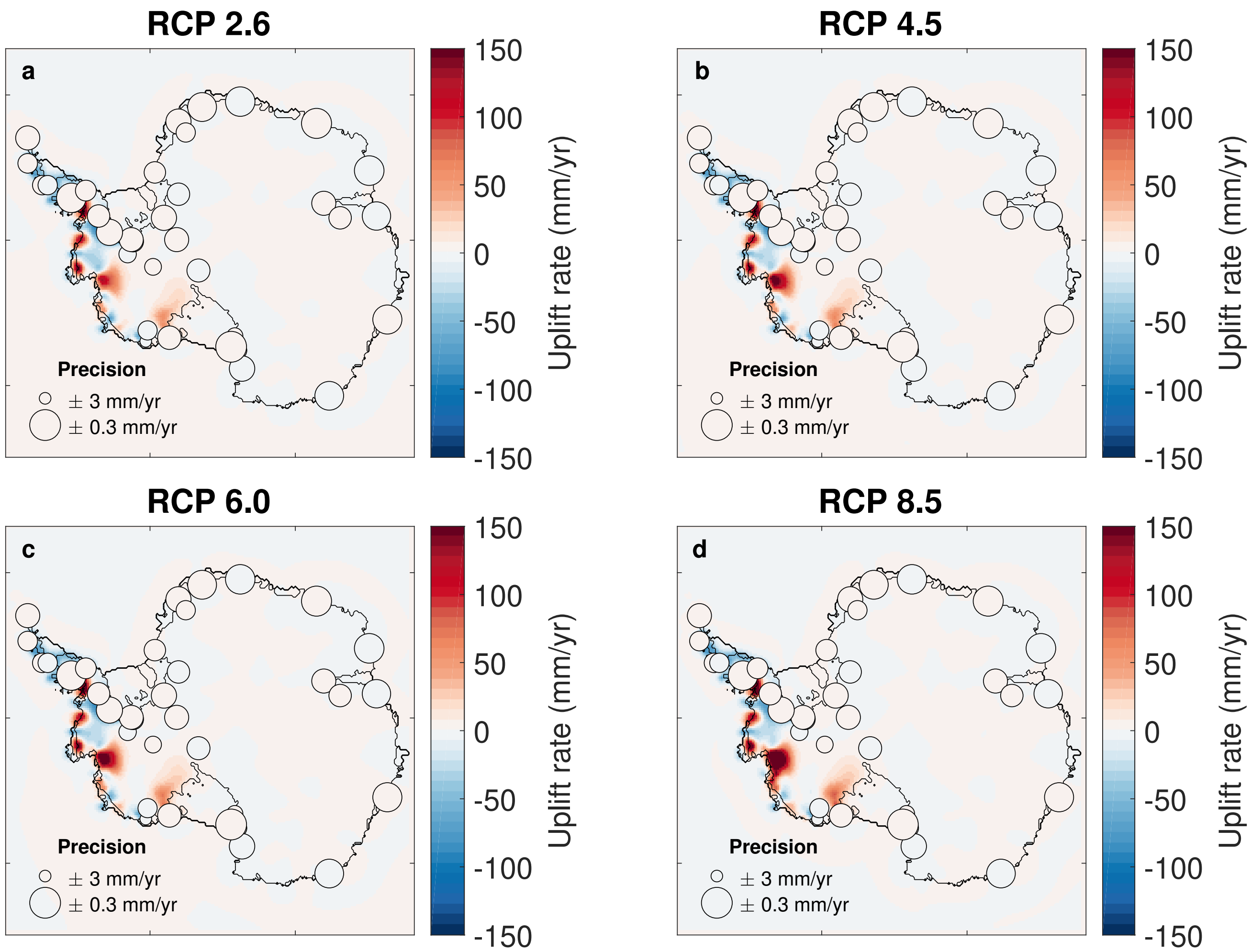

Figure S19. Mean uplift rates maps at 2100 CE predicted by the ensemble of 2000 Monte Carlo simulations under RCP (a) 2.6, (b) 4.5, (c) 6.0, and (d) 8.5. GPS observations of present-day uplift rates from Whitehouse, Bentley, Milne, et al. (2012) are plotted (colored circles) using the same colour scale. The radius of the circle at each GPS site is inversely proportional to the GPS uncertainty at that site.

APPENDIX B

SUPPLEMENTARY INFORMATION FOR CHAPTER 4

Supplementary Information

Violaine Coulon, Ann Kristin Klose, Christoph Kittel,
Ricarda Winkelmann, and Frank Pattyn

1 Ice sheet model setup and initialisation

The f.ETISh model is a vertically-integrated, thermomechanical, hybrid ice-sheet/ice-shelf model that incorporates essential characteristics of ice-sheet thermomechanics and ice-stream flow, such as the mass-balance feedback, bedrock deformation, sub-shelf melting, and calving. The ice flow is represented as a combination of the shallow-ice (SIA) and shallow-shelf (SSA) approximations for grounded ice while only the shallow-shelf approximation is applied for floating ice shelves (Bueler and Brown, 2009; Winkelmann et al., 2011). In order to account for grounding-line migration, a flux condition (Schoof, 2007, related to the ice thickness at the grounding line;) is imposed at the grounding line following the implementation by Pollard and DeConto (2012b, 2020). This implementation has been shown to reproduce the migration of the grounding line and its steady-state behavior (Schoof, 2007) at coarse resolution (Pattyn et al., 2013; Pollard and DeConto, 2020). Numerical simulations of the AIS using a flux condition have also been able to simulate marine ice-sheet behavior in large-scale ice-sheet simulations (Pollard and DeConto, 2012b; DeConto and Pollard, 2016; Pattyn, 2017; Sun et al., 2020). While the use of such a flux condition has been challenged, especially with respect to ice shelf buttressing and regimes of low driving and basal stresses (Haseloff and Sergienko, 2018; Pegler, 2018; Reese et al., 2018; Sergienko and Wingham, 2019), Pollard and DeConto (2020) demonstrate that the algorithm gives similar results under buttressed conditions compared to high-resolution models. Basal sliding is introduced as a Weertman sliding law, i.e.,

$$v_b = -A_b|\tau_b|^{m-1}\tau_b \tag{1}$$

where τ_b is the basal shear stress, v_b the basal velocity, A_b the basal sliding coefficient – whose values are inferred following the nudging method of Pollard and DeConto (2012a) – and $m = 3$ a sliding exponent. Basal melting underneath the floating ice shelves may be determined by different sub-shelf melt parameterisation schemes, such as the PICO model (Reese et al., 2018), the Plume model (Lazeroms et al., 2019), and simple parameterisations (Jourdain et al., 2020; Burgard et al., 2022). Calving at the ice front depends on the combined penetration depths of surface and basal crevasses, relative to total ice thickness. The depths of the surface and basal crevasses are parameterised as functions of the divergence of ice velocity, the accumulated strain, the ice thickness, and (if desired) surface liquid water availability, similar to Pollard et al. (2015) and DeConto and Pollard (2016). Prescribed input data include the present-day ice-sheet geometry and bedrock topography from the Bedmachine dataset (Morlighem et al., 2019) and the geothermal heat flux by Shapiro and Ritzwoller (2004). Present-day mean surface air temperature and precipitation are obtained either from van Wessem et al. (2018), based on the regional atmospheric climate model RACMO2.3p2, or from Kittel et al. (2021), based on the regional climate model MARv3.11. In order to correct the surface mass balance for elevation changes, we assume that a 1°C increase in air temperature accounts for a ∼5% increase in precipitation. Surface temperatures are corrected for elevation changes according to a vertical lapse rate (Pollard and DeConto, 2012b). Surface melt is determined from a Positive Degree-Day model (Huybrechts and De Wolde, 1999). We employed data by either Schmidtko et al. (2014) or Jourdain et al. (2020) for present-day ocean temperature and salinity on the continental shelf. Changes in bedrock elevation due to changes in ice load are modelled by the commonly used Elastic Lithosphere–Relaxed Asthenosphere

(ELRA) model where the solid-Earth system is approximated by a thin elastic lithosphere plate lying upon a relaxing viscous asthenosphere (Brotchie and Silvester, 1969; Le Meur and Huybrechts, 1996). The viscoelastic properties of the Antarctic solid Earth are considered as spatially-uniform and approximated using an asthenosphere relaxation time τ of 3000 years and a flexural rigidity of the lithophere D of 10^{25} $\mathrm{N\,m}$.

Ice-sheet initial conditions and basal sliding coefficients are provided by an inverse simulation following Pollard and DeConto (2012a), using mass-balance forcing for the year 1950 (anomalies for the period 1945-1955 respective to the period 1995-2014 derived from CMIP5 NorESM1-M climate projection are added to a present-day climatology for the 1995-2014 period provided by a RCM). In the inverse procedure, basal sliding coefficients under grounded ice, and sub-shelf melt rates under floating ice (Bernales et al., 2017) are adjusted iteratively to reduce the misfit with observed ice thickness. The obtained sub-shelf melt rates may therefore be regarded as the balance melt rates and are independent of the ocean boundary conditions (forcing). For consistency, different initial states are only produced for each atmospheric present-day climatology. Therefore, initial ice-sheet conditions (ice thickness, bed elevation, velocity, basal sliding coefficients and internal ice and bed temperatures) are identical in all simulations that use the same present-day atmospheric climatology (either derived from RACMO2.3p2, or MARv3.11) and are in steady-state with the initial atmospheric boundary conditions. To limit an initial shock caused by the transition from the balance sub-shelf melt rates derived during the transient nudging spin-up to the imposed sub-shelf melt parameterisation scheme, a short 20-yr relaxation is run after the model initialisation, before the historical simulation. Our initial states are therefore considered as quasi-equilibrated states. The two initialised ice sheet configurations resulting from the nudging spin-ups are within the range of the ISMIP6 models (Seroussi et al., 2019), and well match observations in terms of ice geometry, grounding-line position, and ice dynamics (Figures 1 and 2). In comparison to other ISMIP6 models, the root mean square error (RMSE) is within the range for both ice thickness (RMSE $\sim 50\,\mathrm{m}$) and ice surface velocity (RMSE $\sim 100\,\mathrm{m\,yr^{-1}}$).

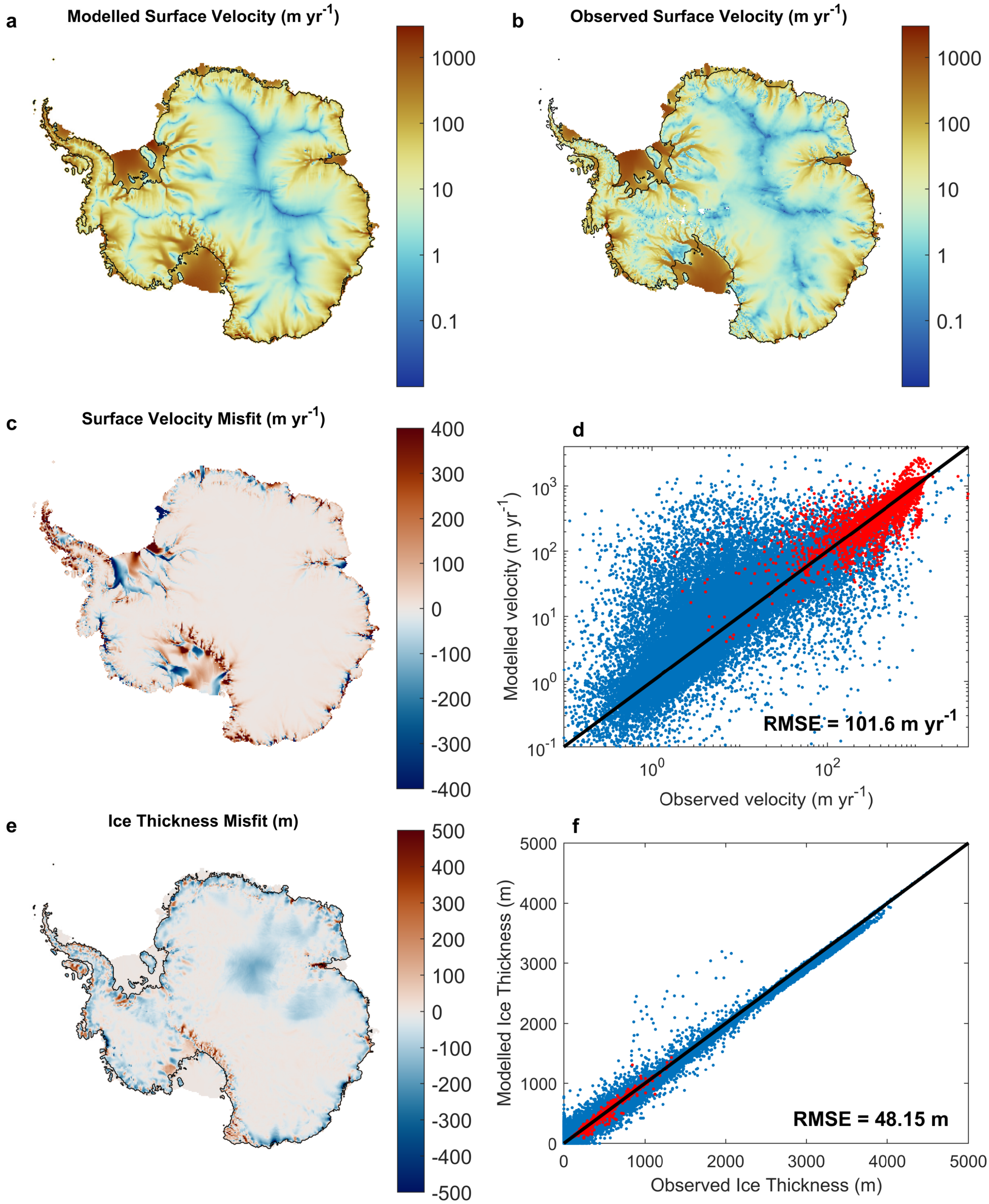

Figure 1: Ice-sheet initial state obtained with the 1995-2014 atmospheric climatology from MARv3.11 (Kittel et al., 2021). Shown is a comparison of the ice sheet thickness and ice velocities as modeled by f.ETISh in the year 1950 (i.e. after the initialisation) to observed ice sheet thickness (Morlighem et al., 2019, Bedmachine;) and velocities (Rignot et al., 2011), using the atmospheric climatology derived from MAR. Modeled and observed surface velocity is illustrated in (a) and (b). Modeled minus observed ice velocity and thickness are given in (c) and (e) with the modeled grounding line in black, respectively, while scatter plots for comparison are shown in (d) and (f).

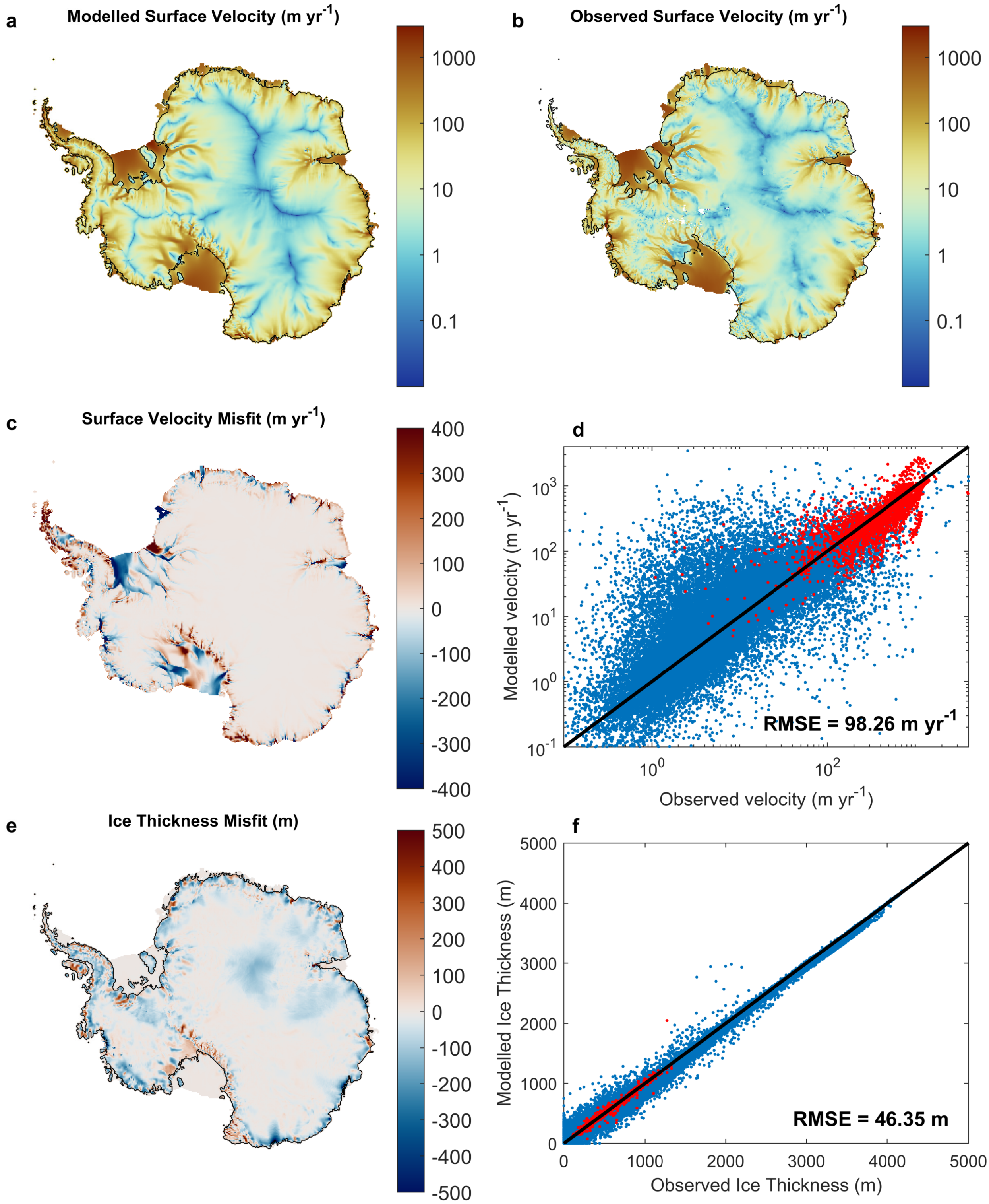

Figure 2: Ice-sheet initial state obtained with the 1995-2014 atmospheric climatology from RACMO2.3p2 (van Wessem et al., 2018). Shown is a comparison of the ice sheet thickness and ice velocities as modeled by f.ETISh in the year 1950 (i.e. after the initialisation) to observed ice sheet thickness (Morlighem et al., 2019, Bedmachine;) and velocities (Rignot et al., 2011), using the atmospheric climatology derived from MAR. Modeled and observed surface velocity is illustrated in (a) and (b). Modeled minus observed ice velocity and thickness are given in (c) and (e) with the modeled grounding line in black, respectively, while scatter plots for comparison are shown in (d) and (f).

2 PDD-based melt-and-runoff model

At the beginning of every year, the air temperature and the precipitation rate are used as inputs to a positive degree-day (PDD) algorithm that calculates the yearly surface mass balance at the ice surface by capturing the basic physical processes of surface melting of ice and refreezing versus runoff in the snow column (Huybrechts and de Wolde, 1999; Seguinot, 2013). More specifically, similar to Tsai et al. (2020), the algorithm involves seasonal cycles of zero-dimensional bulk quantities of snow and embedded melt water, run through several years to equilibrium with a weekly time step, driven by seasonal variations of the air temperatures and precipitation rate interpolated in time to those time steps. A PDD scheme calculates the melt of snow or exposed ice at each weekly timestep (with a uniform normal distribution of standard deviation $\sigma_{PDD} = 4 \deg C$ around the monthly mean T_m, representing diurnal cycles and synoptic variability) while tracking the evolving thickness of the snow layer across the balance year. Surface melt is proportional to the amount of positive degree days, using coefficients of 3 and 8 mm water equivalent of melt per degree (C) day for snow and ice, respectively. Accumulation is assumed equal to precipitation when the daily temperature (also assumed to have a normal distribution around the monthly mean, using a smaller standard deviation of $3.5 \deg C$ to account for the smaller variations in temperature during cloudy days when precipitation occurs) is below 0 °C, and decreasing linearly with temperature between 0 and 2 °C (above which precipitation is then interpreted as rain Seguinot, 2013). After seasonal equilibrium is reached, net annual quantities are used to calculate the refreezing of melt water (which depends on the cold content of the upper ice sheet layers; Huybrechts and de Wolde, 1999), and runoff of excess meltwater once the snow is saturated. Values of all parameters used in this melt-and-runoff scheme were calibrated to outputs from both regional (MAR forced by CMIP6 projections until the year 2100; Kittel et al., 2021) and global climate models (CESM2 until the year 2300 – one of the few CMIP models that include a multi-layered snow model and prognostically calculated snow albedo as a function of snow grain size; Lenaerts et al., 2016; Dunmire et al., 2022) under high-warming scenario. Comparison of the calibrated PDD-based melt-and-runoff models with theses climate models projections are displayed in Figures 3 and 4. It is important to note that since the melt-and-runoff model is not used during the initialisation procedure (see Appendix 1) SMB anomalies derived from the PDD-based melt-and-runoff model are used instead of absolute SMB values in order to maintain the steady-state with respect to initial (1950 CE) atmospheric conditions under unforced conditions. These anomalies are calculated with respect to the SMB reproduced by the melt-and-runoff scheme under the mean 1945-1955 air temperature and precipitation conditions.

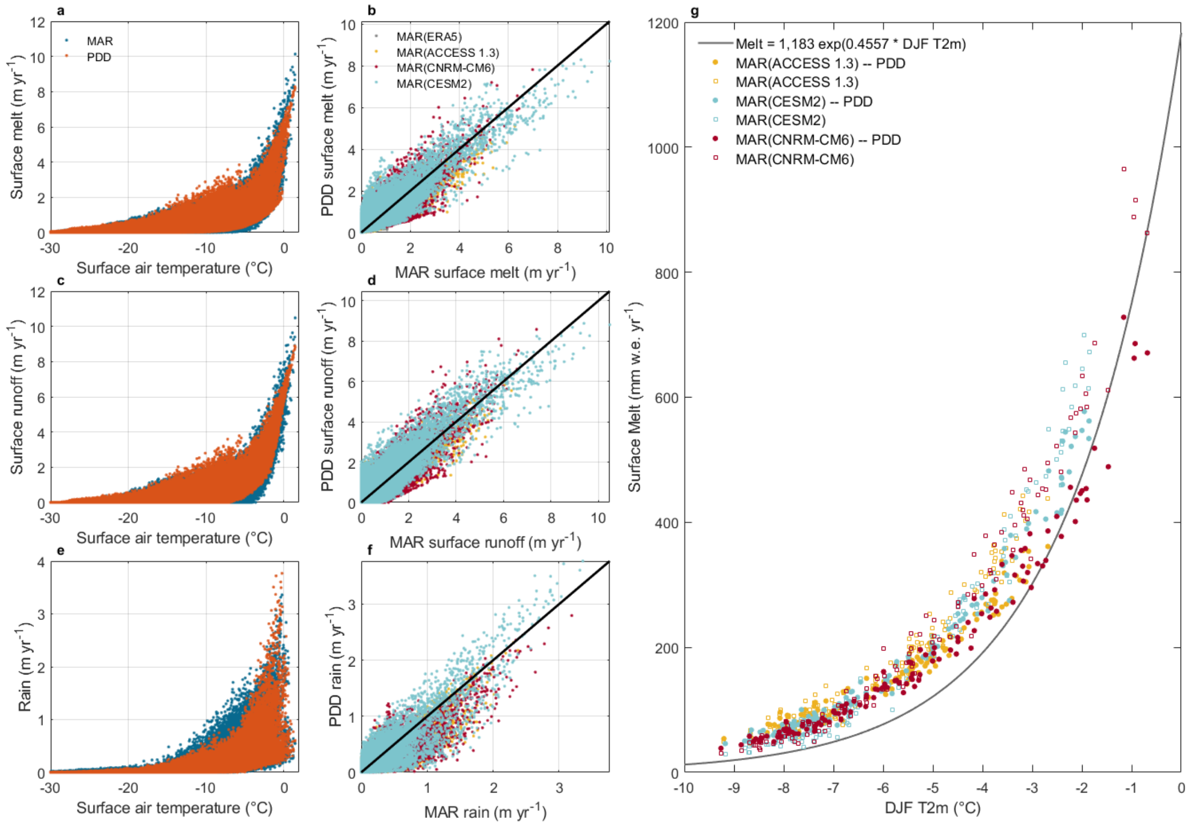

Figure 3: **Comparison of outputs from the positive degree-day (PDD)-based melt-and runoff model with outputs from MAR.** Comparison of yearly surface melt (a-b), runoff (c-d) and rainfall (e-f) rates reproduced by the PDD model with outputs from MAR forced by ERA5 over the 1979-2015 period and by ACCESS1.3, CNRM-CM6 and CESM2 under the RCP8.5 and SSP5-85 scenario, respectively, over the 1980-2100 period. The PDD model uses monthly-mean 2-m air temperature and precipitation rate as inputs, using standard deviations of the daily temperature $\sigma_{PDD} = 4$ °C and $\sigma_{RS} = 3.5$ °C, the precipitation cutoff values $T_{snow} = 0$ °C and $T_{rain} = 2$ °C, the degree-day factor for snow melt K_{snow} of $0.003 w.e.mPDD^{-1}$ and a degree-day factor for ice melt K_{ice} of $0.008 w.e.mPDD^{-1}$. The relation between the surface melt (a), runoff (b) and the yearly rain (c) with respect to the 2-m air temperature are compared in (a,c,e), with the PDD model displayed by the blue dots and MAR outputs by the purple dots. Figures b,d,f, display point-by-point scatter-plots comparing equivalent quantities, with outputs from the different MAR projections represented by different colors. Figure g compares the mean yearly surface melt and DJF 2-m air temperature over the ice shelves, reproduced by the PDD model and by MAR under for the period 1980-2100. The relation derived by Trusel et al. (2015) is shown for comparison.

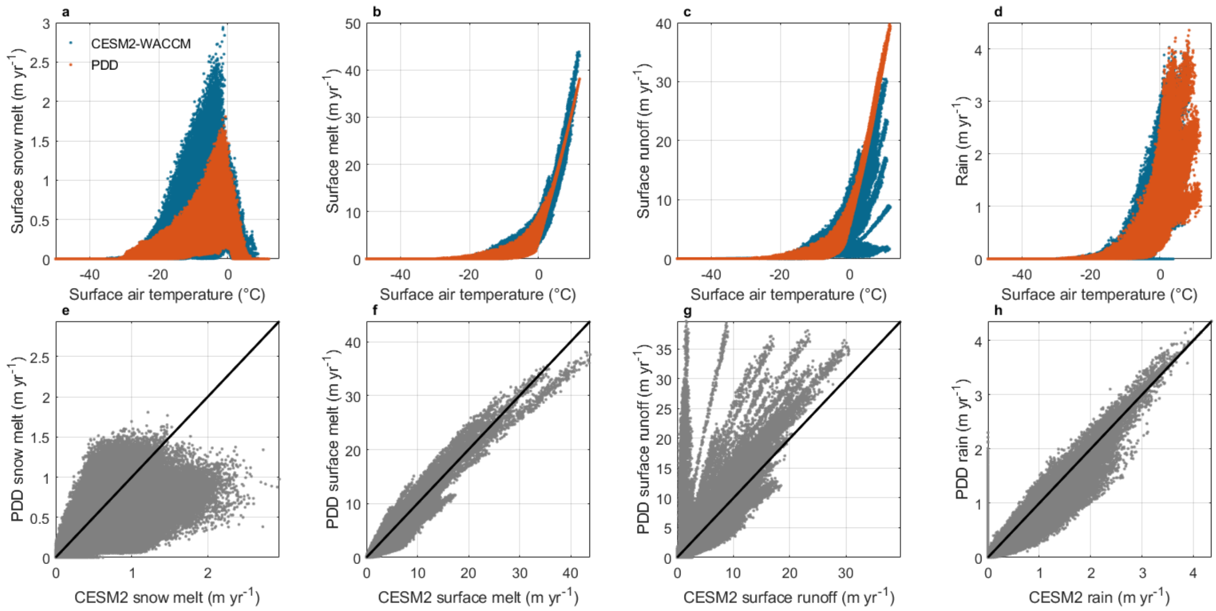

Figure 4: **Comparison of outputs from the positive degree-day (PDD)-based melt-and runoff model with outputs from CESSM2-WACCM.** Comparison of yearly surface melt (a, d), runoff (b,e) and rain (c,f) reproduced by the PDD model with outputs from CESM2 under the SSP5-85 scenario over the 2015-2300 period. The PDD model uses monthly-mean 2-m air temperature and precipitation rate as inputs, using standard deviations of the daily temperature $\sigma_{PDD} = 4$ °C and $\sigma_{RS} = 3.5$ °C, the precipitation cutoff values $T_{snow} = 0$ °C and $T_{rain} = 2$ °C, the degree-day factor for snow melt K_{snow} of $0.003 w.e.m PDD^{-1}$ and a degree-day factor for ice melt K_{ice} of $0.008 w.e.m PDD^{-1}$. The relation between the snow melt (a), total surface melt (b), runoff (c) and the yearly rain (d) with respect to the 2-m air temperature are compared in (a–d), with the PDD model displayed by the blue dots and CESM2 outputs by the yellow dots. Figures (e–h), display point-by-point scatter-plots comparing equivalent quantities.

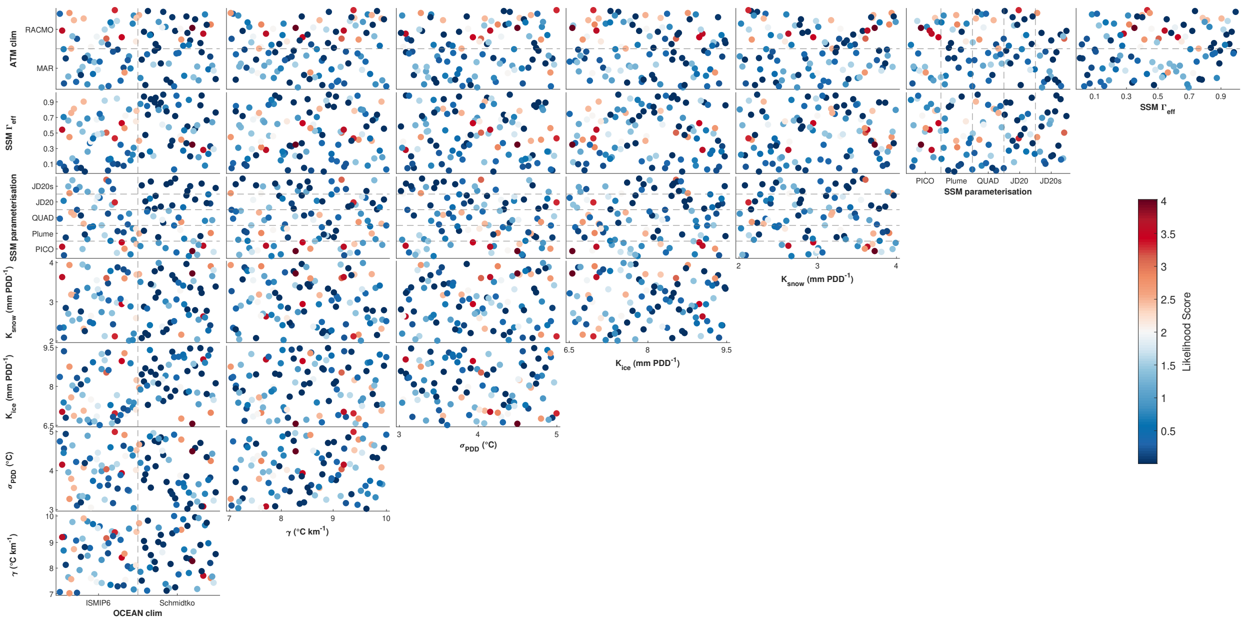

Figure 5: Likelihood weight for the 100-members ensemble of simulations accounting for key uncertainties in ice-ocean and ice-atmosphere interactions over the 8-D parameter space. The parameters are the atmospheric (ATM clim) and oceanic (OCEAN clim) present-day climatologies, the applied sub-shelf melt parameterisation (SSM parameterisation), the effective ice–ocean heat flux (SSM Γ_{eff}), the positive degree-day (PDD) snow melt factor (K_{snow}), the PDD ice melt factor (K_{ice}), the PDD standard deviation of temperature variability (σ_{PDD}), and the atmospheric lapse rate (γ). For visibility, contours were derived by interpolating the obtained weight in the parameter space. Note that for the parameters characterised by discrete values, i.e., ATM clim, OCEAN clim, and SSM parameterisation, the continuous parameter space is divided into a finite number of equal probability regions, or bins, displayed by the dashed lines.

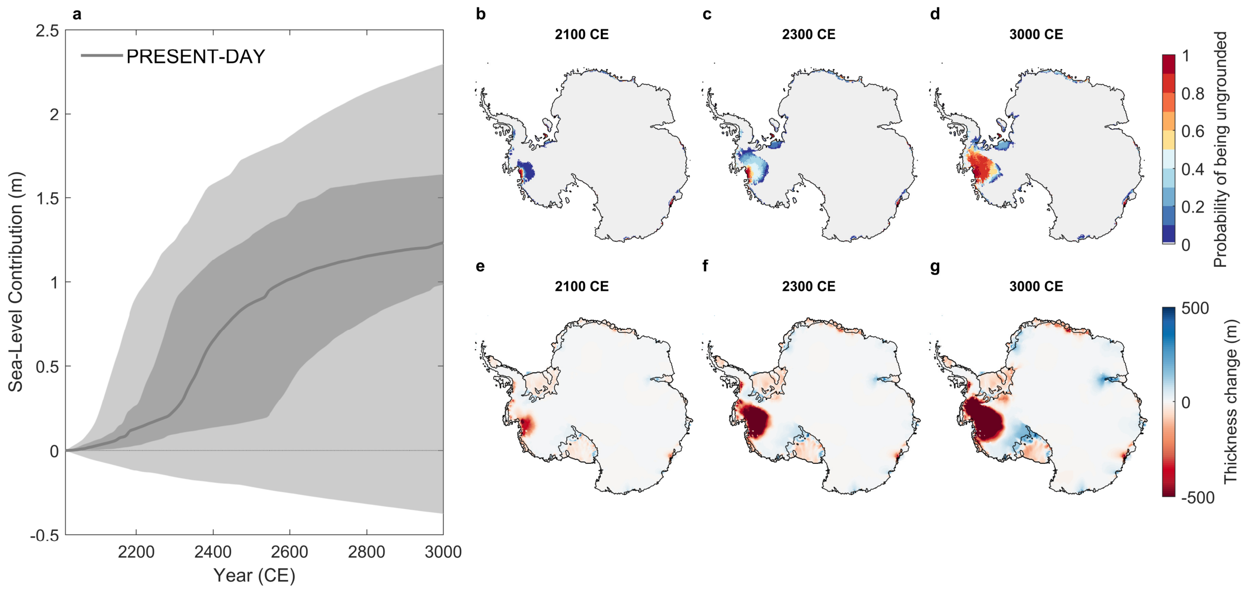

Figure 6: Calibrated probabilistic projections of the Antarctic ice sheet (AIS) contribution to global-mean sea-level rise until the end of the millennia under constant present-day climate conditions. a., Evolution of the ensemble projected contribution to sea-level from the AIS. Solid lines and shaded regions show the median and 25-75% and 5-95% probability intervals (N=100), with 5-year smoothing applied. b-d., Marginal probability of being ungrounded at 2115 (b), 2315 (c) and 3015 (d). Grey regions correspond to locations where there is a 0% probability of being ungrounded. f-g., Mean ice thickness change at 2115 (f), 2315 (g) and 3015 (h). The marginal probability of being ungrounded and the mean thickness change at a given point are computed using the Bayesian calibrated means of the ensemble. Present-day grounding lines are shown in black.

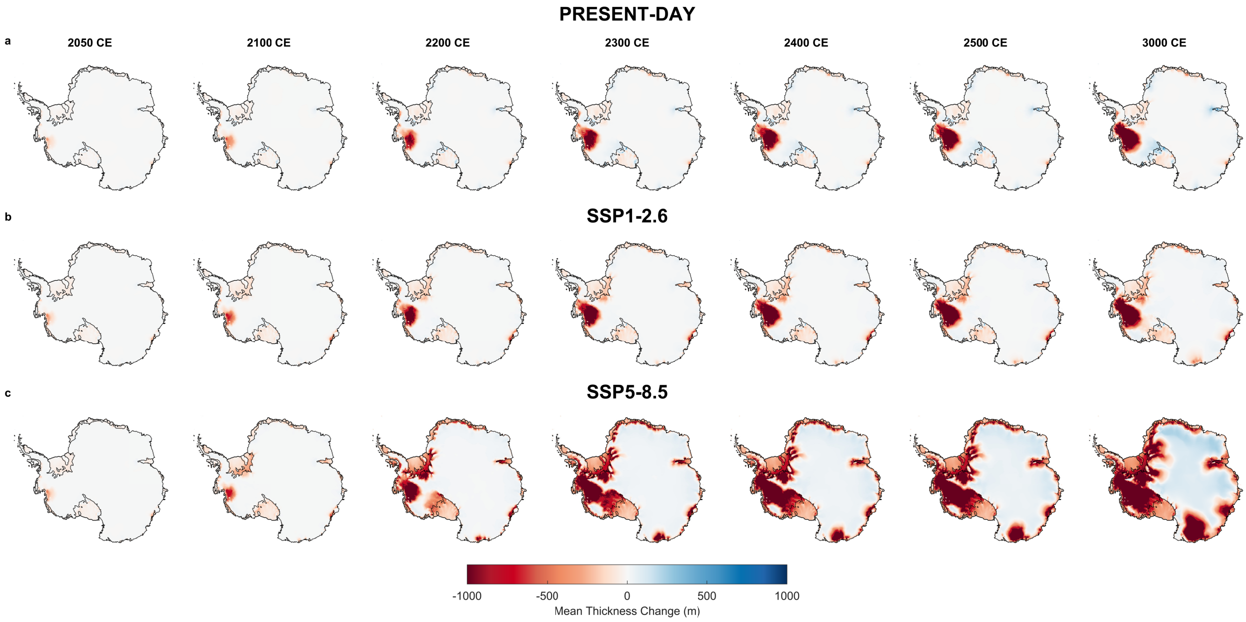

Figure 7: Mean ice thickness change under (a) constant present-day climate conditions (PRESENT-DAY), shared socio-economic pathways (SSP) 1-2.6 (b) and 5-8.5 (c) at different snapshots throughout the millennia. For each scenario, the mean thickness change at a given point is computed using the Bayesian calibrated mean of the ensemble (N=100 for PRESENT-DAY, and N=400 for SSP1-2.6 and SSP5-8.5). Present-day grounding lines are shown in black.

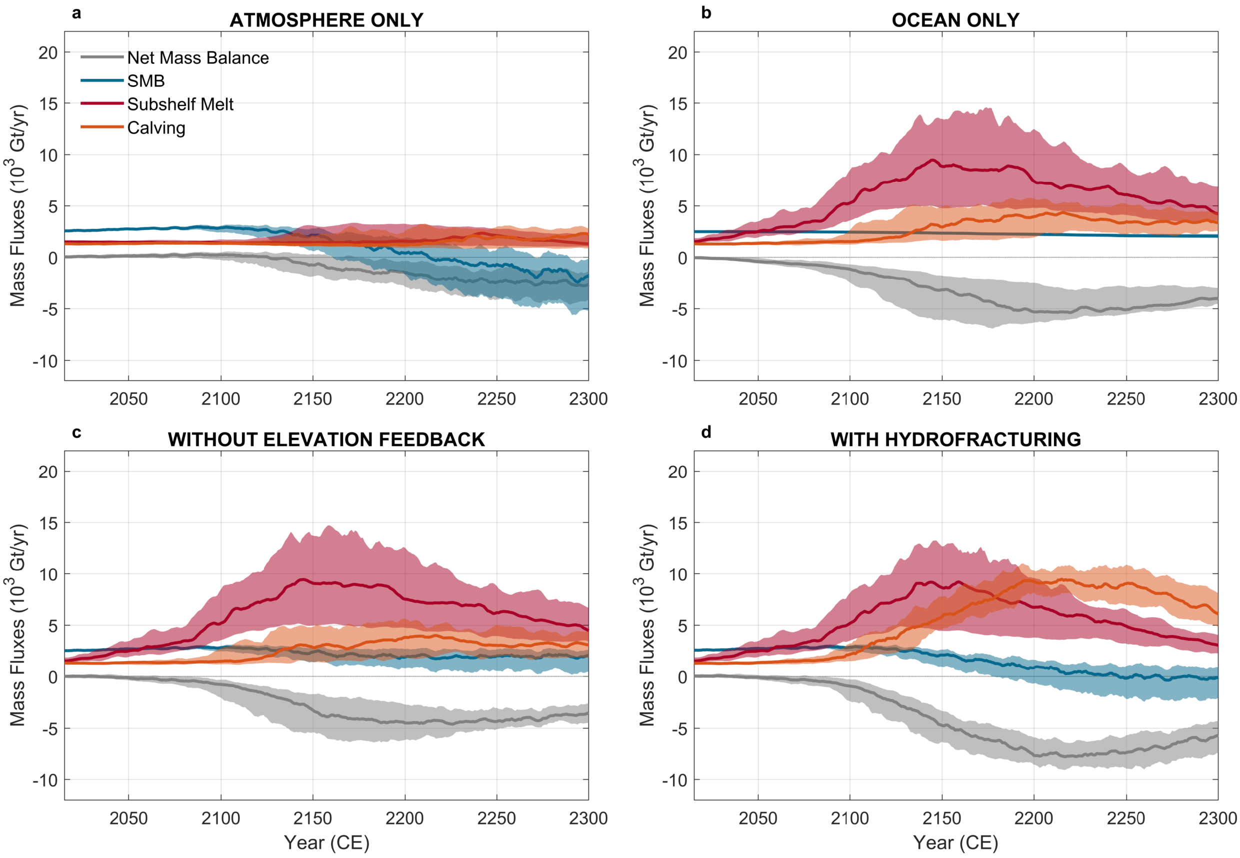

Figure 8: Evolution of the projected main mass balance components in an additional 100-member calibrated ensemble where the choice of the Earth System model (ESM) is included in the Latin hypercube sampled parameter space under the shared socio-economic pathway (SSP) 5-8.5 (a) with the atmospheric forcing only, (b) with the oceanic forcing only, (c) without the elevation feedback, and (d) with hydrofracturing. Time series of the contribution to sea-level over the millennia are color-coded according to the applied ESM. Solid lines and shaded regions show the median and 25-75% probability intervals (N=100 per SSP scenario), with 5-year smoothing applied. The ice-sheet net mass balance net mass balance considers changes in volume above flotation and may therefor be interpreted as the rate of mass change contributing to sea-level rise.

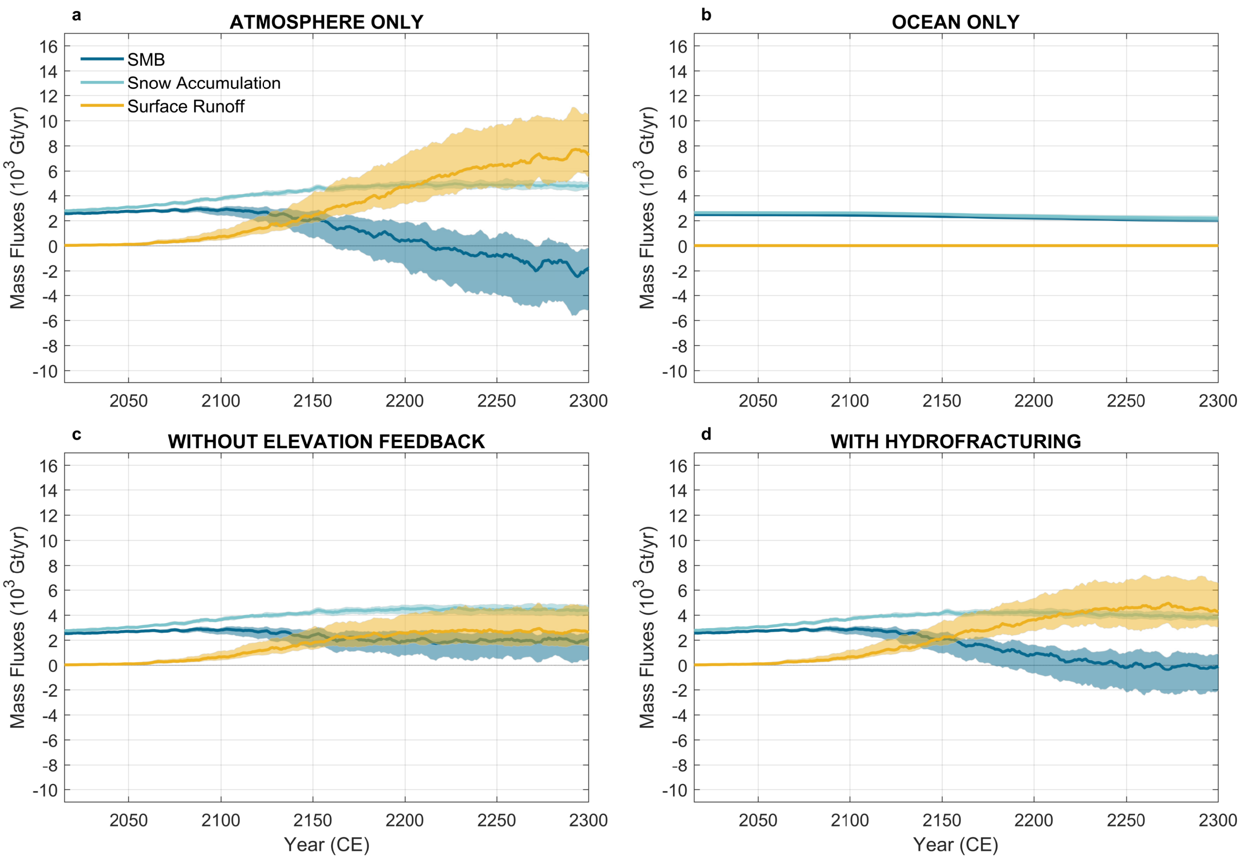

Figure 9: Evolution of the projected main surface mass balance components in an additional 100-member calibrated ensemble where the choice of the Earth System model (ESM) is included in the Latin hypercube sampled parameter space under the shared socio-economic pathway (SSP) 5-8.5 (a) with the atmospheric forcing only, (b) with the oceanic forcing only, (c) without the elevation feedback, and (d) with hydrofracturing. Time series of the contribution to sea-level over the millennia are color-coded according to the applied ESM. Solid lines and shaded regions show the median and 25-75% probability intervals (N=100 per SSP scenario), with 5-year smoothing applied.

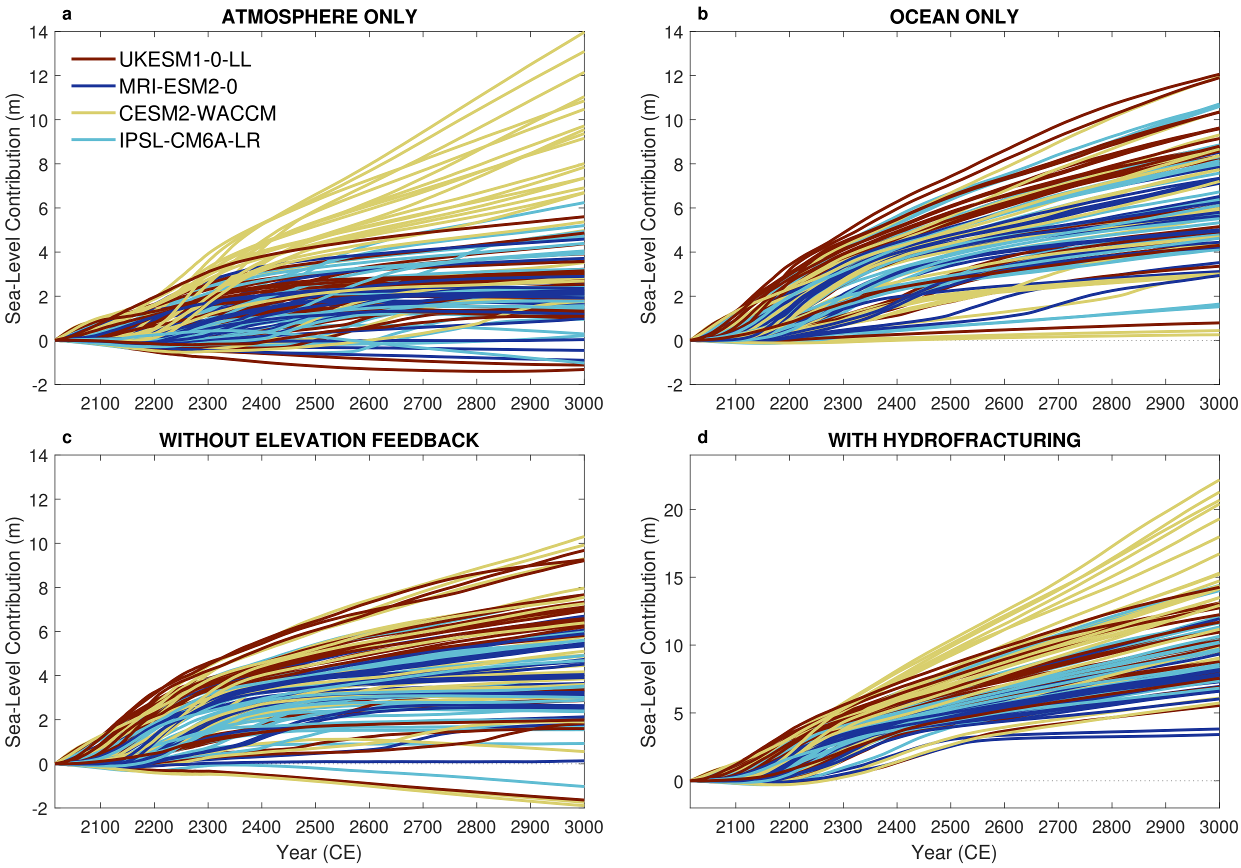

Figure 10: Influence of the climate model on the Antarctic projected sea-level contribution in an additional 100-member calibrated ensemble where the choice of the Earth System model (ESM) is included in the Latin hypercube sampled parameter space under the shared socio-economic pathway (SSP) 5-8.5 (a) with the atmospheric forcing only, (b) with the oceanic forcing only, (c) without the elevation feedback, and (d) with hydrofracturing. Time series of the contribution to sea-level over the millennia are color-coded according to the applied ESM.

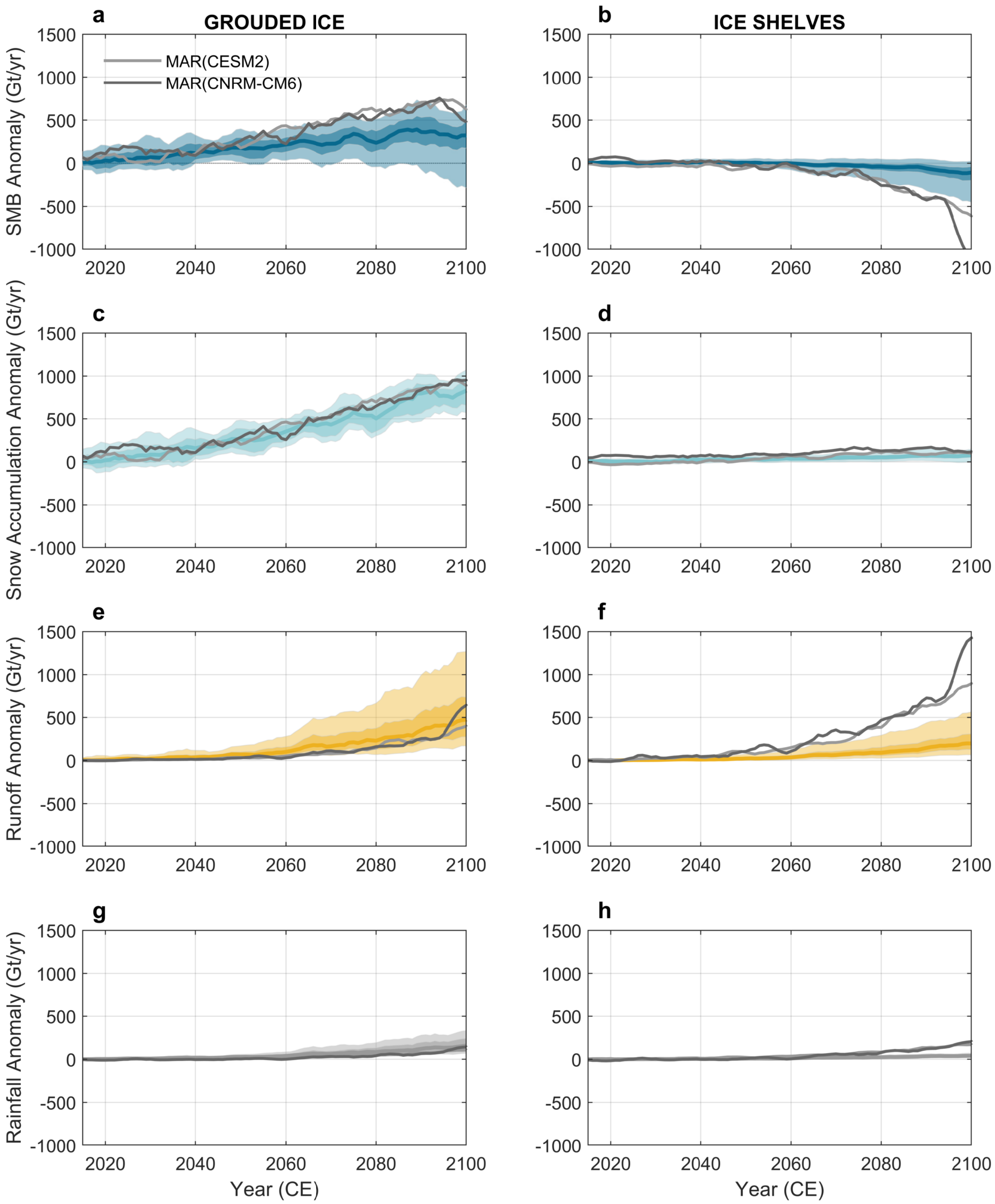

Figure 11: Evolution of the calibrated probabilistic projections of the Antarctic integrated main surface mass balance components until the year 2300 CE over the grounded ice sheet (a,c,e,g) and the ice shelves (b,d,f,h) compared with projections from MAR. Evolution of the ensemble projected anomalies in total surface mass balance (a—b), snow accumulation (c—d), surface runoff (e—f), and rain precipitation (g—h) for the 2015-2300 period under the shared socio-economis pathway (SSP) 5-8.5 over the grounded ice sheet (left) and the ice shelves (right). Colored solid lines and shaded regions show the median, 25-75%, and 5-95% probability intervals (N=400 per SSP scenario), with 5-year smoothing applied. Grey solid lines show time series of the integrated annual SMB components simulated by MAR forced by CNRM-CM6-1 (dark grey), and CESM2 (light grey).

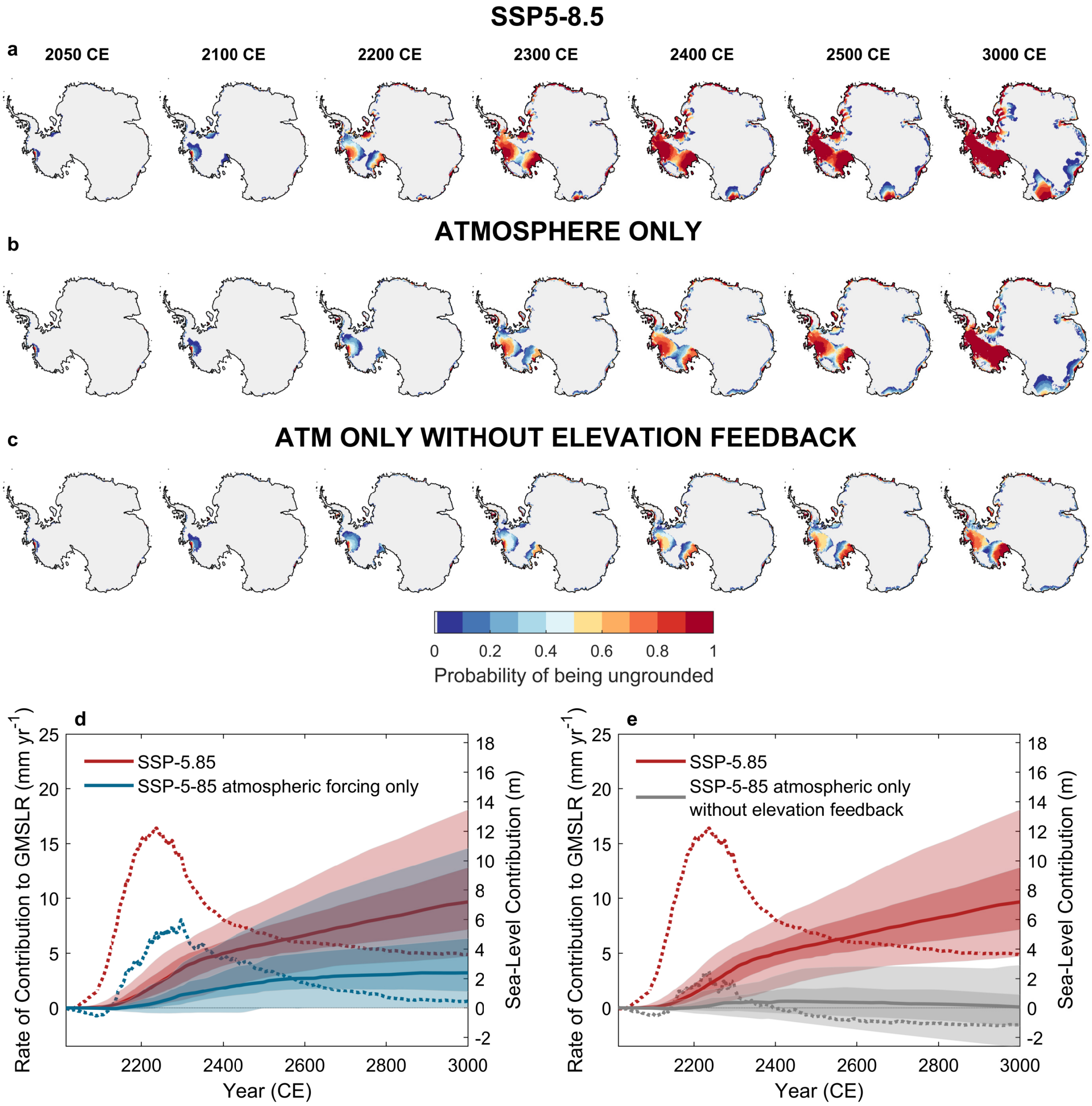

Figure 12: **Contribution of atmospheric forcing and SMB-elevation feedback to projected Antarctic mass changes under high-emission pathway.** Marginal probability of being ungrounded under shared socio-economic pathways (SSP) 5-8.5 considering (a) the combination of atmospheric and oceanic forcings (b) the atmospheric forcing only, and (c) the atmospheric forcing only without the elevation feedback, at different snapshots throughout the millennia. For each, the marginal probability of being ungrounded at a given point is computed using the Bayesian calibrated mean of the ensemble (N=100 for atmospheric/oceanic forcing only, and N=400 for SSP5-8.5). Grey regions correspond to locations where there is a 0% probability of being ungrounded. Present-day grounding lines are shown in black. Figures e—f show the evolution of the calibrated projected contribution to global mean sea-level rise (GMSLR) from Antarctica under SSP5-8.5 until 3000 CE, compared with a smaller calibrated ensemble of projections considering (e) the atmospheric forcing only, and (f) the oceanic forcing only. Solid lines and shaded regions show the median and 25-75% and 5–95% probability intervals with 5-year smoothing applied. Dashed lines show the median rate of contribution to GMSLR. Projections with atmospheric forcing only are applied to a 100-members ensemble of simulations for which the ESM is part of the Latin hypercube sampling (i.e., 9-D parameter space).

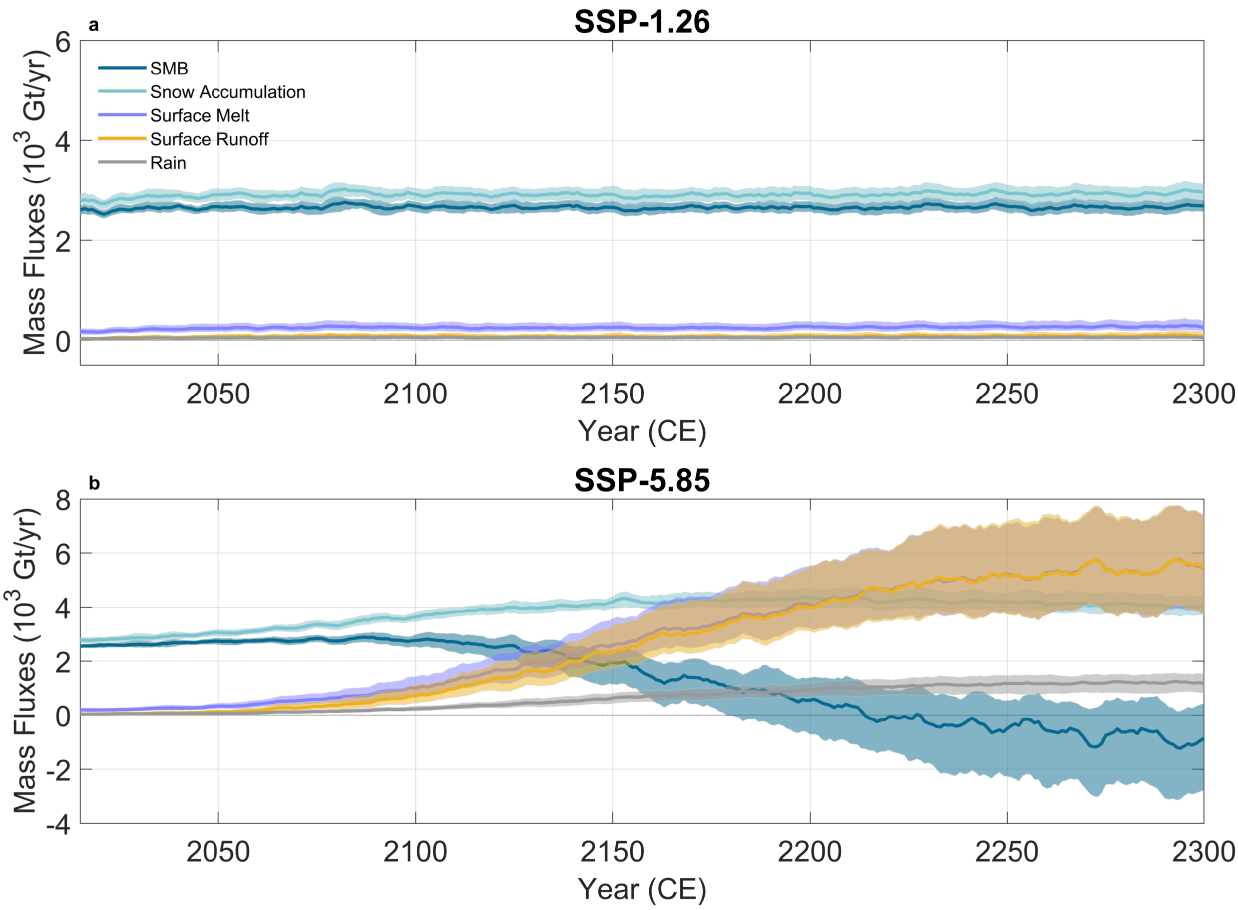

Figure 13: Evolution of the calibrated probabilistic projections of the Antarctic integrated main surface mass balance components until the year 2300 CE over under (a) SSP1-2.6 and (b) SSP5-8.5. Colored solid lines and shaded regions show the median, 25-75%, and 5-95% probability intervals (N=400 per SSP scenario), with 5-year smoothing applied.

References

Bernales, J., Rogozhina, I., and Thomas, M. (2017). Melting and freezing under antarctic ice shelves from a combination of ice-sheet modelling and observations. *Journal of Glaciology*, 63(240):731–744.

Brotchie, J. F. and Silvester, R. (1969). On Crustal Flexure. *Journal of Geophysical Research*, 74(22):5240–5252.

Bueler, E. and Brown, J. (2009). Shallow shelf approximation as a “sliding law” in a thermomechanically coupled ice sheet model. *Journal of Geophysical Research: Earth Surface*, 114(F3).

Burgard, C., Jourdain, N. C., Reese, R., Jenkins, A., and Mathiot, P. (2022). An assessment of basal melt parameterisations for antarctic ice shelves. *The Cryosphere Discussions*, 2022:1–56.

DeConto, R. M. and Pollard, D. (2016). Contribution of Antarctica to past and future sea-level rise. *Nature*, 531:591–597.

Dunmire, D., Lenaerts, J. T. M., Datta, R. T., and Gorte, T. (2022). Antarctic surface climate and surface mass balance in the community earth system model version 2 (1850–2100). *The Cryosphere Discussions*, 2022:1–28.

Haseloff, M. and Sergienko, O. V. (2018). The effect of buttressing on grounding line dynamics. *Journal of Glaciology*, 64(245):417–431.

Huybrechts, P. and de Wolde, J. (1999). The dynamic response of the greenland and antarctic ice sheets to multiple-century climatic warming. *Journal of Climate*, 12(8):2169–2188.

Huybrechts, P. and De Wolde, J. (1999). The dynamic response of the Greenland and Antarctic ice sheets to multiple-century climatic warming. *Journal of Climate*, 12(8):2169–2188.

Jourdain, N. C., Asay-Davis, X., Hattermann, T., Straneo, F., Seroussi, H., Little, C. M., and Nowicki, S. (2020). A protocol for calculating basal melt rates in the ismip6 antarctic ice sheet projections. *The Cryosphere*, 14(9):3111–3134.

Kittel, C., Amory, C., Agosta, C., Jourdain, N. C., Hofer, S., Delhasse, A., Doutreloup, S., Huot, P.-V., Lang, C., Fichefet, T., and Fettweis, X. (2021). Diverging future surface mass balance between the antarctic ice shelves and grounded ice sheet. *The Cryosphere*, 15(3):1215–1236.

Lazeroms, W. M. J., Jenkins, A., Rienstra, S. W., and van de Wal, R. S. W. (2019). An Analytical Derivation of Ice-Shelf Basal Melt Based on the Dynamics of Meltwater Plumes. *Journal of Physical Oceanography*, 49(4):917 – 939.

Le Meur, E. and Huybrechts, P. (1996). A comparison of different ways of dealing with isostasy: examples from modelling the Antarctic ice sheet during the last glacial cycle. *Annals of Glaciology*, 23:309–317.

Lenaerts, J., Vizcaíno, M., Fyke, J., van Kampenhout, L., and Van den Broeke, M. (2016). Present-day and future Antarctic ice sheet climate and surface mass balance in the Community Earth System Model. *Climate Dynamics*, 47.

Morlighem, M., Rignot, E., Binder, T., Blankenship, D., Drews, R., Eagles, G., Eisen, O., Ferraccioli, F., Forsberg, R., Fretwell, P., Goel, V., Greenbaum, J. S., Gudmundsson, H., Guo, J., Helm, V., Hofstede, C., Howat, I., Humbert, A., Jokat, W., Karlsson, N. B., Lee, W. S., Matsuoka, K., Millan, R., Mouginot, J., Paden, J., Pattyn, F., Roberts, J., Rosier, S., Ruppel, A., Seroussi, H., and Smith, E. C. (2019). Deep glacial troughs and stabilizing ridges unveiled beneath the margins of the Antarctic ice sheet. *Nature Geoscience*.

Pattyn, F. (2017). Sea-level response to melting of Antarctic ice shelves on multi-centennial timescales with the fast Elementary Thermomechanical Ice Sheet model (f.ETISh v1.0). *Cryosphere*, 11:1–28.

Pattyn, F., Perichon, L., Durand, G., Favier, L., Gagliardini, O., Hindmarsh, R. C. a., Zwinger, T., Albrecht, T., Cornford, S., Docquier, D., Fürst, J. J., Goldberg, D., Gudmundsson, G. H., Humbert, A., Hütten, M., Huybrechts, P., Jouvet, G., Kleiner, T., Larour, E., Martin, D., Morlighem, M., Payne, A. J., Pollard, D., Rückamp, M., Rybak, O., Seroussi, H., Thoma, M., and Wilkens, N. (2013). Grounding-line migration in plan-view marine ice-sheet models: Results of the ice2sea MISMIP3d intercomparison. *Journal of Glaciology*, 59:410–422.

Pegler, S. S. (2018). Suppression of marine ice sheet instability. *Journal of Fluid Mechanics*, 857:648–680.

Pollard, D. and DeConto, R. M. (2012a). A simple inverse method for the distribution of basal sliding coefficients under ice sheets , applied to Antarctica. *The Cryosphere*, 6:953–971.

Pollard, D. and DeConto, R. M. (2012b). Description of a hybrid ice sheet-shelf model , and application to Antarctica. *Geoscientific Model Development*, 5:1273–1295.

Pollard, D. and DeConto, R. M. (2020). Improvements in one-dimensional grounding-line parameterizations in an ice-sheet model with lateral variations (psuice3d v2.1). *Geoscientific Model Development*, 13(12):6481–6500.

Pollard, D., DeConto, R. M., and Alley, R. B. (2015). Potential Antarctic Ice Sheet retreat driven by hydrofracturing and ice cliff failure. *Earth and Planetary Science Letters*, 412:112–121.

Reese, R., Albrecht, T., Mengel, M., Asay-Davis, X., and Winkelmann, R. (2018). Antarctic sub-shelf melt rates via pico. *The Cryosphere*, 12(6):1969–1985.

Rignot, E., Mouginot, J., and Scheuchl, B. (2011). Ice flow of the antarctic ice sheet. *Science*, 333(6048):1427–1430.

Schmidtko, S., Heywood, K. J., Thompson, A. F., and Aoki, S. (2014). Multidecadal warming of Antarctic waters. *Science*, 346(6214):1227–1231.

Schoof, C. (2007). Ice sheet grounding line dynamics: Steady states, stability, and hysteresis. *Journal of Geophysical Research: Earth Surface*, 112:1–19.

Seguinot, J. (2013). Spatial and seasonal effects of temperature variability in a positive degree-day glacier surface mass-balance model. *Journal of Glaciology*, 59(218):1202–1204.

Sergienko, O. V. and Wingham, D. J. (2019). Grounding line stability in a regime of low driving and basal stresses. *Journal of Glaciology*, 65(253):833–849.

Seroussi, H., Nowicki, S., Simon, E., Abe-Ouchi, A., Albrecht, T., Brondex, J., Cornford, S., Dumas, C., Gillet-Chaulet, F., Goelzer, H., Golledge, N. R., Gregory, J. M., Greve, R., Hoffman, M. J., Humbert, A., Huybrechts, P., Kleiner, T., Larour, E., Leguy, G., Lipscomb, W. H., Lowry, D., Mengel, M., Morlighem, M., Pattyn, F., Payne, A. J., Pollard, D., Price, S. F., Quiquet, A., Reerink, T. J., Reese, R., Rodehacke, C. B., Schlegel, N.-J., Shepherd, A., Sun, S., Sutter, J., Van Breedam, J., van de Wal, R. S. W., Winkelmann, R., and Zhang, T. (2019). initmip-antarctica: an ice sheet model initialization experiment of ismip6. *The Cryosphere*, 13(5):1441–1471.

Shapiro, N. M. and Ritzwoller, M. H. (2004). Inferring surface heat flux distributions guided by a global seismic model : particular application to Antarctica. *Earth and Planetary Science Letters*, 223:213–224.

Sun, S., Pattyn, F., Simon, E. G., Albrecht, T., Cornford, S., Calov, R., Dumas, C., Gillet-Chaulet, F., Goelzer, H., Golledge, N. R., and et al. (2020). Antarctic ice sheet response to sudden and sustained ice-shelf collapse (abumip). *Journal of Glaciology*, 66(260):891–904.

Trusel, L., Frey, K., Das, S., Karnauskas, K., Munneke, P., Meijgaard, E., and Van den Broeke, M. (2015). Divergent trajectories of antarctic surface melt under two twenty-first-century climate scenarios. *Nature Geoscience*, 8.

Tsai, C.-Y., Forest, C., and Pollard, D. (2020). The role of internal climate variability in projecting antarctica's contribution to future sea-level rise. *Climate Dynamics*, 55.

van Wessem, J. M., van de Berg, W. J., Noël, B. P. Y., van Meijgaard, E., Amory, C., Birnbaum, G., Jakobs, C. L., Krüger, K., Lenaerts, J. T. M., Lhermitte, S., Ligtenberg, S. R. M., Medley, B., Reijmer, C. H., van Tricht, K., Trusel, L. D., van Ulft, L. H., Wouters, B., Wuite, J., and van den Broeke, M. R. (2018). Modelling the climate and surface mass balance of polar ice sheets using racmo2 – part 2: Antarctica (1979–2016). *The Cryosphere*, 12(4):1479–1498.

Winkelmann, R., Martin, M. A., Haseloff, M., Albrecht, T., Bueler, E., Khroulev, C., and Levermann, A. (2011). The potsdam parallel ice sheet model (pism-pik) – part 1: Model description. *The Cryosphere*, 5(3):715–726.